FEDERAL UNIVERSITY OF SANTA CATARINA - ARARANGUÁ CAMPUS

Rodrigo Schmidt Lucchesi

BACHELOR FINAL PROJECT IN ENERGY ENGINEERING

Araranguá

2017

RODRIGO SCHMIDT LUCCHESI

TRABALHO DE CONCLUSÃO DE CURSO DE GRADUAÇÃO EM ENGENHARIA DE ENERGIA

Trabalho de conclusão de curso na modalidade de artigo científico para a aprovação na disciplina de Trabalho de Conclusão de Curso do curso de Engenharia de Energia da Universidade Federal de Santa Catarina – Campus Araranguá

Aprovado em: 30 / 11 / 2017

Prof. Dr. Leonardo Elizeire Bremermann (Orientador)

Prof. Dr. César Cataldo Scharlau (Examinador)

Prof. Dr. Éverton Fabian Jasinski (Examinador)

SAFE POWER MANAGEMENT SYSTEM FOR ELECTRIC VEHICLES USING FUZZY LOGIC CONTROL

Rodrigo Schmidt Lucchesi[1], **Leonardo Elizeire Bremermann**[2], **Anderson Luiz Fernandes Perez** [3]

ABSTRACT

The vehicular technology is going through a new paradigm. Guidelines must be determined, in the emissions control and the smart usage of the non-renewable energy sources becomes reality. Nowadays, electric vehicles are an option to mitigate these issues. Viewed as an electronic device, the electric vehicle's consumption has to be managed efficiently due to a limited battery life and the high cost of these energy storage devices. In this bachelor final project, a Safe Power Management System (SPMS) of an electric vehicle, which is a subsystem of an Energy Management System (EMS), is developed. EMS is a power split manager focused on distribute the power to the vehicle main subsystems, always seeking the integrity of the whole set and the reduction on energy consumption. The system uses a Fuzzy Logic Controller, as the control strategy to the electric energy consumed by the electric vehicle.

Keywords: Electric vehicle, Energy Management System, Safe Power Management System, Energy consumption, Fuzzy Logic Control

[1]Undergraduate student of Energy Enginnering at the Federal University of Santa Catarina, Araranguá Campus, Rodovia Governador Jorge Lacerda, 3201, Jardim das Avenidas Araranguá, Santa Catarina, Brasil, CEP 88905-355. E-mail: rodrigo.lucchesi@grad.ufsc.br

[2]Professor.Dr, Advisor in the Bachelor Final Project

[3]Professor.Dr, Co-Advisor in the Bachelor Final Project

LIST OF ABBREVIATIONS AND ACRONYMS

AC	*Alternating Current*
BEV	*Battery Electric Vehicle*
BMS	*Battery Management System*
CB	*Chemical Battery*
CG	*Center of Gravity - Rigid Body*
COG	*Center of Gravity - Function*
DC	*Direct Current*
DoD	*Deep of Discharge*
EDC	*European Driving Cycles*
EM	*Electric Motor*
E.M.F	*Electromagnetic Force*
EMS	*Energy Management System*
EV	*Electric Vehicle*
FC	*Fuel Cell*
FCEV	*Fuel Cell Electric Vehicle*
FEV	*Fully Electric Vehicle*
FIS	*Fuzzy Inference System*
FLC	*Fuzzy Logic Controller*
FTP-75	*Federal Test Procedure - 75*
HEV	*Hybrid Electric Vehicle*
HM	*Height Method*
HWFET	*Highway Fuel Economy Driving Schedule*
ICE	*Internal Combustion Engine*

ICEV	*Internal Combustion Engine Vehicle*
JDC	*Japanese Driving Cycles*
LA	*Lead Acid*
MISO	*Multiple inputs - Multiple outputs*
MF	*Membership Function*
NC	*Nickel Cadmium*
SC	*Santa Catarina*
SEV	*Solar Electric Vehicle*
SoC	*State of Charge*
SoH	*State of Health*
SPMS	*Safe Power Management System*
USDC	*United States Driving Cycles*
USEPA	*United States Environmental Agency*

1 INTRODUCTION

A new era are becoming to exist in the vehicular industry. With the zero emission politics, environmental problems, and high oil prices, new technologies are needed to mitigate and solve these issues. The internal combustion engine, used vastly worldwide in traction vehicles, are allowing grounds to the electrification of the powertrain.

Seen as the future of mobility, electric vehicles technology is growing up fast, gaining supporters in all sectors. It is well know that, in order to introduce a new form of thinking, the solution must be gradually presented to the market. Therefore, many companies, such as Toyota, Nissan, BMW and others, are building the path for the evolution. To catalyze the process, the company named Tesla Motors, showed to the world a new futuristic vision about electric vehicles. Solving partially the short driving range problem with its new battery technology, the company put a step forward of the competitors, with its high technology embedded in its products.

Therefore, a good analogy of an electric vehicle (EV) is a battery powered electronic device, like an smart phone. Even with the development of new chemical batteries, the low autonomy is the weakness of the electric cars segment. On these devices, an option to overcome this problem is the insertion of bigger batteries. However, higher weight in a vehicle, straightly affects its energy consumption, due to the extra force needed to push a heavier object. Thus, new approaches to manage the electric energy consumed in the vehicle are needed to avoid this solution.

Energy management systems are power split managers, which decides where the energy should be used. It is like the human brain choosing what are the main functions to be conserved for surviving. The brain decides where the chemical energy must go in real emergencies, for example. Those human body natural controllers are activated to perform in a more effective way these tasks. In the same way, an electric vehicle needs an economic performance in low battery situations.

In order to represent this feature, a Fuzzy logic controller (FLC) could be implemented to perform those actions, searching a more efficient electricity consumption by the electric vehicle. Fuzzy sets are a natural system observation in probabilities way, instead numeric intervals, modelling complex dynamic systems in a more human thinking manner. Considering this approach, all the control variables are described with the linguistic expressions.

In this case, a Safe Power Management System is created to the electric vehicle battery emergency situations. These issues occur when the battery reach low state of charge (low en-

ergy). Therefore, the controller acts straight in the vehicle performance, decreasing the vehicle speed when these states are reached. Seeking the system analysis, a simulation was performed using the programming tool *Matlab*, to obtain the speed values using this modern controller.

This study is organized with the following structure. Firstly, the Literature Review with the topics used to understand the main parts of the project development is done. Secondly, the models used to compose the EV powertrain are detailed: Battery model, Motor model and the Vehicle model. Also in this section, the FLC development is described, which is the Safe Power Management System proposed to reduce energy consumption. Nonetheless, is introduced a section with the results from scenarios developed to analyze the EV behaviour. Finally, the final conclusions of the main situations proposed in the simulation are deeply analyzed in this section.

2 LITERATURE REVIEW

In this section the literature review will be presented, summarizing the topics used to the study's construction.

2.1 EV hystory and development

Electric vehicle (EV) technology has been developed for more than a hundred years with the advent of chemical batteries as energy storage device, providing electricity to the vehicle powertrain. Powertrain is the group of components that deliver power to the driving wheels including engine or electric motor (KLOMP, 2010). In the late 1800s, engineers from France, England, United States, and other countries started to expand the construction of electric vehicle prototypes. In 1897, the first commercial electric vehicle was introduced into the New York City taxi fleet. Creating a new market in the automotive industry, *Pope Manufacturing Co.* took advantage of this opportunity and became the first large-scale electric cars manufacturer in United States (EMADI, 2014). An interesting fact occurred in 1899 with the Belgium racing driver *Camille Jenatzy*, who drove the car called *La Jamais Content*, exceeding 100 km/h with an electric car, setting an important mark to the evolution of the technology (LARMINIE; LOWRY, 2004).

However, with the use of internal combustion engines and the reduction of gasoline price in 1920s, the electric vehicles production started to decline. Its low battery capacity, causing a short driving range, became the weaker point of the segment. In comparison of available energy, the 9000 $\mathrm{Wh\,kg^{-1}}$ of the fuels, utilized in internal combustion engine vehicles (ICEVs), were

much bigger than the 30 $\mathrm{Wh\,kg^{-1}}$ of the lead acid batteries used in electric cars. This situation made the engineers rethink about the on-board technology and pushed to a new era of mobility with the extinction of electric vehicles in 1935 (EMADI, 2014).

Since the 1990s, increased concerns about soaring oil prices, depleting fossil fuels reserves, and environmental issues caused by the exhaust emissions of ICEVs, influenced the automotive industry to return with the production of EVs (EMADI, 2014). As mentioned in Emadi (2014), with comparison of conventional ICEVs, electric vehicles has several advantages such as: high electric machine efficiency versus internal combustion engine efficiency ; low level of environmental pollution, improving local air quality ; lower noise ; smoother operation ; a variability of electricity sources whom could be obtained from renewable, such as hydro, wind and solar ; a variate of on-board energy storage devices such as batteries, supercapacitors, flywheels and fuel cells ; regenerative breaking to recover the kinetic energy of the vehicle.

The majority of the vehicle manufacturers adopted the new tendency, boosted by zero-emission politics, new researches have begun to strengthen the technology. In California, Tesla Motors was created and installed, changing dramatically the future of the EVs. The visionary, creator and Tesla CEO, Ellon Musk, introduced a new paradigm to the market. Solving partially the battery range problem and introducing new production modes to the industry, this company become the best one in any ways on the sector. Nowadays, many vehicle companies started to invest in the segment, pushing the market to new limits. In Japan, Germany, Italy, for example, manufacturers such as Honda, BMW and Fiat has been working on producing new products to reduce the cost of EVs, indeed having high prices due to the new components to supply the innovations embedded in the vehicles (MUNEER; KOLHE; DOYLE, 2017).

Thus, the future of the powertrain electrification is going towards of new sources of electric energy also with the smart cities integration. New types of charging stations should be implemented using renewable energy as the primary source. Electric vehicle batteries can also be employed as power banks. With all these cases, autonomous-driving and the mentioned trends are becoming the future of the automotive industry, being also a solution to greenhouse effect and urban mobility (PISTOIA, 2010). This transition from ICEVs to EVs is not a easy task to perform. Petrol production countries as Saudi Arabia, causes difficult obstacles due to the strong politics and its big economy influences (RAJHI et al., 2012). So the gradually introduction of electric vehicles turns a solution to this task.

Whereas in places as US, China and some European countries like Germany and Netherlands, some government incentives to EVs production are turning easier the technology introduction. China is a strong example. In the most populated cities as Beijing, Shanghai and Hong

Kong, to purchase an internal combustion engine vehicle, the customer needs to obtain a different license plate to be able to run with these vehicles on the streets. It is a much higher cost compared to the electric vehicles license. Also, the government provides subsides to buy EVs in China (WANG; PAN; ZHENG, 2017). However, if the electric energy consumed by the vehicle is not generated from renewable energy sources, as wind and solar, the whole system does not become a sustainable choice to mitigate the footprint caused by the emissions of Thermal power stations, the main power generation source in the country (JI et al., 2012). In the next section, the background on hybrid and electric vehicles will be explored.

2.2 Background on hybrid and electric vehicles

This section provides a general view about electric vehicles technology. Electrification of cars powertrain can be classified as Hybrid Vehicles (HEVs) and pure electric vehicles (EVs), which include battery-powered electric vehicles (BEVs) , fuel cell electric vehicles (FCEVs) and solar electric vehicles (SEVs). In fully electric vehicles, no internal combustion engine is applied on the system (MELO; ARAUJO; CASTRO, 2011).

2.2.1 Hybrid electric vehicles (HEVs)

HEVs uses an ICE, combining power with electric motor. This structure is generally used to improve the efficiency of the system. This technology is the first step to introduce electric vehicles to the market. There are three different configurations to connect the ICE and electric motor, that will be described in next subsections.

2.2.1.1 Series hybrid electric vehicles

The ICE generates mechanical power to an electric generator or is used to propel the wheels via the same electric motor and mechanical transmission. In this case, there is no mechanical connection between the ICE and the traction load. The ICE works as a range extender, offering a solution to the short driving range of pure electric vehicles. The decoupling between the ICE and the driving wheels has the advantage of flexibility for fixing the engine operating states. Nevertheless, it has three propulsion devices (ICE, generator, electric motor). Therefore, the efficiency of series HEVs are generally lower (MELO; ARAUJO; CASTRO, 2011).

2.2.1.2 Parallel hybrid electric vehicles

According to Melo, Araujo and Castro (2011), in a parallel HEV, the ICE and the electric motor are able to deliver power to drive the wheels. Power distribution between the engine and the motor is varied, so both run in their optimum operating region as long as possible. There is no separate generator in a parallel hybrid configuration. Whenever the generator's operation is needed, the motor works as generator to charge the battery in two ways: regenerative braking and absorbing power from the ICE when its output is greater than that required to drive the wheels. An advantage over the series case is that a smaller ICE and a smaller electric motor can be used to get the same performances.

2.2.1.3 Series-Parallel hybrid electric vehicles

This configuration allows the vehicle been propelled by the ICE, electric motor or both. It is necessary a power split controller to determine which power source will be used. Generally, the vehicle is driven by the electric motors in low speeds and the ICE is activated, when the car needs a higher energy. Toyota Prius is an example of Series-Parallel HEV (PISTOIA, 2010).

2.2.2 Fully electric vehicles (FEVs)

According to Melo, Araujo and Castro (2011), there are several electric motor topologies for FEVs: a single electric motor; an electric motor in each of the steering wheels; a motor for each rear wheel and one motor per wheel. As energy source used to the vehicle, it could be mentioned chemical batteries (CB), fuel cells and solar panels (providing energy to be stored in CBs).

2.2.2.1 Battery electric vehicles (BEVs)

Battery Electric Vehicles (BEVs) are powered only by batteries, an electrochemical device to store chemical energy, converted later to electricity during the EV operation. There are a few drawbacks in this technology, highlighting especially the battery weight, its short driving range and high recharging time. Compared to fossil fuels, it has a lower power density as well. There are several types of chemical batteries, which can be mentioned like Nickel Metal Hydride (NiMH), Lead Acid (Pb Acid), and Lithium Ion (Li-Ion)(LARMINIE; LOWRY, 2004). Most of the automotive companies has been using Li-Ion batteries, due to its higher power den-

sity, faster recharging and greater durability, being nowadays the best choice for EVs (MELO; ARAUJO; CASTRO, 2011).

The inclusion of power electronic converters at the storage devices, are turning the whole EV system more efficient than years ago. Battery Management Systems (BMS) are used to improve the efficiency on battery usage. This system allows the fast charging, equalization of the battery cells and optimization of the battery discharging, for example. Another case is the EMS developed to reduce electric energy consumption and optimize power distribution in the EV. For instance, this management systems shows improvements in the capability of storing the braking energy, together with the control of Joule losses (PISTOIA, 2010).

2.2.2.2 Fuel cell electric vehicles (FCEVs)

FCEVs run on electricity generated by the fuel cells on-board. The fuel cells use many combination of fluids to the electrochemical process, but hydrogen and oxygen are the most utilized in the electric energy generation. The by-products of fuel cells are only water and heat, and has a much more efficient energy conversion system, compared with ICE and chemical batteries (EMADI, 2014). A fuel cell is an electrochemical energy conversion device, which uses a combination of fluids and a proton exchange membrane to produce electricity. This membrane is high cost priced, being nowadays a disadvantage to the technology.

Another challenges for the FCEVs are the waste water vapor management, hydrogen preparation, storage, transportation and distribution. Those are very important issues to be properly dealt with, to the consolidation of this energy device (EMADI, 2014). The powertrain of a FCEVs can be a combination of energy storage devices. A FC system can be the primary source or work alone to provide energy to the vehicle. As a developing technology, the research in FCEVs are growing fast, and has been considered the future of electric cars (CHAN, 2007).

2.2.2.3 Solar electric vehicles (SEVs)

Allan Freeman in England built up the first solar-powered vehicle in 1979. SEVs capture energy from the sun and converts it to electricity. The electric energy generated from the solar panels, is used to charge batteries or power the vehicle directly (EMADI, 2014). The conventional solar-powered powertrain with the static solar panel is easy to implement and operate, however has a short drive range, limited acceleration capacity, low efficiency and is highly sensitive to weather conditions (LOVATT; RAMSDEN; MECROW, 1998). To overcome the low efficiency of the system, a maximum power point tracking system is implemented in the vehicle. Nevertheless,

the solution to use solar panels to recharge batteries is a promising option. Using as battery banks, the solar utilities could help on stationary events, while the vehicle is parked, for example (EMADI, 2014). In the next section driving cycles will be detailed.

2.3 Driving cycles

A driving cycle is made up of micro-trips (trip between two idling intervals) and has a period of 10 to 40 min. This duration has to contain enough micro-trips reflecting real-world driving behaviour (ARUN et al., 2017). The driving cycles could be laboratory made or real ones. These last mentioned are constructed with sensors to capture the main variables, as velocity, acceleration, distance and slope.

When talking about driving cycle development, three steps are important: route selection, data collection and cycle construction. The route selection involves selecting the course to describe the cycle. It consist of determining if the route is a highway with constant velocity, arterial roads or city driving, for example. Data collection, is the ability to collect the parameters with the right sensors to describe the driving cycle. Finally, the cycle development consists of splitting the entire data into micro-trips and creating a time domain function of the vehicle velocity (ZHANG; GUO; HUANG, 2017).

There are two types of driving cycles: the modals and the transient ones. The primary difference between those types, is the driver behavior. The modal driving cycles are a compilation of acceleration in straight line in periods of constant velocity. They do not represent real driver actions. In the transient cycles, many variation of the velocity are occurred, being a more realistic scenario (ARAÚJO, 2015).

According to (BENTO, 2015), there are several models of driving cycles and the main ones are divided in three big groups: European driving cycles (EDC), American driving cycles (USDC - United States Driving cycles) and Japanese driving cycles (JDC). During a vehicle design stage, a proper mathematical model to describe the powertrain is needed, to achieve good results in simulations. The driving cycles are the inputs to the code, being used for the desired analysis of the vehicle. For example, a driving cycle should be performed until drain the EV battery (LARMINIE; LOWRY, 2004). This execution is used to analyze driving range and the behavior of the battery, during the time that model has been exposed.

2.4 Fuzzy logic controller (FLC)

In this section the Fuzzy logic controller will be explored, also with the mathematical theory behind it, describing the tools to develop a project which is inserted as the control system technique.

2.4.1 Fuzzy set

A fuzzy set (class) A in X is characterized by a membership function $fa(x)$ which associates with each point in X a real number in the interval $[0, 1]$, with the value of $fa(x)$ at x representing the "grade of membership" of x in A. Thus, the nearer the value of $fa(x)$ to one, the higher the grade of membership of x in A (ZADEH, 1965). For example, the control variable Hot related to the linguistic variable internal temperature of a room, has a range $[20, 35]$. If takes an aleatory value as $27\,^{\circ}\mathrm{C}$, this temperature will have a grade of membership to the interval, such as $finT(27) = 0.7\ (70\%)$ (RIADI et al., 2007).

A classical set, described by Boolean logic, has "sharp" boundaries, having a similar analogy to a digital signal. Applying more flexibility to these structures, fuzzy sets are smoother than the classical ones, appearing more an analog signal, giving a broader range of possibilities to describe the interval [0-1] (JANG, 1993). This partial membership is described in Figure 1, where member $x4$ and $x5$ do not belong to the set B in the view of a classical set, but they can be considered partials in fuzzy (BAI; WANG, 2006).

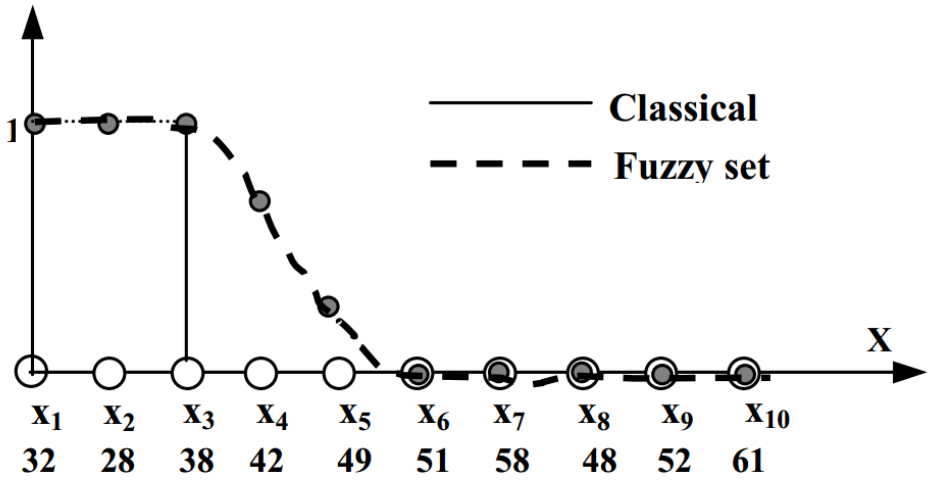

Figure 1 – The comparison between classical and fuzzy sets. Source: (BAI; WANG, 2006)

2.4.2 Fuzzy inference system (FIS)

To design a fuzzy logic control, it is highly necessary understand the types of controllers existing in the literature. The most used are the Mamdani and Sugeno FIS (FARIAS, 2014). A Mamdani FIS is developed by three steps: fuzzification, inference rules and defuzzification (CARBONI; RAGAINI; FERRERO, 2017). Each parameter is described as a linguistic variable, having its own control variables, splitting those in a more human thinking way. As mentioned before, the input internal temperature could be divided in many subgroups as: Cold, Medium, Hot; being those the control variables of the linguistic variable internal temperature.

According Kaur and Kaur (2012), the most fundamental difference between Mamdani-type FIS and Sugeno-type FIS is how the crisp output is generated from the fuzzy inputs. Mamdani-type FIS uses the technique of defuzzification with membership functions to a fuzzy output, while Sugeno-type FIS uses weighted average to compute the crisp output. A Mamdani FLC was projected to this study, so the theory to create it is described below.

2.4.2.1 Fuzzification and membership functions

Fuzzification is the process of making a crisp quantity fuzzy or a possibility. This process gives to the data an uncertainty characteristic. All the interval of vagueness could be described for a membership function (SZCZEPANIAK; LISBOA, 2012). Membership function (MF) characterizes the fuzziness in a fuzzy set. The main purpose of them is to transform a crisp data to a possibility in the interval of $[0, 1]$ (SZCZEPANIAK; LISBOA, 2012). According to Bai and Wang (2006), the membership functions can be represented in many ways, such as: triangular, trapezoidal, piecewise linear, gaussian, singleton, sigmoidal, sinusoidal and many other function types.

The most used membership functions are the Triangular, Trapezoidal and Gaussian. The Trapezoidal membership function has four values as its calculation parameters, containing two peak numbers. The Equation 2.1 represents it. Different to the Trapezoidal, a Triangular membership function, a special case of the Trapezoidal MF, has three numbers for the rules combination which are explained in the Equation 2.2. It has one maximum point where fuzziness is 1. In FLC, a Trapezoidal membership function could be used to describe a Triangular MF, its peak parameters must be the same value (JANG, 1993). The letters, illustrated below, represents the parameters of the numerical interval to be fuzzyfied from the MFs.

$$f(x:a,b,c,d) = \begin{cases} 0, & x \leq a \\ \frac{x-a}{b-a}, & a < x \leq b \\ 1, & b < x < c \\ 0, & x > d \\ \frac{d-x}{d-c}, & c < x \leq d \\ 0, & x > c \end{cases} \tag{2.1}$$

$$f(x:a,b,c) = \begin{cases} 0, & x \leq a \\ \frac{x-a}{b-a}, & a < x < b \\ \frac{c-x}{c-b}, & b < x \leq b \\ 0, & x > c \end{cases} \tag{2.2}$$

The intervals where the membership functions will act are called Control Variables, sectioning the variables used in the FLC project, called Linguistic Variable (LV). As example, for the input internal temperature, this space is subdivided in three control variables $(Cold, Medium, Hot)$. For the cold control variable the internal temperature varies from $(0-15\,^{\circ}\mathrm{C})$ representing a variable to be fuzzified for a MF (RIADI et al., 2007). The fuzziness represents how deep is the value inserted to that situation. If internal temperature of $15\,^{\circ}\mathrm{C}$ has 1 as grade of membership in the Medium control variable, so this state is totally inserted in the Medium interval.

2.4.2.2 Defuzzification

The defuzzification process is meant to convert the fuzzy output, back to the crisp or classical output value. This action is resumed as the transformation of a linguistic variable to a number for a MF. Three defuzzification techniques are commonly used: mean of maximum method, center of gravity method and the height method (BAI; WANG, 2006).

The Center of Gravity method (COG) is the most applied defuzzification technique used in FLC projects. The process is analogous to calculate centroid of an area. The Equation 2.3 describe the output generated from the process (BAI; WANG, 2006).

$$COG(\mu(x)) = \frac{\int \mu(x)x dx}{\int \mu(x) dx} \tag{2.3}$$

The parameter $\mu(x)$ is the value calculated from the membership function and x is a quantity from the control variable. The Height method (HM) is valid only for the case where the output membership function is an aggregated union result of symmetrical functions (BAI;

WANG, 2006). This method can be divided into two steps. First, the consequent membership function F_i can be converted into a crisp consequent $x = \Phi$ where F_i is the center of gravity of Φ. Then the COG method is applied to the rules with crisp consequents, which can be expressed on the Equation 2.3 (BAI; WANG, 2006).

$$x = \frac{\sum_{i=1}^{M} w_i f_i}{\sum_{i=1}^{M} w_i} \tag{2.4}$$

In the Equation 2.4 above, w_i is the degree which the ith rule matches the input data. Its simplicity is the advantage of this method. At last, Mean of Maximum method search for the highest grade of membership, even if more than one peaks appeared in the set. Avoiding an aleatory value, a mean value is calculated between the maximum values in the system output. The Equation 2.5 describes how the maximum values are calculated, which u represents the maximum points of pertinence degrees and M are the values encountered in the data set.

$$u = \sum_{i=1}^{M} \frac{u_i}{M} \tag{2.5}$$

2.5 Energy management system (EMS)

According to Kley, Lerch and Dallinger (2011), electric vehicles and autonomous driving are the future of mobility. However, the EVs autonomy is smaller than ICE vehicles (HOWEY et al., 2011). To overcome this problem, many solutions have been created in the past years. The answer for these questions are the utilization of multiple Energy Storage Systems (ESS), regenerative breaking (RB) or even the hybridization of the powertrain with IC engine, called range extenders (EMADI, 2014).

As an electronic device, the energy in an EV has to be managed to obtain lower energy consumption values (DIB et al., 2014). Therefore, a Battery Management System (BMS) and Energy Management System (EMS) are, nowadays, the options to manage the system in a more efficiently mode. Allied with power electronic devices and control techniques, these subsystems have being deeply studied for their better results on energy consumption overall (EMADI, 2014).

The BMS regulates the chemical battery used in electric vehicles, as the cells equalization, charging and discharging, for example (CHENG et al., 2011). An EMS has the objective of managing the energy used in the system (BEAUDIN; ZAREIPOUR, 2015). For an EV, an EMS works as a power split manager, aiming to a better system efficiency and a reduction of electricity consumption (MELO; ARAUJO; CASTRO, 2011).According to Emadi (2014), for energy management problems, there are two kinds of solutions: the optimization-based strategies and

the heuristic-based strategies. The optimization options and researches related to it are found in Emadi (2014) and illustrated in Table 1:

Table 1 – Strategies using optimization techniques and articles related

Strategies using optimization techniques	**Description**
1) Strategies that consider EMS operation restrictions;	1) In Sakhdari and Azad (2015), the heater power and internal temperature are used to minimize the battery power and energy consumed;
2) Strategies that consider FC/engine efficiency;	2) As example, Wang et al. (2017);
3) Strategies that consider battery State of Health (SOH) or longevity;	3) As mentioned in Serrao et al. (2011);
4) Strategies based on analytical solutions;	4) As mentioned in Li et al. (2015);
5) Online and offline strategies;	5) In Melo, Araujo and Castro (2011) talks about offline and online procedures to control energy consumption;

Source: Adapted from Emadi (2014)

The Emadi (2014), mentioned the solutions using heuristic-based strategies that are described in Table 2 below:

Table 2 – Strategies heuristic-based solutions and articles related

Strategies heuristic-based solutions	**Description**
1) Piecewise continuous description of the power split	1) As listed in Armenta et al. (2015);
2) Frequency based power split	2) Is the same kind of strategy mentioned above, perhaps utilizing the frequency domain instead of the time domain;
3) Fuzzy controllers	3) Is an option for the controlling system. Fuzzy Logic is used in Hemi, Ghouili and Cheriti (2014);
4) Neural Networks;	4) Which Moreno, Ortúzar and Dixon (2006) and Murphey et al. (2012) uses machine learning techniques to develop the EMS;

Source: Adapted from Emadi (2014)

In this work, a Safe Power management System using fuzzy logic control is developed, to be utilized as the Eco-Mode option, found in the vehicle Nissan Leaf Armenta et al. (2015). The strategy used for the study was based in (GALDI; PICCOLO; SIANO, 2006). This study proposes a FLC to limit the power extracted from the battery when the vehicle reaches limiting conditions in the deep of discharge ($DoD > 70\%$). The next sections will describe how the work was developed and the results obtained.

3 METHODOLOGY

In this study, a subsystem of an Energy Management System (EMS) is implemented. This block could be resumed in applying a fuzzy logic controller to reduce the vehicle velocity when critical battery deep of discharge is reached. The FLC is switched on when ($DoD > 70\%$), seeking the reduction of EV electric energy consumption. It is well know that, if the EV is on a highway and the Safe Power Management System (SPMS) decrease the cars velocity, an accident could be occurred for low speed. To avoid this situation, the driver should stop for battery recharging or keep hazard warning lights on, for a safety way. The government policies about this situation must be studied, finding the best solution for these new mobility problems (YOUNG et al., 2013).

Since SPMS affects directly the vehicle performance, this system must be used on emergency situations (Low battery and far recharging station). In Galdi, Piccolo and Siano (2006), the authors suggest a similar approach. As mentioned in the other section, EMS are power split managers. Optimum scenarios or other desired situations could be proposed to this block, taking as target the reduction of vehicle consumption. It is developed, to the vehicle analysis, simulation scenarios using a mathematical model of the EV powertrain.

To emphasize how a electric vehicle works, an analogy to a battery powered electronic device, as a mobile phone, could be made. The energy is supplied by the CB when the vehicle is switched on. When the driver press the accelerator pedal, working as a potentiometer, electric power is required from the battery. To describe this sequence, a functional model, covered with mathematical equations, are modeled for the analysis. The modeling approach uses the following devices: battery, electric motor and the longitudinal vehicle dynamics describing the vehicle motion.

Therefore, a block diagram of the system control, represents the mathematical models to describe the system dynamics and the controllers embedded in the EV. How the controller would be applied in the system is a metric for its development. It could work in a close loop system, when the controller has a feedback from the plant output, or in an open loop system,

with no output signal comparison is done (NISE, 2012). In this study, a open loop system control method is applied with the FLC mentioned and described in Figure 2. In the next subsections, will be demonstrated how these modelling blocks were developed.

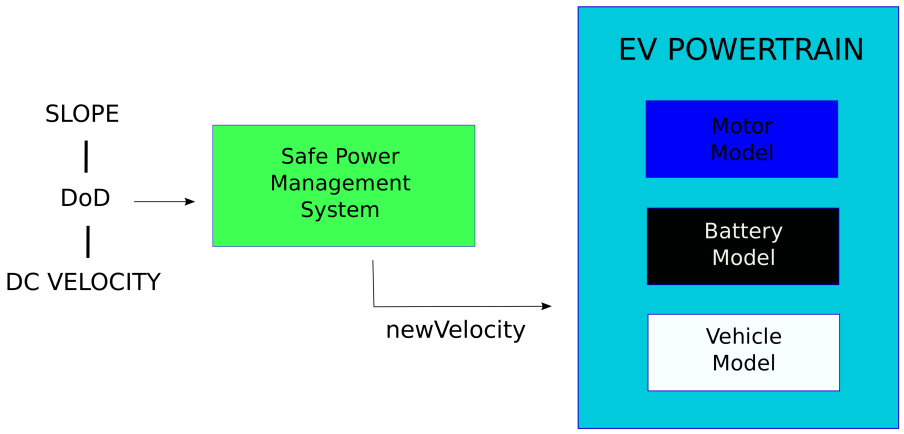

Figure 2 – Block Diagram of the system control. Source: The author

3.1 Battery modelling

Most of the EV nowadays, are running with Li-Ion batteries. Whereas a decade ago, this technology was in the majority cases utilized for racing cars, due to its high price. During this period and before, many other types of chemical batteries were used in EV. For the development of this model, a research in the literature was made and many articles were found about this topic such as (HAIZHOU, 2017; FOTOUHI et al., 2016; LARMINIE; LOWRY, 2004). In Larminie and Lowry (2004), a well explained example of Lead-acid and Niquel-cadmium, are introduced with a battery internal resistance model, thus used in this study.

The chemical battery can be represented as an equivalent electric circuit. The chosen model was a DC source represented by the internal resistance model, illustrated in Figure 3. As Larminie and Lowry (2004) mentioned, the battery can be treated as a black box. It means the equations to describe the model are obtained from data analysis of the dynamical system. Unfortunately, this model does not represent with accuracy the lag during the battery open voltage drop. These issue are discussed in the literature (JOSSEN, 2006). Therefore, the simpler model is adopted, and the results obtained are a good approximation of the real scenario (LARMINIE; LOWRY, 2004).

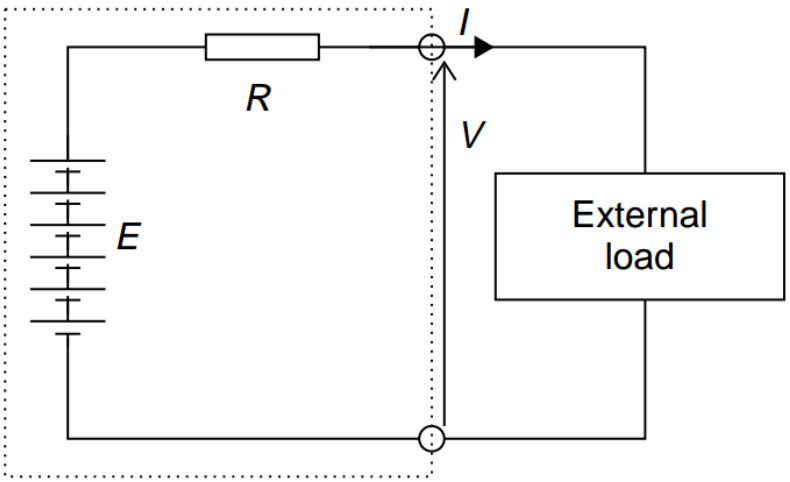

Figure 3 – Internal resistance circuit model of a chemical battery. This battery is composed of 6 cells. Source: (LARMINIE; LOWRY, 2004)

According Larminie and Lowry (2004), Lead Acid (LA) and Nickel Cadmium (NC) batteries are the most consolidate types to be used in traction cases. Enhancing the battery choice, the Ragone plot, illustrated in Figure 4, is used to determine the battery type. It is a graphical representation of specific energy and specific power. Specific energy is the amount of electric energy stored for every kilogram of battery mass $(\mathrm{Wh\,kg^{-1}})$. Specific power is the amount of power obtained per kilogram of battery $(\mathrm{W\,kg^{-1}})$.

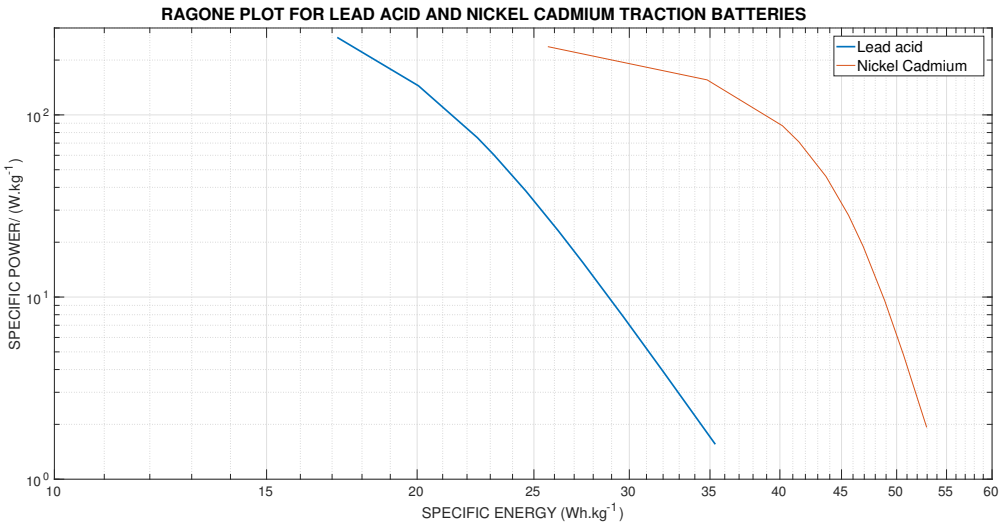

Figure 4 – A Ragone plot - Specific Power versus Specific Energy - for typical lead acid and nickel cadmium batteries. Source: Edited from Larminie and Lowry (2004)

A similar behaviour is verified on Figure 4, for both battery types, since the specific

power is inversely proportional to the specific energy. In the power range of 1 to $100\mathrm{W\,kg^{-1}}$ the $NiCad$ battery shows slightly less changes. However, above that point, in $100\mathrm{W\,kg^{-1}}$ the $NiCad$ battery specific power falls much faster than the Lead acid. The Ragone plot concludes, ignoring other factors such as cost, that the $NiCad$ battery performs better if power densities are lower than $100\mathrm{W\,kg^{-1}}$ are required. Nonetheless, at higher values up to $250\mathrm{W\,kg^{-1}}$ or even higher, the Lead acid becomes more attractive with its higher specific power, fitting well with high speed electric motors.

As the powertrain requires a high power from the battery, the Lead-Acid (LA) is chosen. An advantage of LA batteries is its low internal resistance, described in the Equation 3.1. That means a lower energy loss in the process is occurred. In order to determine the parameters of the model, firstly it has to be calculated the battery open voltage, related to the deep of discharge (DoD). DoD is the inverse of SoC mentioned before. On the range from $0-100\%$ and describes the remain energy stored in the battery. First of all, it must be mentioned that the Li-Ion open voltage model was not adopted for its implementation complexity. In Weng, Sun and Peng (2014), illustrates the open voltage modelling for this type of chemical battery. As Larminie and Lowry (2004) confirm, the Lead Acid is a good approximation for range calculation analysis, performed in this study.

$$R_{in} = No.ofcells \times \frac{0.022}{C_{10}}\mathrm{Ohms} \tag{3.1}$$

As mentioned in Larminie and Lowry (2004), for been direct proportional to the battery deep of discharge, the most important parameter for CB analysis is the open circuit voltage model. The Equation 3.2 illustrates the relation with DoD. The variable n is the number of cells in the chemical battery.

$$E = n \times (2.15 - DoD \times (2.15 - 2.00)) \tag{3.2}$$

Therefore, the next part is the battery capacity modelling. Capacity, is the electric charge that a battery can supply. The *Peukert* capacity is introduced in Equation 3.3, which describes the electric charge removed from the battery. Where the *Peukert* coefficient exponentially acts in the battery current on discharging. The charging current has no *Peukert* coefficient. Thus in discharging mode, electric charges are removed from the battery in a faster process.

$$CR_{n+1} = CR_n + \frac{\delta \times I^k}{3600}\mathrm{Ah} \tag{3.3}$$

The DoD is the ratio of the charge removed from the battery by the original battery capacity. The Equation 3.4 shows the nth iteration.

$$DoD_n = \frac{CR_n}{C_p} \tag{3.4}$$

The following modeling, is the current drawn from battery. The power required from the powertrain is calculated as shown in Equation 3.5:

$$P = V \times I \tag{3.5}$$

Combining the open voltage calculation from the battery equivalent circuit, Figure 3, the Equation 3.6 is developed:

$$V = E - IR \tag{3.6}$$

The power extracted from the battery calculation is illustrated in Equation 3.7:

$$P = V \times I = (IE - IR) \times I = EI - RI^2 \tag{3.7}$$

So the current drained from the battery is developed as follows in the Equation 3.8 :

$$I = \frac{E - \sqrt{E^2 - 4RP}}{2R} \tag{3.8}$$

To represent the charging mode, occurred when the regenerative breaking is applied or normal battery charging situations, the charge supplied to the battery is illustrated in Equation 3.9. Regenerative breaking is a range extender technique, used in the powertrain model. It converts the kinetic energy from the brakes and generate power to the battery, increasing the SoC or decreasing the DoD.

$$CR_{n+1} = CR_n - \frac{\delta \times I}{3600}\text{Ah} \tag{3.9}$$

The current in charging mode is lower than discharging and this is represented from the *Peukert* coefficient. The same analogy with human body can be made. A certain person requires more time to recharge the battery (8 hours sleep) than spending it in a exercise (1 hour) for example (LARMINIE; LOWRY, 2004). The calculation of the electric current supplied to the battery is demonstrated in the Equation 3.10.

$$V = E + IR$$

$$P = V \times I = (IE + IR) \times I = EI + RI^2$$

$$I = \frac{-E + \sqrt{E^2 + 8RP}}{4R} \tag{3.10}$$

In Figure 5 is illustrated a schematic of the procedures of charging and discharging inside a CB. Therefore, with the battery model described with the equations to be applied in the simulation, the parameters to used in the analysis, as cited in Larminie and Lowry (2004), are described in Table 3.

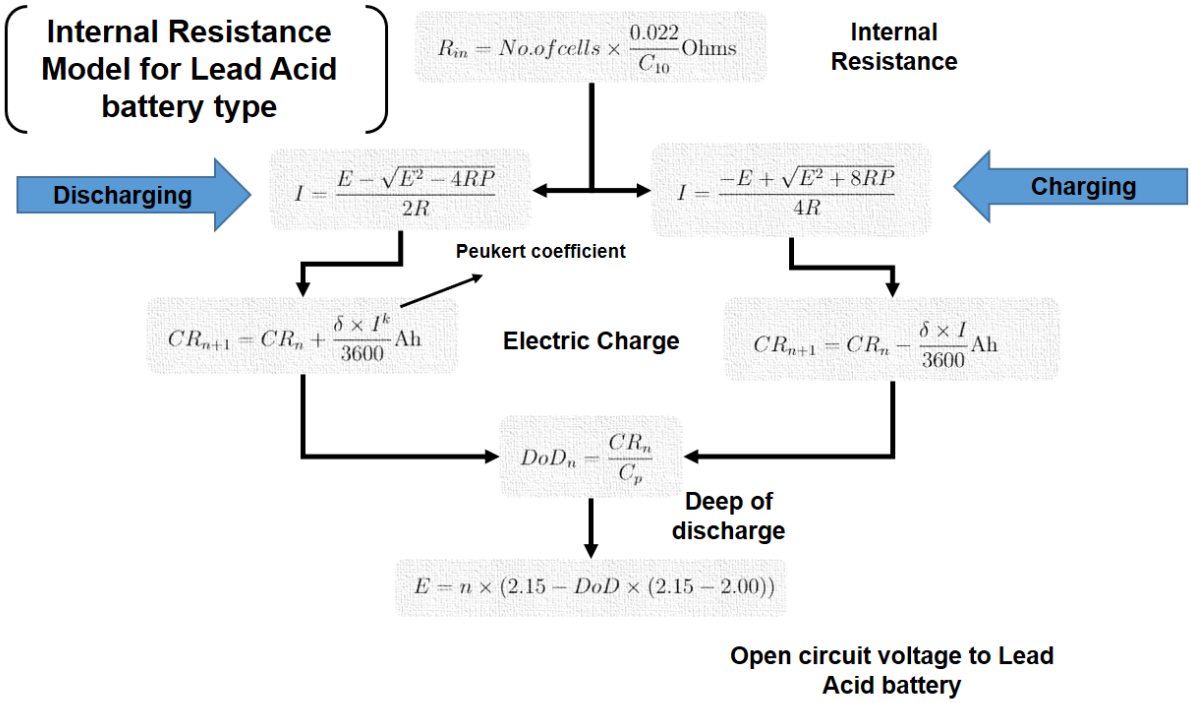

Figure 5 – Schematic of the procedures of charging and discharging inside the chemical battery. Source: Edited from Larminie and Lowry (2004)

Table 3 – Coefficients to describe the Lead acid battery model

Battery type	Number of cells	Peukert Coefficient	Battery capacity (Ah)
Lead Acid	156	1.12	60

Source: Adapted from Larminie and Lowry (2004)

3.2 Electric motor modelling

The electric motor (EM) is the main part to be described mathematically in the EV powertrain. An induction motor, used for this study, has 2 main parts: the Stator and Rotor. The Stator is the stationary part and the rotor is the rotating part. A Stator is made by stacking thin-slotted highly permeable steel laminations inside a steel or cast iron frame. Winding passes through slots of the Stator. When a 3 phase AC current passes through the winding produces a rotating magnetic field (CHAPMAN, 2013).

Assume you are putting a closed conductor inside such a rotating magnetic field. Since the magnetic field is fluctuating an electromagnetic force (E.M.F) will be induced in the loop according to Faraday's law. The E.M.F will produce a current through the loop. The situation has become as if a current carrying loop is situated in a magnetic field. This will produce a magnetic force in the loop according to Lorentz law, so the loop will start to rotate (CHAPMAN, 2013).

A similar phenomenon also happens inside an induction motor. Instead of a simple loop, a squirrel-cage rotor is used. A squirrel-cage rotor has got bars which are shorted by end rings. A 3 phase AC current passing through a Stator winding produces a rotating magnetic field. So as explained, current will be induced in the bars of the squirrel-cage and it will start to rotate. This is due to the rate of change of magnetic flux in one squirrel bar pair which is different from another, due to its different orientation. This variation of current in the bar will change over time (CHAPMAN, 2013).

That's why the name induction motor is used, electricity is induced in rotor by magnetic induction rather than direct electric connection. To aid such electromagnetic induction, insulated iron core lamina are packed inside the rotor. Varying the frequency of AC current in the electric motor with the EV accelerator pedal, the motor angular velocity increases, generating a greater torque in the power shaft, transmitting mechanical power to a transmission system to moves the vehicle in a linear motion. However, between the power input and output, there will be numerous energy losses associated with the motor (CHAPMAN, 2013; EMADI, 2014).

In this section, the electric motor efficiency with the losses involved, are developed. This approach is an energy analysis of the system block. According to Larminie and Lowry (2004), some losses are the same for all types of electric motors, being a good approximation to obtain the final results proposed to this study. Those losses are divided in four types detailed below:

- Copper Losses:

These losses are caused by the electric resistance of the motor wires and brushes. It is a heating energy loss. The variable τ is the motor torque and the constant Kc depends on the

resistance of the brushes and the coil, and also the magnetic flux Φ. (LARMINIE; LOWRY, 2004). The Equation 3.11 represents this parameter.

$$P_{CopperLosses} = K_c \tau^2 \quad (W) \tag{3.11}$$

- Iron losses:

Those losses are caused by magnetic effects in the motor, particularly in the rotor. The magnetic field is continually changing in this part while the motor is operating. The iron inside this motor piece, causes two types of losses. The first is called "hysteresis" loss, and is resumed in the energy required to continually magnetize and demagnetize the iron, aligning and re-aligning the magnetic dipoles. "hysteresis" is the lag between this process. The second iron loss results from the changing magnetic field, generating a current in the iron, by the normal methods of electromagnetic induction. It is another heating energy loss. The Ki is a constant depending on magnetic field and w is the motors angular velocity (LARMINIE; LOWRY, 2004). The Equation 3.12 illustrates the sum of these energy losses.

$$P_{IronLosses} = K_i \omega \quad (W) \tag{3.12}$$

- Friction power and windage power:

The friction power come from bearings and brushes of the motor. The rotor will also have a wind resistance, which might be quite large if a fan is fitted to the rotor for cooling. The parameter Tf is the friction torque and Kw is a constant depending mainly on the size and shape of the rotor, even if a cooling fan is fitted (LARMINIE; LOWRY, 2004). The Equations 3.13 and 3.14 represents those losses.

$$P_{Friction} = T_f \omega \quad (W) \tag{3.13}$$

$$P_{Windage} = K_w \omega^3 \quad (W) \tag{3.14}$$

- Constant losses (C):

According Larminie and Lowry (2004), losses in the system occur even if the motor is totally stationary. The total power losses in a electric motor, developed for this study, are compiled in the Equation 3.15. Doing some mathematical manipulations, the Equation 3.16

is obtained, which describes the electric motor efficiency with the respect of energy losses. The motor efficiency is described by the ratio of the mechanical power by the electric power (Output/Input). Returning to what was mentioned, electric power is the power given by the battery to produce the mechanical power derived from the torque generated from the rotating magnetic field.

The torque of the output power (mechanical power) has a simplification adopted by the author (LARMINIE; LOWRY, 2004). Mechanical power of the electric motor is $P_{mech} = \tau.\omega$, which τ is the torque generated by the E.M.F and ω is the angular velocity of the rotor. The author infers that friction power is the mechanical power. That is, the τ_f is equal to τ.

$$TotalLosses = K_c\tau^2 + K_i\omega + K_w\omega^3 + C \quad (W) \tag{3.15}$$

$$\eta_m = \frac{Output\ power\ (Mechanical\ Power)}{Input\ power\ (Electric\ Power)} = \frac{Output\ power}{Output\ power + Losses}$$

$$\eta_m = \frac{\tau_f\omega}{\tau_f\omega + K_c\tau^2 + K_i\omega + K_w\omega^3 + C} \tag{3.16}$$

As one of the main EV problems, the short driving range could be mitigated with some techniques called *range extenders*. One of those techniques, is called regenerative braking (RB). While the vehicle braking, the vehicle kinetic energy could be converted into electric energy by the motor. How this works is easiest to understand in the case of the classical DC motor with brushes, but broad principles apply to all motor types (LARMINIE; LOWRY, 2004). As mentioned in (LARMINIE; LOWRY, 2004), if the motor is unplugged from the battery from a switch, rotating with a certain angular velocity ω , this operation generates a certain voltage in the motor. To explain that, suppose the voltage of the battery is Vb, and the motor is turning at angular velocity ω, then the current that will flow out from the motor, is given by the Equation 3.17 below:

$$I_m = \frac{V}{R} = \frac{K_m\Phi\omega - Vb}{Ra} \tag{3.17}$$

The Ra is the armature resistance, Km is constant related to the magnetic poles, Φ is the magnetic flux and Vb the battery voltage. To normalize the voltage generated in the motor, a DC/DC converter is used, increasing the DC voltage generated by the process. Without power electronics the battery would not charge due to the low voltage generated from that situation. The power given by the RB is taken in the Equation 3.18, where η_c is the efficiency of the converter. The sub-index m is related to the motor as b to the battery. So current flows to the

battery recharging it in active braking situations.

$$P_{RB} = V_b \times I_b = \eta_c \times V_m \times I_m \tag{3.18}$$

The motor efficiency detailed in Equation 3.16 has the used parameters to the simulation, from Larminie and Lowry (2004), detailed in the Table 4 . To the DC/DC converter, an efficiency of $\eta = 0.5$ is adopted, being the RB efficiency (LARMINIE; LOWRY, 2004).

Table 4 – Typical values of 100 kW, high speed induction motor

Parameter	**100 kW, high speed induction motor**
kc	0.3
ki	0.01
kw	5.0$\times$ 10^{-6}
C	600

Source: Adapted from Larminie and Lowry (2004)

3.3 Longitudinal vehicle dynamics modelling

In this section, the longitudinal vehicle dynamics model will be detailed. This part is literally the equations to describe mathematically the cars motion. In this study, the vehicle is represented as a rigid body (RAJAMANI, 2011). To develop the equations, the vehicle external forces should be point out. Using the Newton's second law $\sum \vec{F} = m \times \vec{a}$, forces, accelerations and its directions must be represented, to describe the system dynamics. Also, the torques generated by the external forces, related to a chosen point k must be illustrated as $\sum \vec{M}_k = I_k \times \vec{\alpha}$, where M_k is the torque related to the point k, I_k is the moment of inertia due to the same point and $\vec{\alpha}$ is the rigid body angular velocity. In some cases, the center of inertia (C_G) is a good reference point to calculate the torques (HIBBELER, 2016).

The vehicle body motion could be simplified to a only translational motion. The rigid body rotational motion is not occurred due to the road restrictions with the wheels in the vertical axis (SHAKOURI et al., 2010).However, in real conditions, torques related to the external forces must be considered. The Equations in 3.19 illustrate the equations of motion applied in the vehicle free-body diagram, represented in Figure 6, where a bi-dimensional analysis ($x - y$ /

horizontal-vertical) of the system in a road with slope θ is applied (RAJAMANI, 2011). In this situation the C_G was the point chosen by the author, to calculate the torques generated by the external forces and the moment of inertia. However, the vehicle linear acceleration, represented by $\ddot{x}$, has the opposite direction to the rigid body motion.

$$\begin{aligned} \sum F_x &= m(a_g)_x \\ \sum F_y &= m(a_g)_y \\ \sum M_g &= I_g\alpha \end{aligned} \tag{3.19}$$

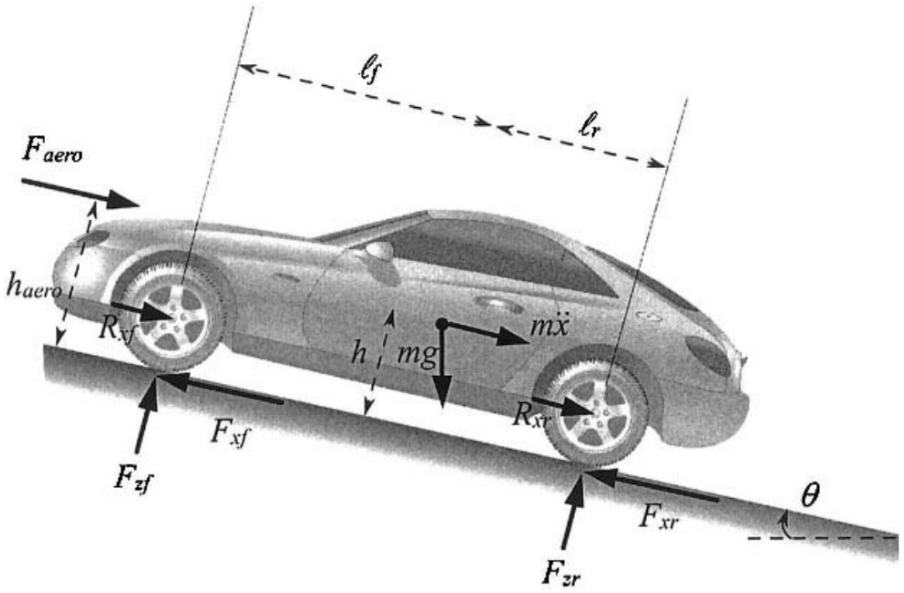

Figure 6 – Longitudinal vehicle dynamics. Source: (RAJAMANI, 2011)

In Figure 6 the related forces are: F_{aero} is the drag force, R_x is the rolling resistance force, F_x is the longitudinal tire force and F_z is the normal force, proportional to the vehicle mass. The first three forces would be more detailed in the chosen model, illustrated in Figure 7. The other parameters included in the Figure 6, are the vehicle length measures, which are used to calculate the torques generated by the external forces acting in the vehicle body. Therefore, l_f and l_r are the distances between the front and rear wheel to the vehicle center of inertia. The parameter h_{aero} is the distance between the road and the point where the drag force acts, h is the distance between the road and C_G.

However, this model explored in Rajamani (2011) is not used to the proposed study. In the uphill scenario, described in the next section, this representation had high battery power values, discharging the battery to fast, consequently. Even on plain road scenarios the vehicle had higher values in all the parameters analyzed, presenting an undesirable behaviour. Due those situations, the model covered in Larminie and Lowry (2004), illustrated in the Figure 7, was adopted. This is a simplified model of the vehicle longitudinal dynamics illustrated in Figure 6. During the proposed simulation, the battery open voltage drop, proportional to the tractive force shown in Figure 7, had a smoother behaviour. In order that situation, the electric charges were drained slower, resulting in a more realistic way to the battery discharging.

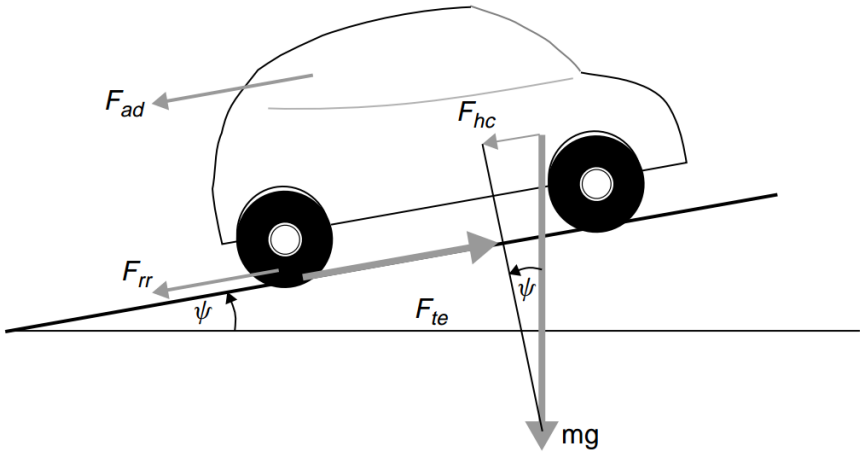

Figure 7 – Longitudinal vehicle dynamics adopted in the study. Source: (LARMINIE; LOWRY, 2004)

The simplifications adopted by the author are described as follows. Firstly, there is no acceleration in y axis and there is just one normal force N_r acting in the rear wheel, caused by the vehicle weight. Neither moments generated from the forces are considered, where none distance are described in the model, which are directly used to calculate the moment of external forces. By those simplifications, the only equations remained from the Equations 3.19 are $\sum F_x = m(a)_x$ that will generate the tractive force Fte and $\sum F_y = 0$ that will generate the Normal force $N_r = mg\cos(\psi)$. Tractive force is the force to propel the vehicle forward, transmitted to the ground through the drive wheels.Consider a vehicle of mass m, proceeding at a velocity v, up a slope of angle ψ, as in Figure 7, the forces used in the model are described below:

3.3.1 Rolling resistance force

The rolling resistance force, Equation 3.21, is primarily due to the friction of the vehicle tire with the road. It is direct proportional to the vehicle weight. According to Shakouri et al. (2010), the rolling resistance coefficient is hardly dependent of the vehicle velocity and is illustrated in Equation 3.20. To determine the rolling resistance force, the Equation 3.21 is used (LARMINIE; LOWRY, 2004). The parameters listed in both equations are: N_r = Normal force in rear wheel; v_x = vehicle velocity in x axis.

$$\mu_{rr} = 0.01 \left(1 + \frac{v_x}{100}\right) \tag{3.20}$$

$$\vec{F_{rr}} = \mu_{rr} N_r \quad [\hat{\imath}] \tag{3.21}$$

3.3.2 Aerodynamic drag

According to Larminie and Lowry (2004), this force is due to the friction of the vehicle body moving through the air. The formula for this component is illustrated in Equation 3.22. The parameters in the Equation are: ρ = air density; A_f = frontal area of the vehicle; v = velocity; C_d = drag coefficient.

$$\vec{F_{ad}} = \frac{1}{2} \rho A_f C_d v_x^2 \quad [\hat{\imath}] \tag{3.22}$$

The drag coefficient C_d can be reduced by good vehicle design. A typical value for a saloon car is 0.3, but some electric vehicle designs have achieved values as low as 0.19. To calculate this parameter is a hard task. Many mathematical approaches are needed, using especially fluid dynamics (MUNSON; YOUNG; OKIISHI, 2004). The coefficient used for the simulation is an approximation to the GM EV1, vehicle proposed by Larminie and Lowry (2004). For the frontal area determination, the Equation 3.23 is adopted (SHAKOURI et al., 2010), which is a polynomial approximation to define this parameter for any vehicle with mass m.

$$A_f = 1.6 + 0.00056(m - 765) \tag{3.23}$$

3.3.3 Hill climbing force

This force is related to the streets and highways road slopes. It is a important aspect to be studied, as will be deeply discussed in the Results and Discussion section. High electric currents are drawn from the battery in uphill cases due to an extra weight force acting in the opposite direction of the vehicle motion (YANG et al., 2014). As shown in Equation 3.24, the force is straightly related to the road slope ψ and the vehicle mass.

$$\vec{F_{hc}} = mg\,\text{sen}(\psi) \quad [\hat{\imath}] \tag{3.24}$$

3.3.4 Acceleration force

If the velocity of the vehicle is changing, then clearly a force will need to be applied in addition to the forces shown in Figure 7. This force will provide the linear acceleration of the vehicle (LARMINIE; LOWRY, 2004). The acceleration is calculated with the formula $a(n) = v(n) - v(n-1)$, from the driving cycle inserted as input of the simulations used to the system analysis. The Equation 3.25 express this item.

$$\vec{F_{la}} = ma_x \quad [\hat{\imath}] \tag{3.25}$$

$$\vec{F_{te}} = (F_{rr} + F_{ad} + F_{hc} + F_{la}) \quad [\hat{\imath}] \tag{3.26}$$

Therefore, the tractive force F_{te} or the resultant force acting in the x axis is calculated, which is illustrated in Equation 3.26. An observation to be made, that no tire model is developed to the simulation. In Larminie and Lowry (2004), the relationship between the motors and

wheels angular velocity, can be negligible, being represented with the same value. The Table 5 illustrates the parameters adopted in the simulation. Those are based in the vehicle EV1, a full electric vehicle produced in late 1900s for General Motors. Even as a old vehicle, the parameters used are not to significant than a newer models.

Table 5 – Typical parameter values for the GM EV1

Parameter	**Electric Vehicle GM EV1**
ρ	1.225 $\frac{kg}{m_3}$
c_d	0.19
m_v	1540 kg
G_{eff}	0.95

Source: Adapted from Larminie and Lowry (2004)

3.4 Fuzzy logic controller (Safe Power Management System)

In this section the FLC development and its functionality are described. Firstly, the idea of what kind of controller would be applied, was an unknown quantity. In Farias (2014), an experimental test was created to obtain electric energy consumed by an electric toy car, used as experimental test for the controllers proposed. The main objective of this work, was applying two types of controllers (FLC and if-else statements), to verify which one would work more effective in controlling the vehicle prototype energy consumption. The FLC was developed using the Mamdani inference system and COG function as deffuzification technique. Trapezoidal MF's were used for the fuzzification step. The input variables adopted from the author to this controller structure were: road slope θ and battery state of charge SoC. The output was the vehicles velocity. In this project results, the FLC performed better to control the energy consumed.

Based on these results, a deeper research about FLC was made to find the best control configurations to reduce the EV consumption with this type of controller. In Emadi (2014), a part of an EMS is developed, mentioning the heuristic approach, which characterizes the FLCs. EMS as a power split manager, controls all the embedded systems in the vehicle, connected via

the controller area network (CAN), the vehicle network used to communicate all the controlled devices (BECKER; SCHAEPER; SAUER, 2012). Based on work of Galdi, Piccolo and Siano (2006), a new approach was adopted to the EMS. The authors elaborated a Safe Power Mode to the EV using Fuzzy controllers. It is a block of an EMS, which works juts on battery critical $SoC's$.

Following this research, a Safe Power Management System (SPMS) with FLC is developed in this study, working during low battery states, seeking the EV integrity and giving a chance to the driver reaches the next charging station. Using a FLC controller to actuate only in emergency situations ($DoD > 70\%$), being directly applied on the vehicles performance (GALDI; PICCOLO; SIANO, 2006). The SPMS slows down the vehicle speed in critical battery energy states, seeking the reduction on electric energy consumption, as it is straight connected to the EV velocity. This controller works in different environments (plain road slope, uphill and downhill scenarios). This is a range extender technique (EMADI, 2014). With these concerns, this study selected a combination of these two projects illustrated in Farias (2014), Galdi, Piccolo and Siano (2006), to develop the methodology for the FLC controller construction.

The FLC adopted uses a Mamdani Fuzzy inference sytem (FIS) and COG as defuzzification method. The Mamdani FIS has the procedures mentioned in the subsection about Fuzzy in the Literature Review: fuzzification, (IF-THEN) rule based for inference process and defuzzification; being that a better option to describe heuristically the system. The COG method is used for been the most applied method in the FLC projects (FARIAS, 2014). It has two membership functions (MF), the triangular and trapezoidal MF, for the fuzzification step, which describes the linguistic variables.

The Fuzzy logic deals with simplicity and effectiveness to the control actions required from the controller, managing battery depletion under low battery $SoC's$, since it codifies the system knowledge in a set of fuzzy rules (GALDI; PICCOLO; SIANO, 2006). Due to the FLC ability to be used in situations where the system dynamics modelling is a hard task to be done, that situation enhanced the choice to use it FLC as the control unity (MAMDANI, 1976; KALAVATHI; REDDY, 2012). Also, the FLC does not require knowledge of a detailed mathematical model of the control system, unlike a classical controller does. Variables as flames colour of a combustion system could be model by knowing the intensity of those type of variables (BAŠIĆ; VUKADINOVIĆ; POLIĆ, 2013).

According to Tang and Mulholland (1987), when a FLC is well designed, it behaves similar to a nonlinear controller or even like a set of linear PID controllers, operating differently according to the stimuli or inputs. Therefore, as the modelling blocks are not hardly detailed, with a few of simplifications to the development, the usage of this approach of controlling system is a reasonable choice. Therefore, the controller is a MISO type (multiple inputs and

single output), having as its inputs: road slope, deep of discharge and current velocity from the driving cycle; as output: the new vehicle velocity. The programming software Matlab was used to to structure the FLC, demonstrated in Figure 8. At this picture, the left parameters are the inputs: slope-DoD-Velocity; on the right is the output newVelocity.

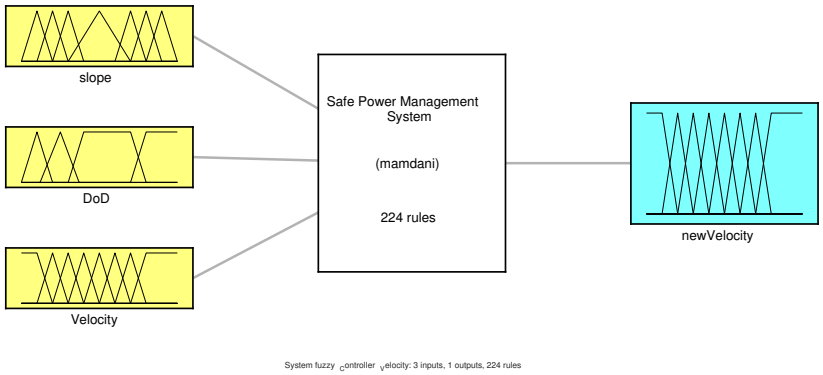

Figure 8 – The visual structure of the FLC. Source: The Author

The controller tasks are resumed of slowing the EV velocity to reduce the vehicle energy consumption. Firstly, the inputs slope, derived from the road gradient, Deep of discharge DoD, calculated from the battery modelling and the vehicle velocity, from the driving cycle used as input of the simulation, are performed inside the FIS rules of the FLC. A great number of rules (224) are created to the Mamdani system, seeking a more accurate response from the controller and a smoother behaviour to the velocity gradients. The inputs/output represented as linguistic variables are shown in Figure 9.

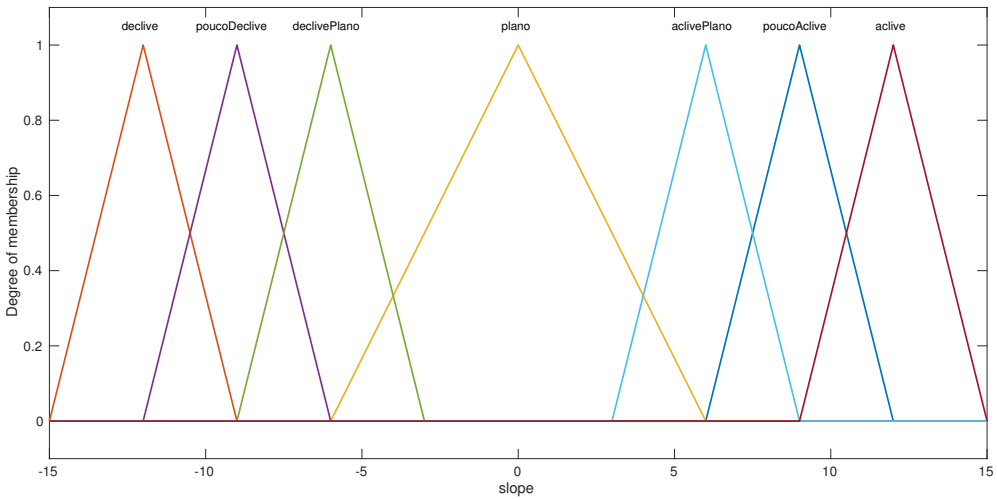

(a)

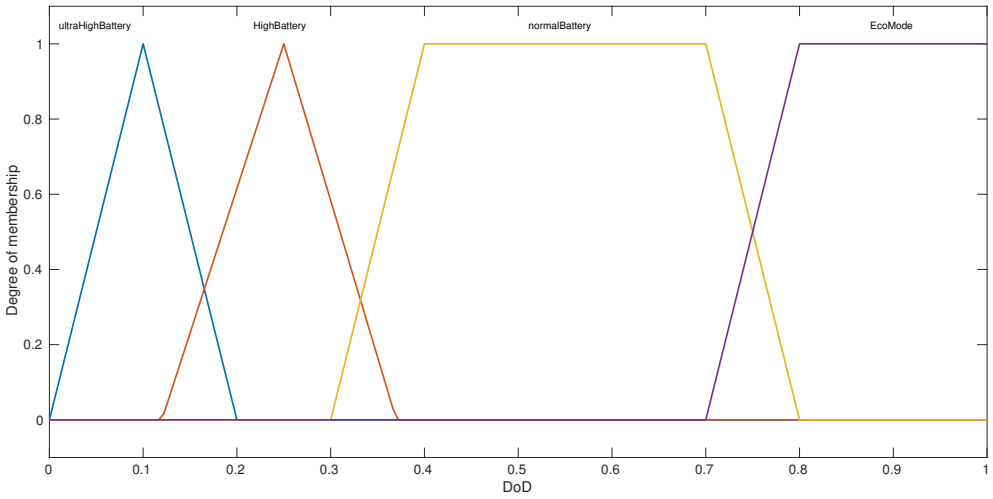
ultraHighBattery
HighBattery
normalBattery
EcoMode
Degree of membership
DoD
0
0.1
0.2
0.3
0.4
0.5
0.6
0.7
0.8
0.9
1
0
0.2
0.4
0.6
0.8
1

(b)

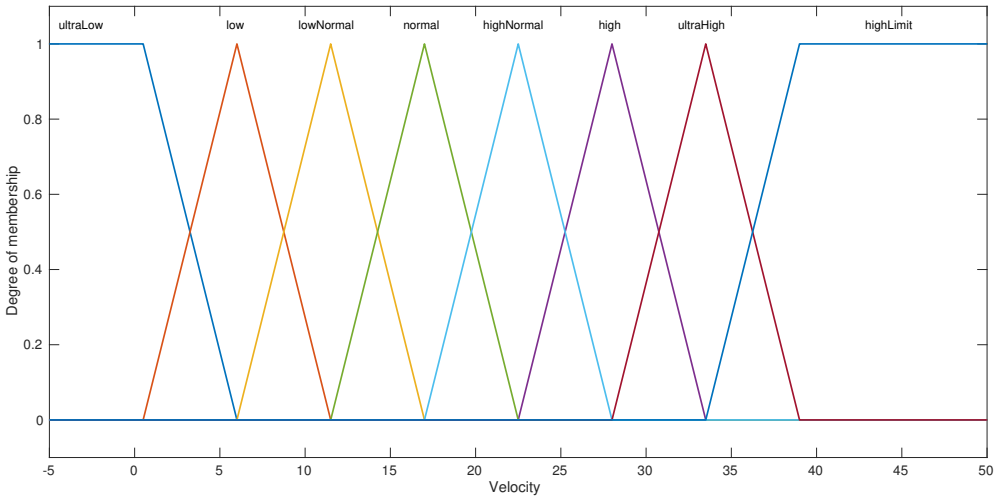
ultraLow
low
lowNormal
normal
highNormal
high
ultraHigh
highLimit
Degree of membership
Velocity
-5
0
5
10
15
20
25
30
35
40
45
50
0
0.2
0.4
0.6
0.8
1

(c)

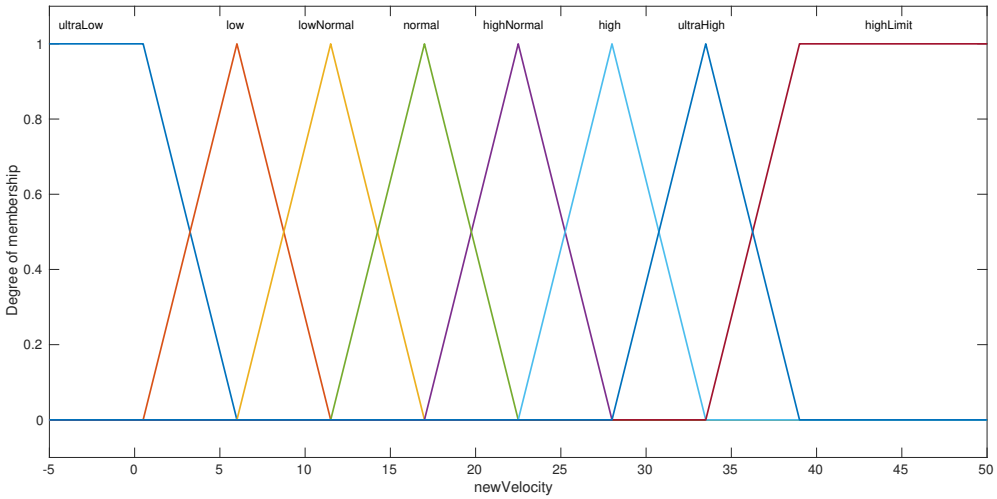

(d)

Figure 9 – The Fuzzy Inference System of the FLC developed. Inputs: a) Slope, b) DoD, c) velocity; Output: newVelocity. Source: The Author

As mentioned in Wu (2012), Trapezoidal MF are indicated to a big set of rules (greater than 100), having a low computational cost to the system controlling. However, as the system is applied offline, slowing data processing, limits this type of controller usability in real-time control applications. Therefore, the Fuzzy inference process combine the inputs inside the FLC with the $IF-THEN$ statements, generating the desirable output, created by the controller developer. For example, one of these rules working inside of the SPMS, is performed by sequence: "slope=plane and DoD=Eco Mode and Velocity=high then newVelocity=lowNormal".

The fuzzy rules utilized in the study are illustrated on Attachment A. To describe why the Trapezoidal and Triangular (a special case of the Trapezoidal MF) are used, some considerations are mentioned in Wu (2012). The author make a comparison between two types of MF's (Gaussian and Trapezoidal), pointing the best situations for each MF usability. The three special cases for the Trapezoidal choice, are highlighted below:

1. *Construction*: It concerns the methods to obtain the membership functions. Generally, there are two methods to create a MF: Model-Driven a mathematical model to describe the plant is needed. Optimization techniques are used to tune the parameters; Knowledge-Driven, the MF is obtained by the knowledge of the model designer about the linguistic variables, in a heuristic way. This last approach, adopted in this study, Trapezoidal MF are easier to model variables like flame colour of a combustion system, used to control the fuel required from the power controller.

2. *Analytic Structure*: The fuzzy controller could be derived to a mathematical model, if a classical controller is needed, for example. The Trapezoidal is easier to implement, due to its simpler structure. As mentioned before, sometimes FLCs are not a good option to fast controlling tasks;

3. *Monotonicity*: It describes how a system conserves the original structure during a process. A monotonic function is expressed as a mathematical expression who not changes the given order. A Trapezoid function performs better than Gaussian and others;

4. *Computational Cost*: In real-time controlling tasks, a low cost algorithm is preferred, in other words, a faster process is performed by the controller. Doing a Mamdani FIS with 50 rules or lower than that, a Gaussian MF seems more favorable. However, with the case of this study, more than 100 rules are used, so the trapezoidal MF performs faster;

Resulting from these concerns, a combination of Triangular and Trapezoidal MF are used to model the linguistic variables. In the next section the simulation results from the proposed scenarios will be explored.

4 RESULTS AND DISCUSSION

In this section, the results from the simulation scenarios will be discussed. The intention on this analysis, is testing the developed SPMS, when the vehicle reaches high DoD situations. The simulation is developed in *Matlab*, which is an easy implementation programming tool due to its mathematical libraries, offering a wide of function choices to be used in the code to be developed (CHAPMAN, 2016). The simulation was planned to be used on the acquisition of some parameters in the time domain. Primarily, a driving cycle is used as input. As discussed before, a driving cycle is a continuous representation of the vehicles velocity in urban,highway or a mix of those scenarios, for instance. In order to emulate these situations, driving cycles from USEPA (United States Environmental Agency) were utilized, which were developed to be used on many researches targets, such as emission of pollutants analysis (CHEN et al., 2007).

Nonetheless to the results comparison, real scenarios of driving cycles were built-up. As the controller acts in different road slopes, seeking a lower energy consumption, a uphill environment was created. All the scenarios, except uphill, runs in zero slope gradient. The simulation pseudo code in the Figure 10 is described below. Its structure was thought to simplify the system analysis in time domain, generating vectors for each magnitude, facilitating the data collection of the mean values.

Algorithm 1 Simulation of the electric vehicle to SPMS test

```
Choose Driving cycle
Initialize NULL vectors
Define parameters
n ← size(NULLvectors)
i ← 1
while (DoD < 95%)||(i < n ) do
    if (DoD < 70%) then
        Calculate the electric motor parameters with controller
    else
        Calculate the electric motor parameters without controller
    end if
    Calculate the battery parameters
    i ← i + 1
end while
```

Figure 10 – Simulation pseudocode. Source: The Author

4.1 Urban driving scenario

In this subsection, two urban driving scenarios are tested to verify the impact of the SPMS in the EV. This test propose a comparison of a real situation and a theoretic one.

4.1.1 EPA driving cycle (FTP-75)

The FTP-75 driving cycle is used as input for the simulation in this case. The FTP-75 (Federal Test Procedure) has been used for emission certification and fuel economy urban driving testing of light-duty vehicles in the United States (WANG et al., 2013). The following are some basic parameters of the cycle: Duration: 1877 s; Distance traveled: 17.77 km; Average speed: 34.12 km/h; Maximum speed: 91.25 km/h. The driving cycle velocity and the controlled velocity are expresses in Figure 11. The SPMS actuation is visible in this figure, also its smooth behaviour with the EV velocity. Thus, the driving cycle is repeated until DoD reaches 95%, reaching a battery empty state to analyzed the extra distance given by the SPMS. This technique is applied in all tests and is mentioned in Larminie and Lowry (2004) for vehicle range calculation.

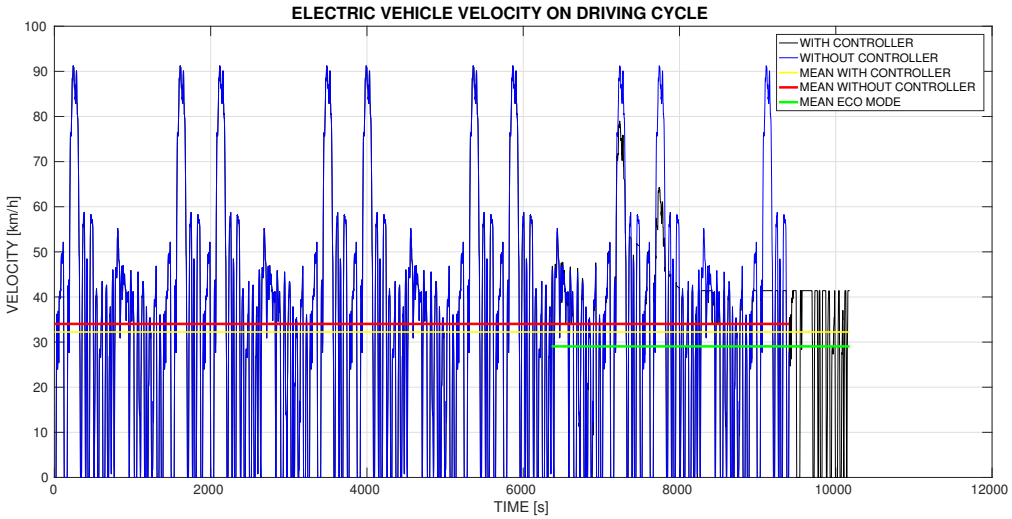

Figure 11 – The EV velocity in the FTP-75 driving cycle. Source: The Author

In the figures below, the performance of the controller dedicated to the EV energy reduction is demonstrated. At the top, the original plot is shown. Below that, a zoomed picture of the original one is utilized to observe with more quality the details of the information inserted. In Figure 12 the blue lines are the driving cycle without the controller and the black ones with it. The driving cycle with the controller has a longer range, elucidated in the plot. This situation repeats for all plots. About the EV consumption, the red line indicate the mean value for the cycle without controller, the yellow line with controller and the green one describes the mean consumption just for the safe power mode. The values obtained from the simulation are described in Table 6. A overall improvement of 6.67 % is occurred with the SPMS.

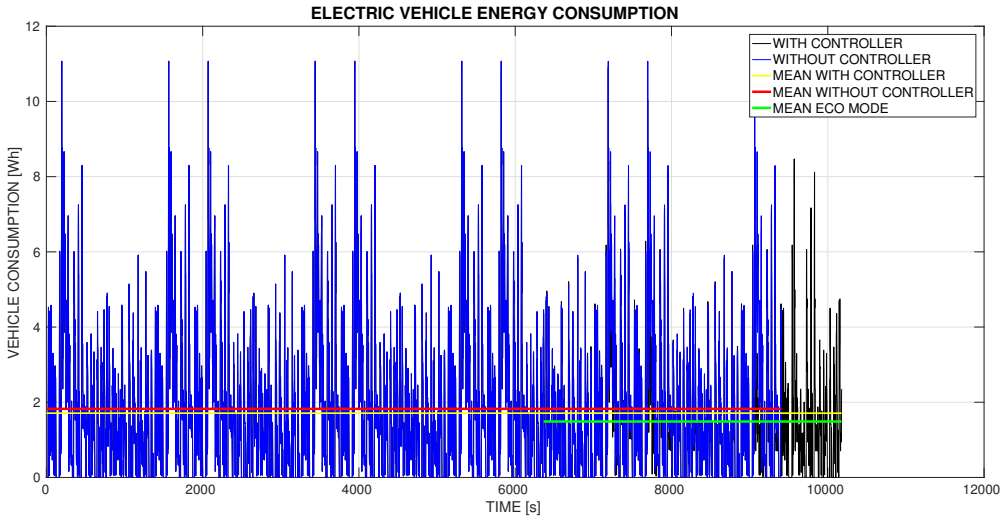

(a)

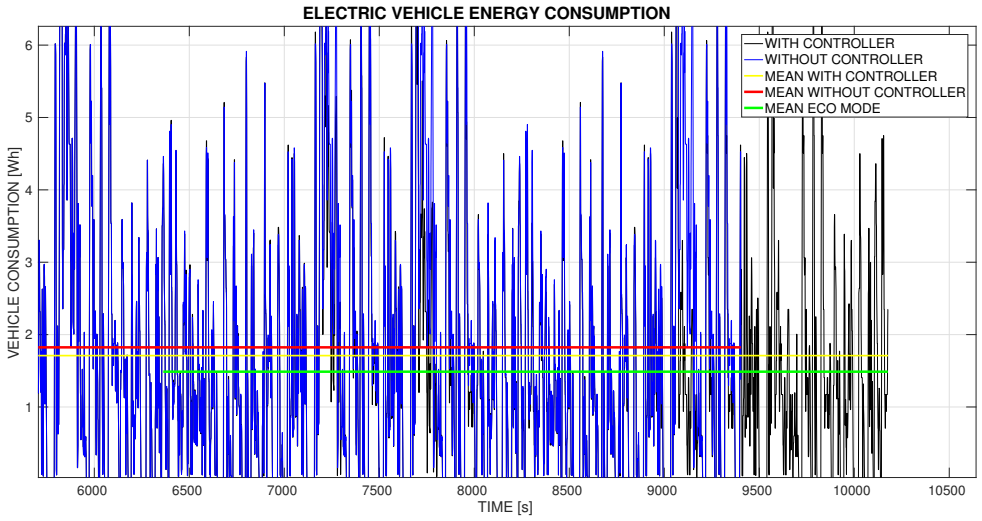

(b)

Figure 12 – The EV consumption in FTP-75 driving cycle. a) Original picture of the energy consumption; b) Zoomed picture of the energy consumption. Source: The Author

Table 6 – Mean values of EV energy consumption in FTP-75 driving cycle

Parameter	**Results for the electric vehicle GM EV1**	**Improvements (%)**
Energy consumption without controller	1.8240 Wh	—
Energy consumption with controller	1.7098 Wh	6.67
Energy consumption in Safe power mode	1.4876 Wh	18.40

Source: The Author

In the next plot, Figure 13, the EV electric motor power losses are described in Equation 3.16. With those losses, the heat loss occurred in the battery $P_{Battery_{Loss}} = I^2 R_{in}$ is added to the analysis. In Table 7, the mean values obtained in the simulation are detailed. A overall improvement of 8.11 % occurred with SPMS application.

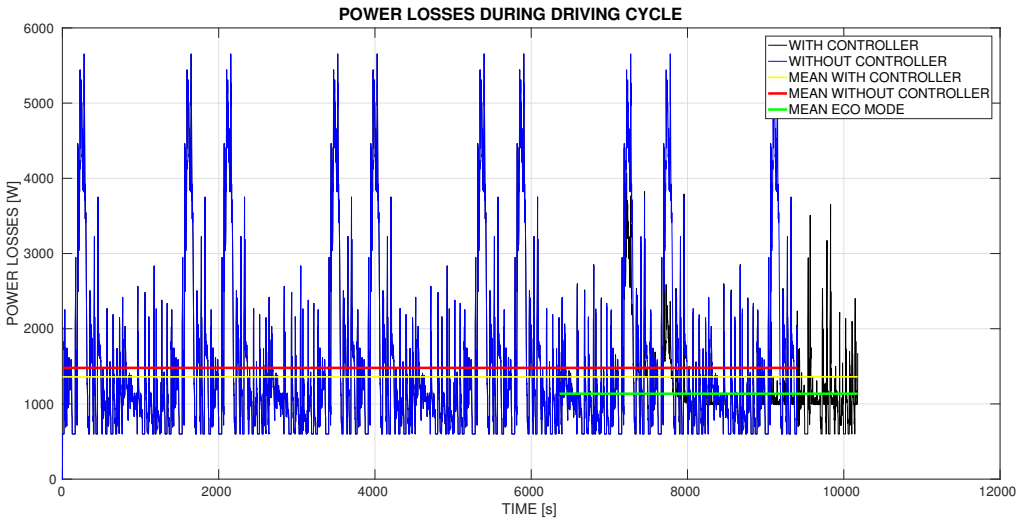

(a)

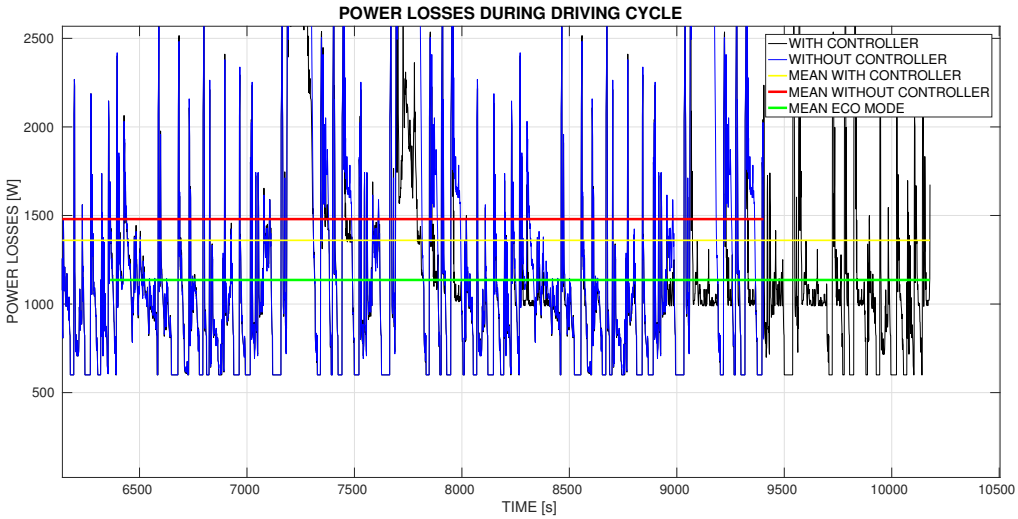

(b)

Figure 13 – The EV powertrain power losses in FTP-75 driving cycle. a) Original picture of the power losses; b) Zoomed picture of the power losses. Source: The Author

Table 7 – Mean values of EV powertrain power losses during the driving cycle

Parameter	**Results for the electric vehicle GM EV1**	**Improvements (%)**
Power losses without controller	1479 W	—
Power losses with controller	1359 W	8.11
Power losses in Safe power mode	1135 W	23.25

Source: The Author

In the next plot, Figure 14, the EV battery electric current linked to the cycle is demonstrated. In Table 8, the mean values obtained in the simulation are detailed. A overall improvement of 6.18 % occurred with SPMS application

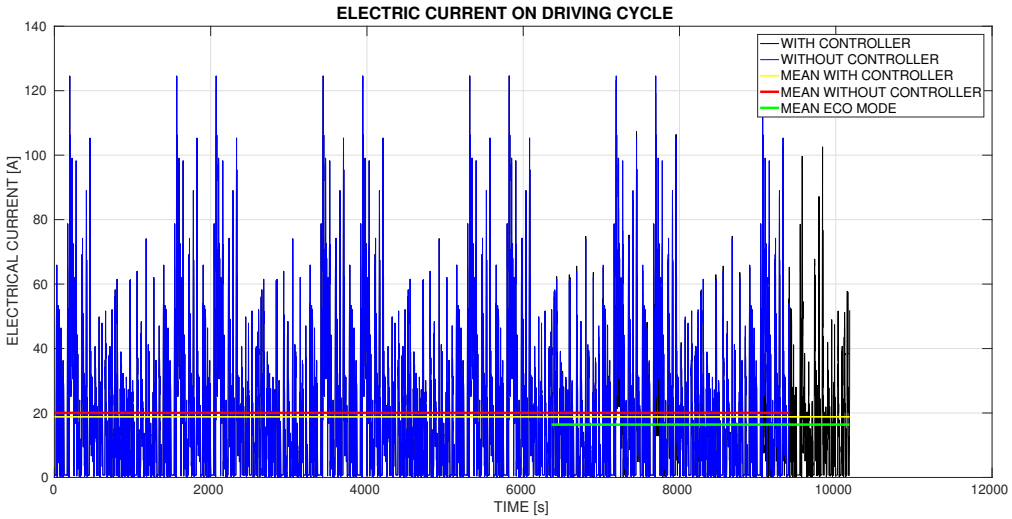

(a)

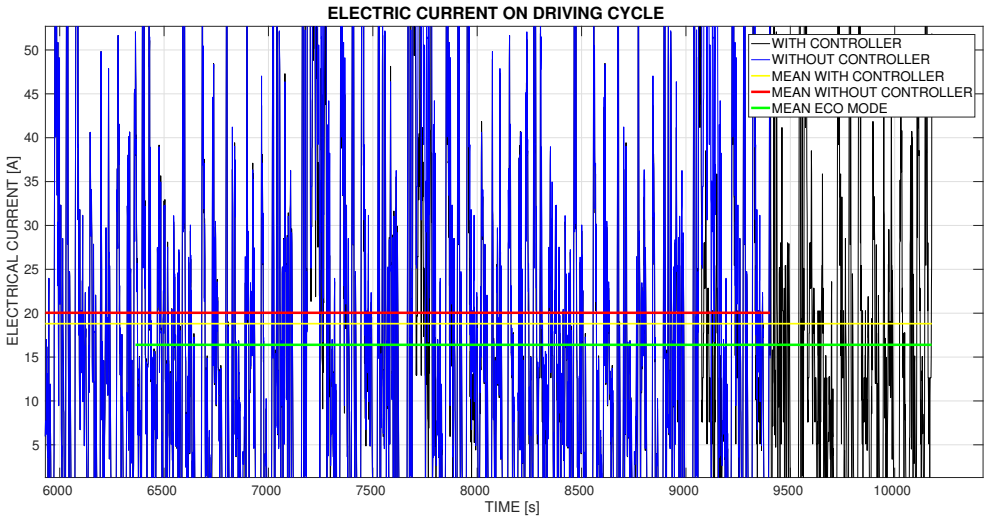

(b)

Figure 14 – The EV battery electric current in FTP-75 driving cycle. a) Original picture of the battery electric current; b) Zoomed picture of the battery electric current. Source: The Author

Table 8 – Mean values of EV battery electric current during the FTP-75 driving cycle

Parameter	**Results for the electric vehicle GM EV1**	**Improvements (%)**
Battery electric current without controller	20.04 A	—
Battery electric current with controller	18.80 A	6.18
Battery electric current in Safe power mode	16.39 A	18.21

Source: The Author

In the Figure 15, deep of discharge versus time is illustrated. The regenerative breaking action could be seen with the peaks as occurred in $4000\,s$. The larger vehicle autonomy is visible when the cycle with controller has a longer time interval to drain the whole battery.

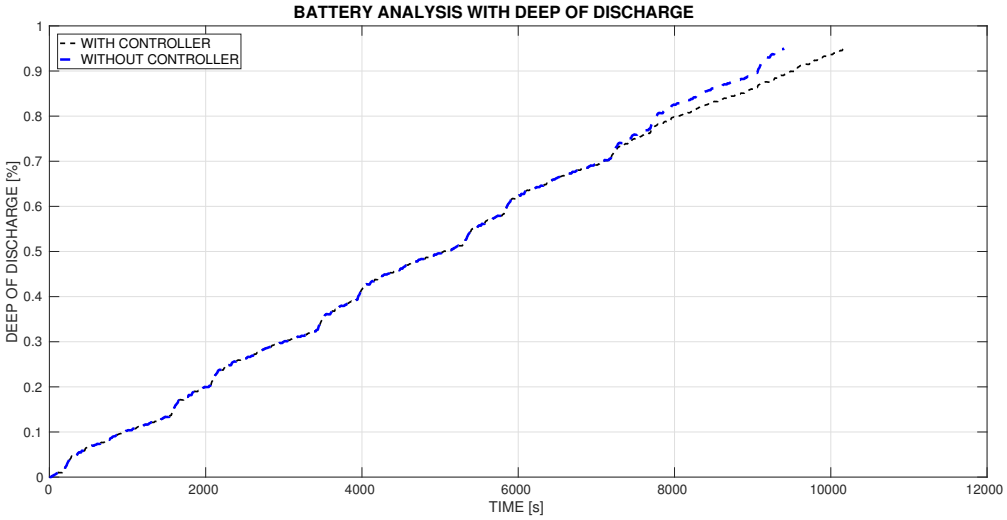

Figure 15 – The EV battery DoD in FTP-75 driving cycle. Source: The Author

The Figure 16, shows the relation of deep of discharge and the distance travelled by the vehicle. In the controlled cycle as might be seen, two extra kilometers are added to the trip.

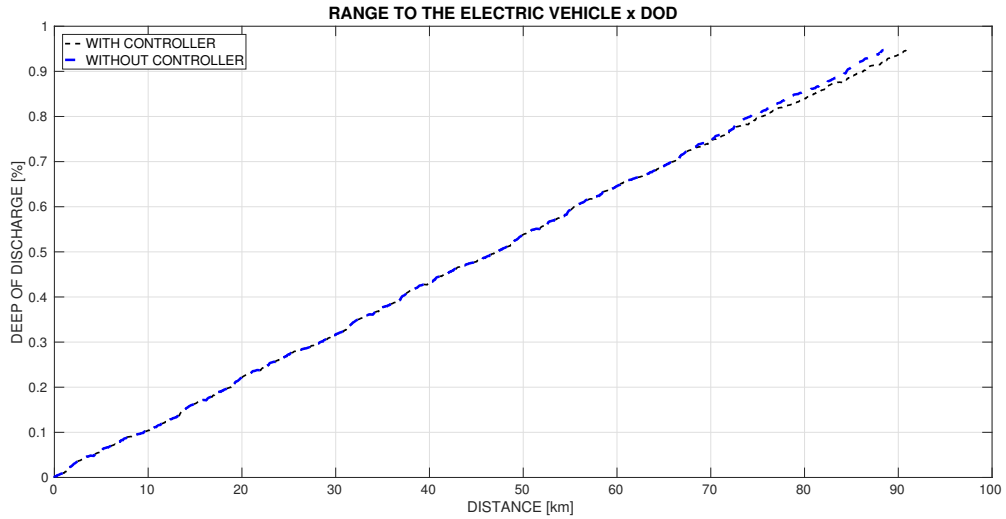

(a)

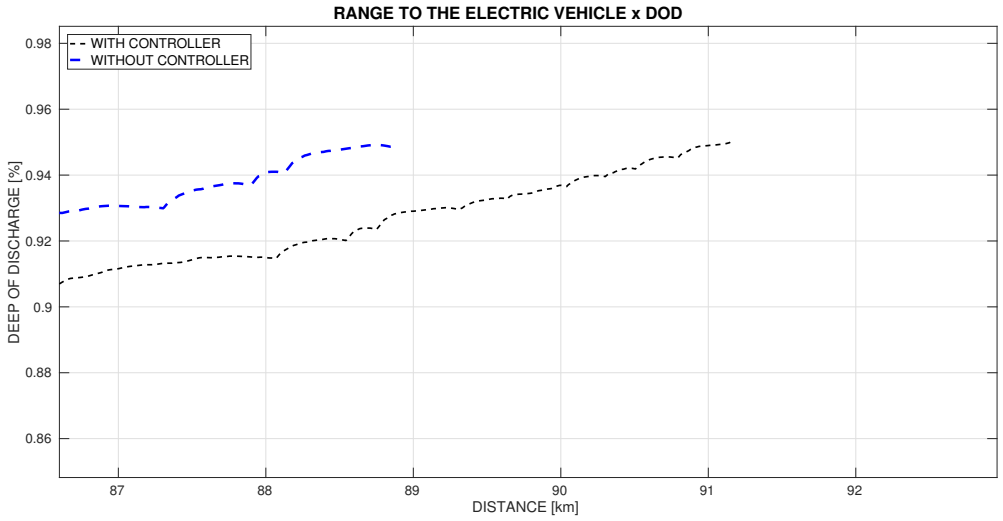

(b)

Figure 16 – The EV battery Dod x Distance travelled in FTP-75 driving cycle. a) Original picture of DoD x Distance travelled; b) Zoomed picture of DoD x Distance travelled. Source: The Author

4.1.2 Real driving cycle (Arroio do Silva/Araranguá)

In Capo (2016), a driving cycle from Arroio do Silva (SC) to UFSC-Araranguá (SC) was made. The author used a camera to record the digital odometer of his car during the trip between these two locations. At the end of the driving cycle, a video edition software was used, to create a time domain cycle. Some parameters of the driving cycle are listed in sequence:

Distance travelled: 9.4 km; Duration: 647 s; Maximum speed: 84 km/h; Mean speed: 52.3 km/h. To simulate the vehicle using the chemical battery until gets flat, the cycle is repeated. This situation is similar to many trips among this two locations without battery recharging. The Figure 17 shows the driving cycle created and the vehicle velocity behaviour with the controller acting in the vehicle performance.

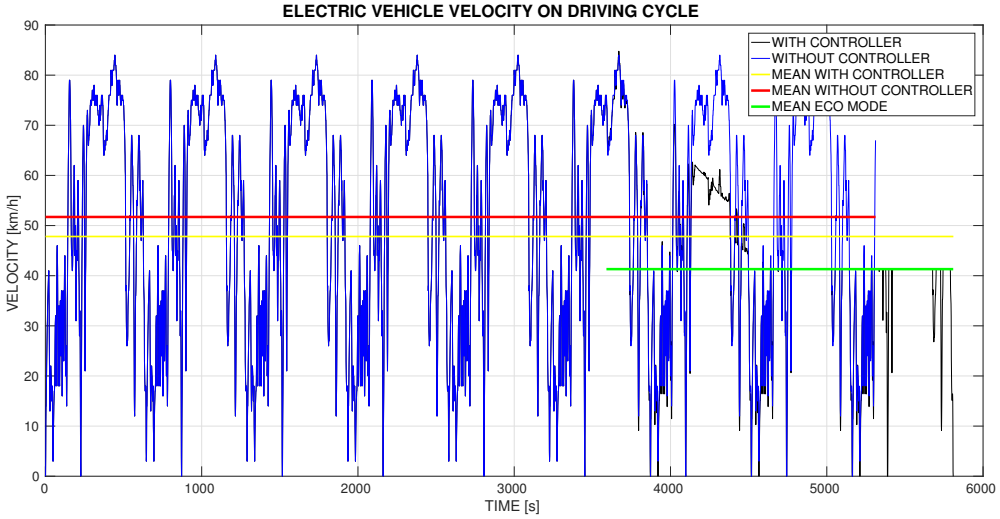

Figure 17 – The EV velocity in Arroio do Silva/Araranguá driving cycle. Source: The Author

As visible in Figure 17, higher velocities than FTP-75 driving cycle are occurred. As result of a mix between urban and light state highway driving (slower speed limit, V = 80km/h compared with V = 110 km/h of a federal highway) higher analyzed parameter values will be generated from the simulation as follows the next Figures and Tables. Therefore, the Figure 18 is illustrated the EV consumption values, obtained in the simulation. To express the mean values on plot, the Table 9 shows the parameters. A overall improvement of 8.48 % occurs with the usage of the SPMS.

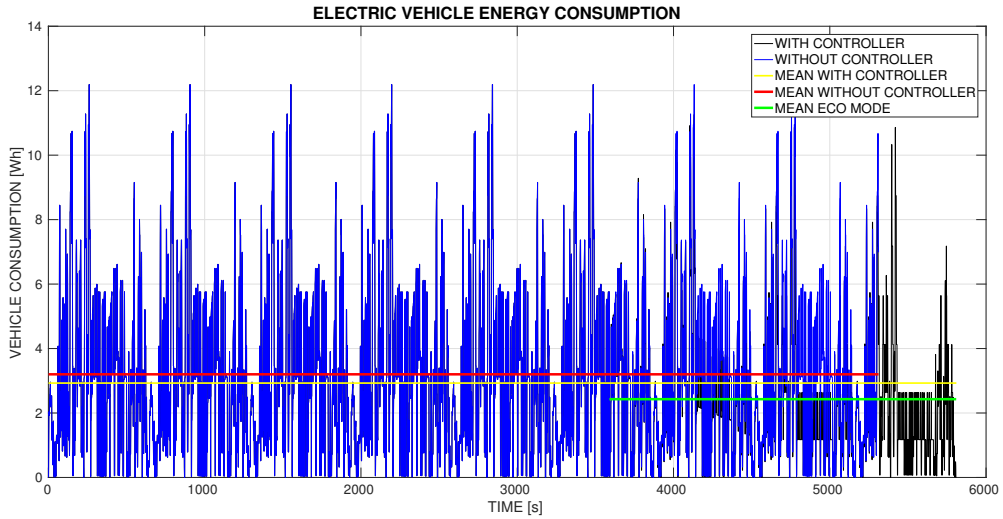

(a)

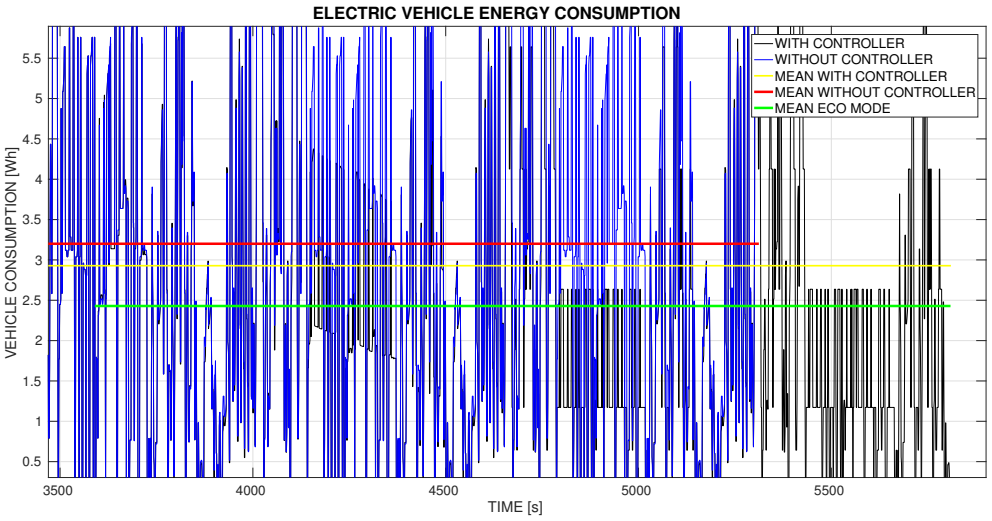

(b)

Figure 18 – The EV consumption in Arroio do Silva/Araranguá driving cycle. a) Original picture of the energy consumption; b) Zoomed picture of the energy consumption. Source: The Author

Table 9 – Mean values of EV energy consumption in Arroio do Silva/Araranguá driving cycle

Parameter	**Results for the electric vehicle GM EV1**	**Improvements (%)**
Energy consumption without controller	3.2004 Wh	—
Energy consumption with controller	2.9284 Wh	8.48
Energy consumption in Safe power mode	2.4290 Wh	24.10

Source: The Author

The Figure 19 illustrates the power losses occurred in the EV powertrain. The heat loss occurred in the battery, $P_{Battery_{Loss}} = I^2 R_{in}$, is included for the computation of the analyzed parameters. In the Table 10 the mean values obtained in the simulation are shown. A overall improvement of 12.24 % occurred with SPMS application.

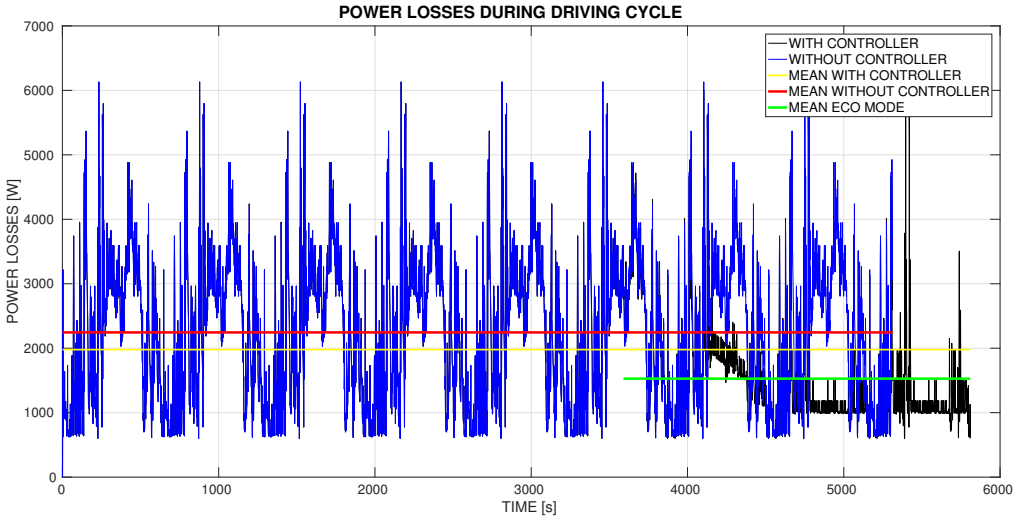

(a)

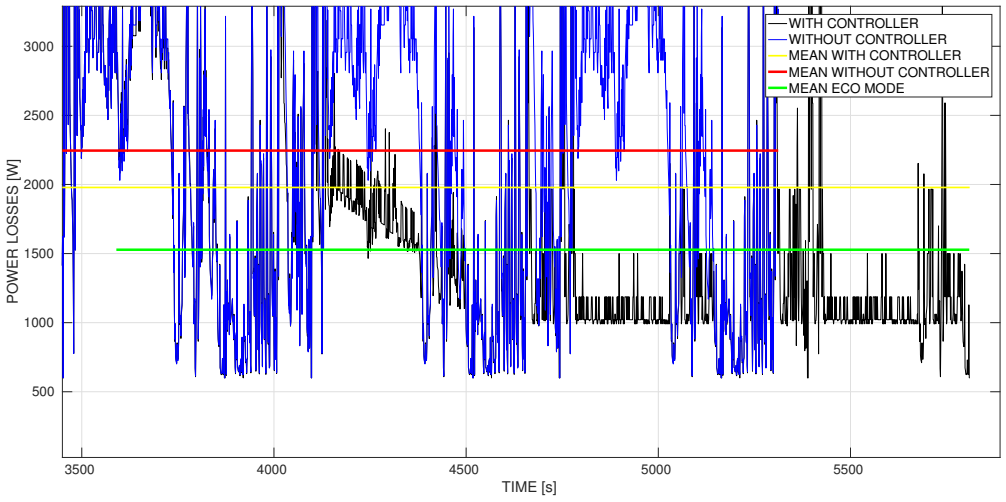

(b)

Figure 19 – The EV power losses in Arroio do Silva/Araranguá driving cycle. a) Original picture of the power losses; b) Zoomed picture of the power losses. Source: The Author

Table 10 – Mean values of EV powertrain power losses during the Arroio do Silva/Araranguá driving cycle

Parameter	**Results for the electric vehicle GM EV1**	**Improvements (%)**
Power losses without controller	2254 W	—
Power losses with controller	1978 W	12.24
Power losses in Safe power mode	1527 W	32.25

Source: The Author

In the next plot, Figure 20, the EV battery electric current used in the cycle is demonstrated. In Table 11 the mean values obtained, are detailed. A overall improvement of 8.58 % occurred with the SPMS application.

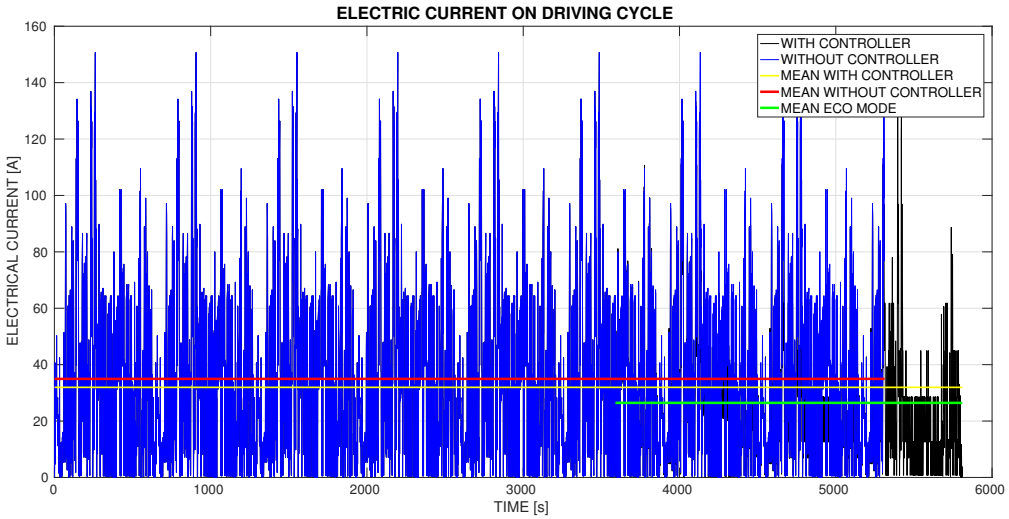

(a)

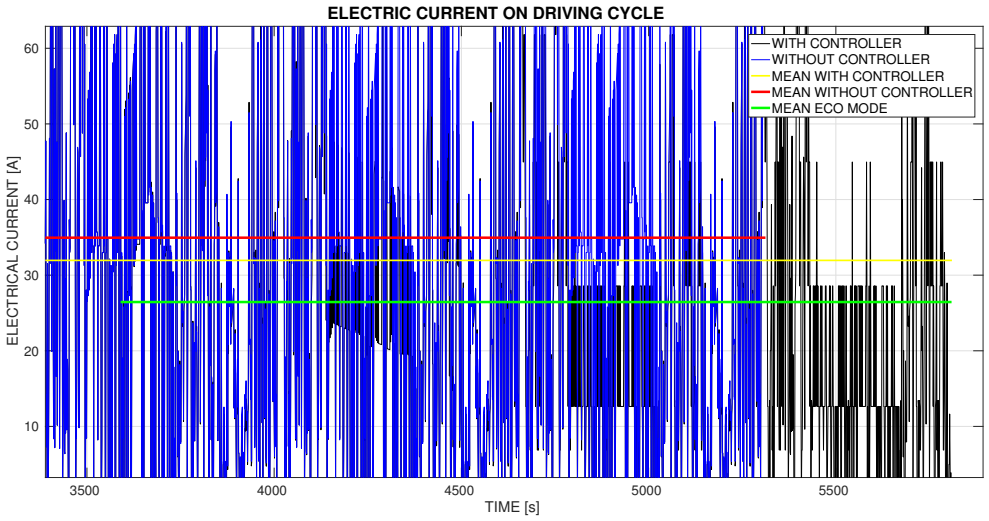

(b)

Figure 20 – The EV battery electric current in Arroio do Silva/Araranguá driving cycle. a) Original picture of the battery electric current; b) Zoomed picture of the battery electric current. Source: The Author

Table 11 – Mean values of EV battery electric current during the Arroio do Silva/Araranguá driving cycle

Parameter	Results for the electric vehicle GM EV1	Improvements (%)
Battery electric current without controller	34.95 A	—
Battery electric current with controller	31.95 A	8.58
Battery electric current in Safe power mode	26.44 A	24.34

Source: The Author

In the Figure 21 the deep of discharge versus time is illustrated. The regenerative breaking action could be seen in the figure with the peaks as occurred between 1700 and $2500\ s$. The larger vehicle autonomy is visible when the EV with controller has a longer time interval to empty the battery.

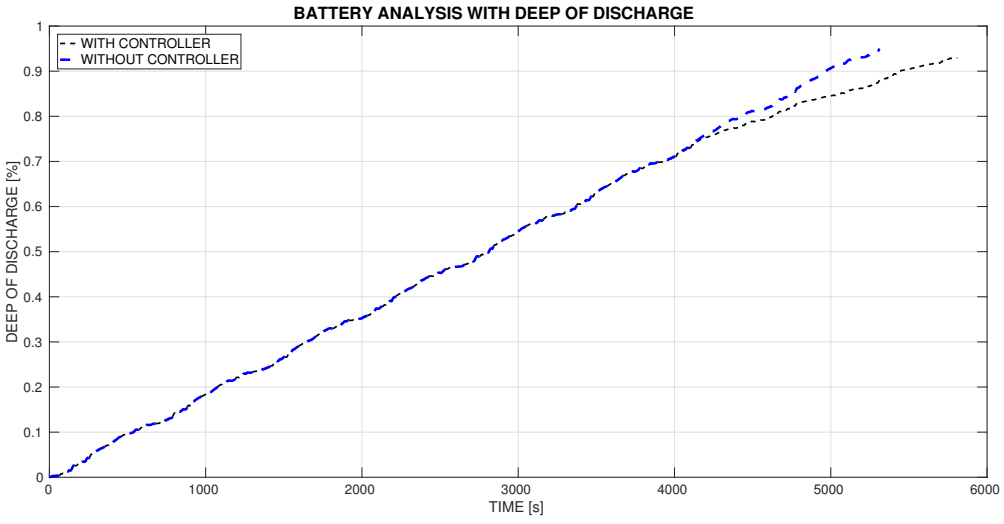

Figure 21 – The EV battery DoD in (Arroio do Silva - Araranguá) driving cycle. Source: The Author

The Figure 22, shows the relation of deep of discharge and the distance travelled by the vehicle. In the controlled cycle, one extra kilometer is added to the trip. This longer range provided by the controller is due to the speed reduction affecting directly the consumption.

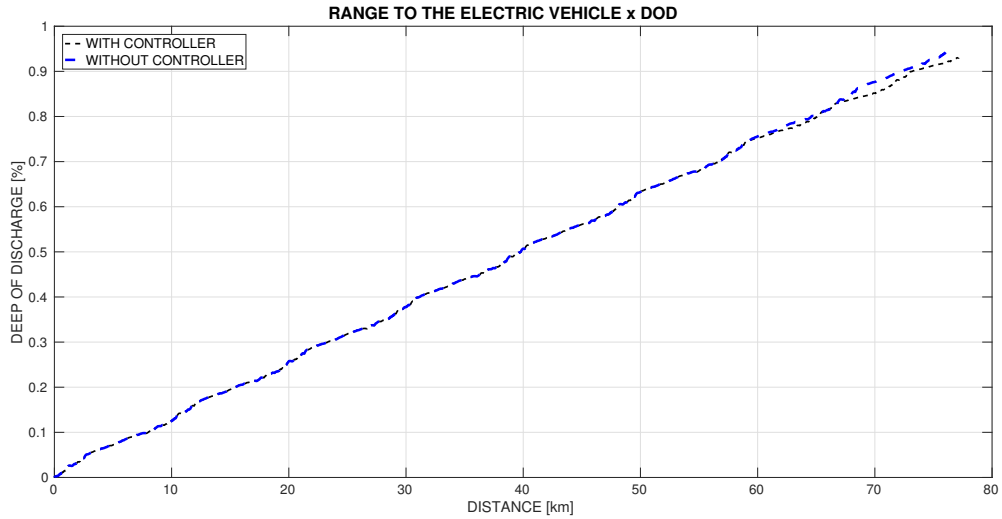

(a)

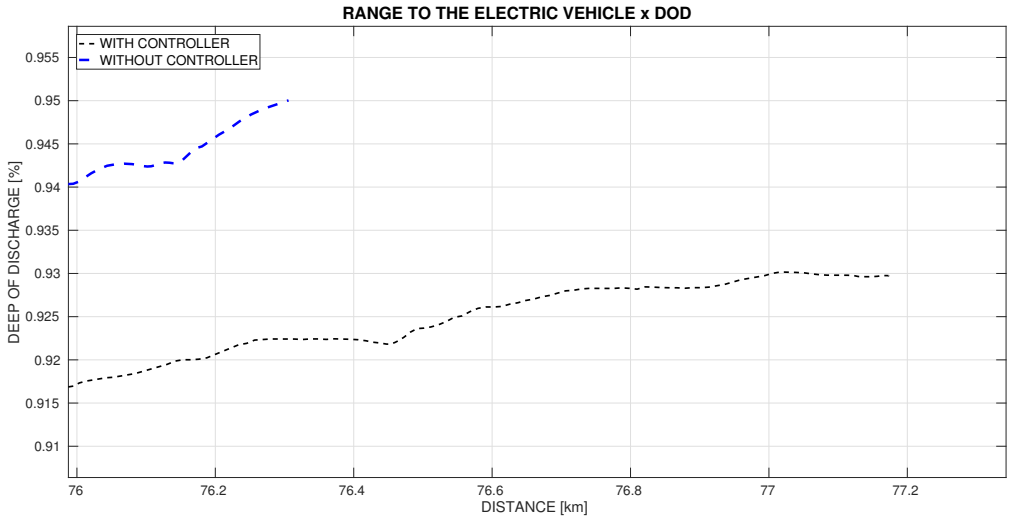

(b)

Figure 22 – The EV battery DoD x Distance travelled in Arroio do Silva/Araranguá driving cycle. a) Original picture of DoD x Distance travelled; b) Zoomed picture of DoD x Distance travelled. Source: The Author

4.2 Highway driving scenario

In this subsection two highway driving scenarios are tested to verify the impact of the SPMS in the EV. The tests proposal, is a comparison of a real situation and a theoretic one.

4.2.1 EPA driving cycle (HWFET)

In the highway artificial scenario used as simulations input, the Highway Fuel Economy Driving Schedule (HWFET) is adopted. It uses a warmed-up engine and makes no stops, averaging 77 km/h with a top speed of 97 km/h over a 16.45 km distance (MIERS et al., 2008). It has a duration of 765 seconds. The driving cycle speed and the controlled one, are illustrated in Figure 23. This input is repeated until DoD reaches 95% in the simulation. The Figure 24 shows the consumption values reached in the simulation. To express the mean values, the Table 12 display the quantities. A overall improvement of 28.25 % occurs with the SPMS application.

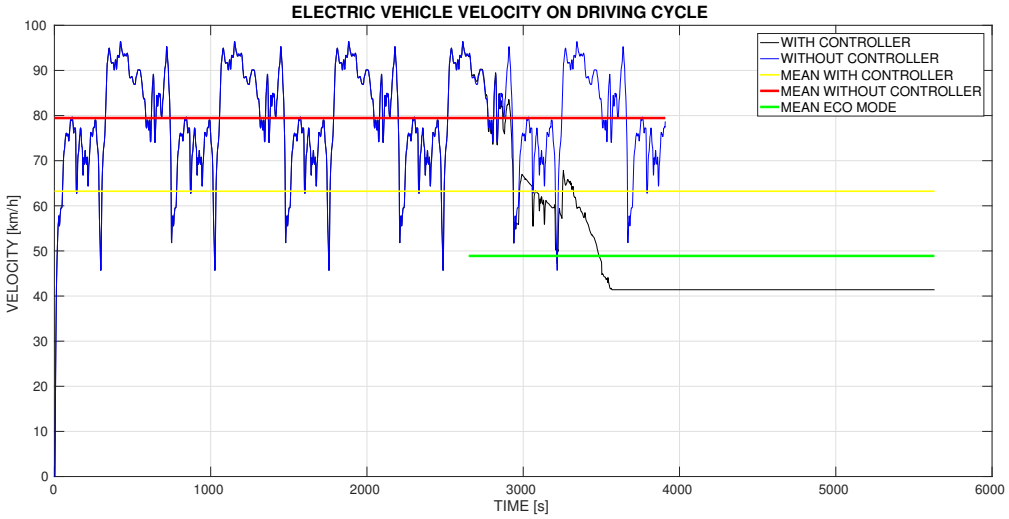

Figure 23 – The EV velocity in HWFET driving cycle. Source: The Author

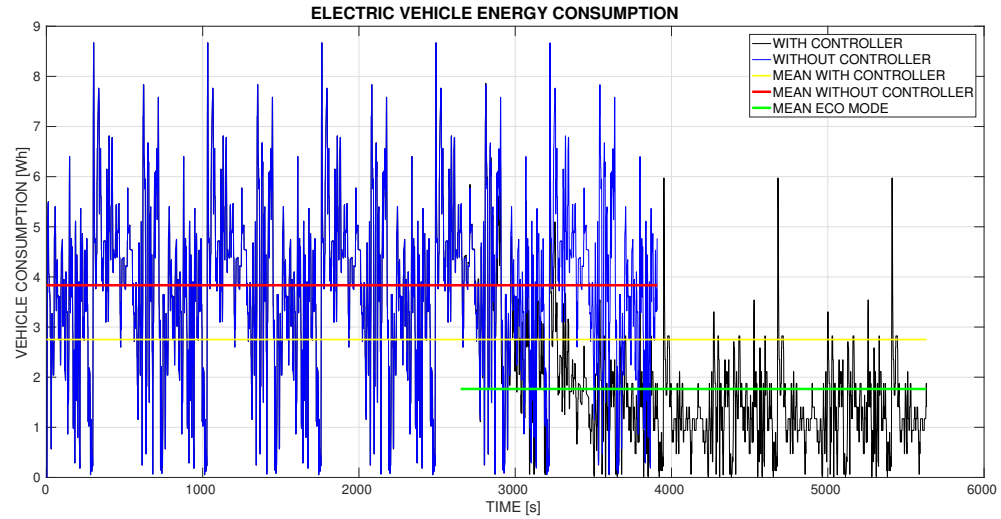

(a)

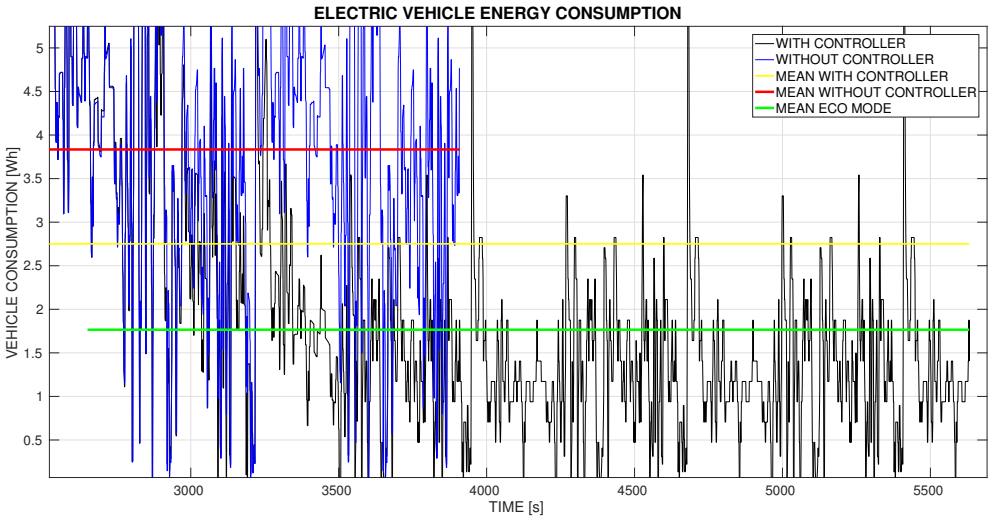

(b)

Figure 24 – The EV consumption in HWFET driving cycle. a) Original picture of the energy consumption; b) Zoomed picture of the energy consumption. Source: The Author

Table 12 – Mean values of EV energy consumption in HWFET driving cycle

Parameter	**Results for the electric vehicle GM EV1**	**Improvements (%)**
Energy consumption without controller	3.8343 Wh	—
Energy consumption with controller	2.7511 Wh	28.25
Energy consumption in Safe power mode	1.7654 Wh	53.96

Source: The Author

The Figure 25, illustrates the power losses generated in the EV powertrain. The heat loss occurred in the battery $P_{Battery_{Loss}} = I^2 R_{in}$ is included for the computation of the parameter. In the Table 13 the mean values obtained in the simulation are shown. A overall improvement of 31.67 % occurred with SPMS application.

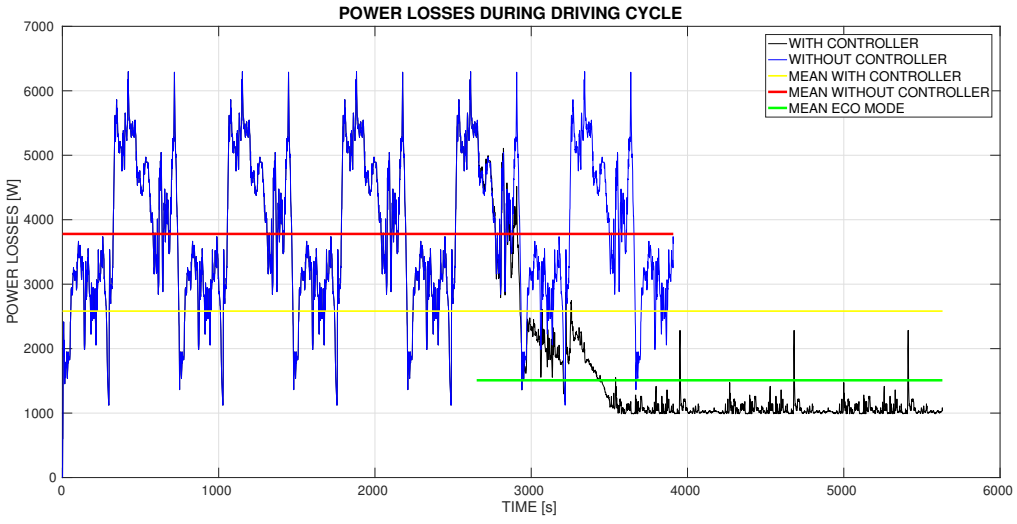

(a)

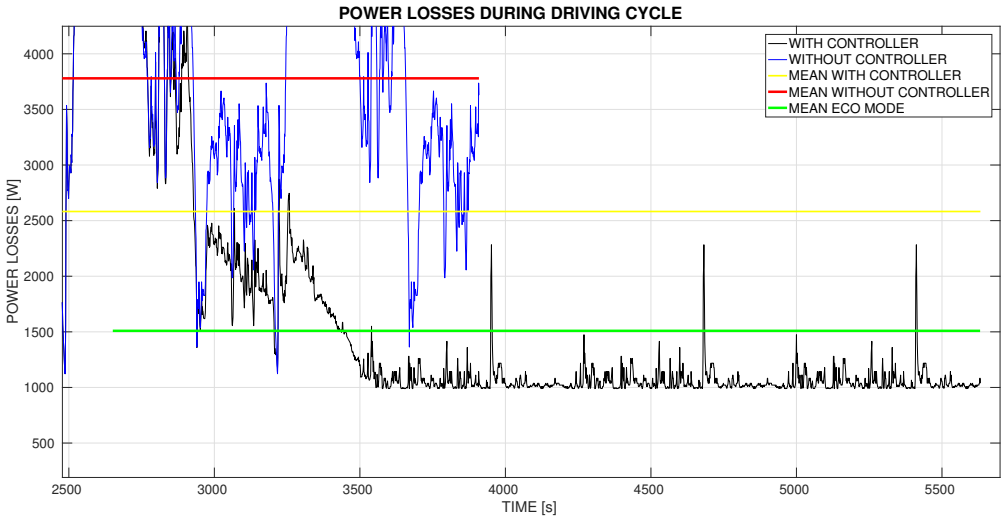

(b)

Figure 25 – The EV power losses in HWFET driving cycle. a) Original picture of the power losses; b) Zoomed picture of the power losses. Source: The Author

Table 13 – Mean values of EV powertrain power losses during the HWFET driving cycle

Parameter	**Results for the electric vehicle GM EV1**	**Improvements (%)**
Power losses without controller	3779 W	—
Power losses with controller	2582 W	31.67
Power losses in Safe power mode	1509 W	60.06

Source: The Author

The next plot, Figure 26, the EV battery electric current consumed in the cycle is demonstrated. In Table 14, the mean values obtained from the simulation are detailed. A overall improvement of 28.42 % occurred with the SPMS application.

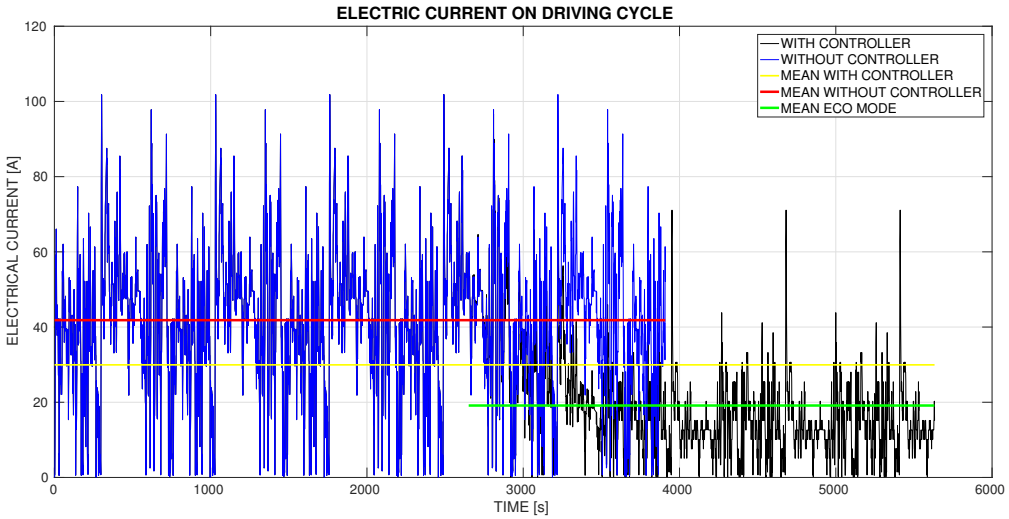

(a)

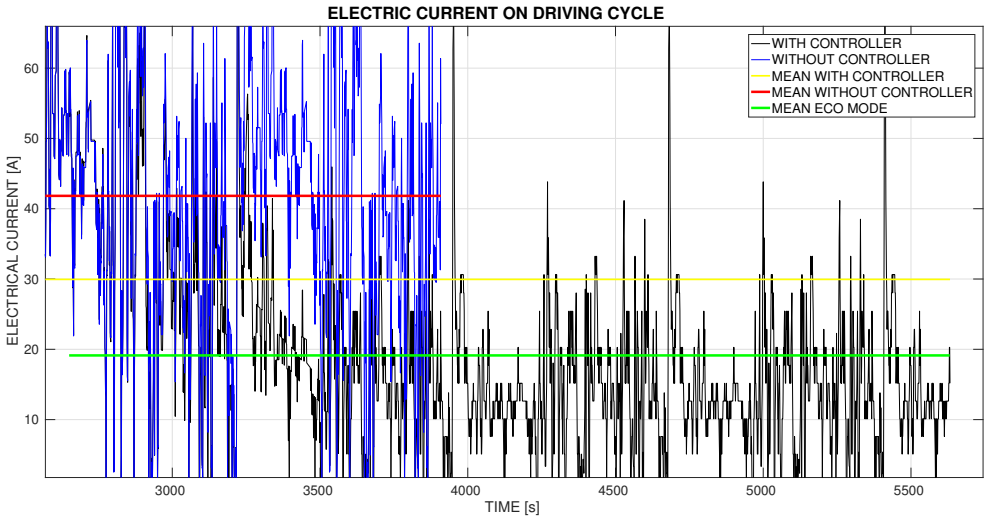

(b)

Figure 26 – The EV battery electric current in HWFET driving cycle. a) Original picture of the battery electric current; b) Zoomed picture of the battery electric current. Source: The Author

Table 14 – Mean values of EV battery electric current during the HWFET driving cycle

Parameter	**Results for the electric vehicle GM EV1**	**Improvements (%)**
Battery electric current without controller	41.83 A	—
Battery electric current with controller	29.94 A	28.42
Battery electric current in Safe power mode	19.13 A	54.26

Source: The Author

In the Figure 27, the deep of discharge versus time is illustrated. Could be seen the regenerative breaking action in the figure with the peaks as occurred between $1700 - 2500s$. As in highways, the active braking are rarely occurred compared to passive braking, the vehicle slows down just from inertia force in those cases. For that reason, these peaks are smaller and wider than in the city driving cycle. The larger vehicle autonomy is visible when the EV with controller has a longer time interval to drain the battery.

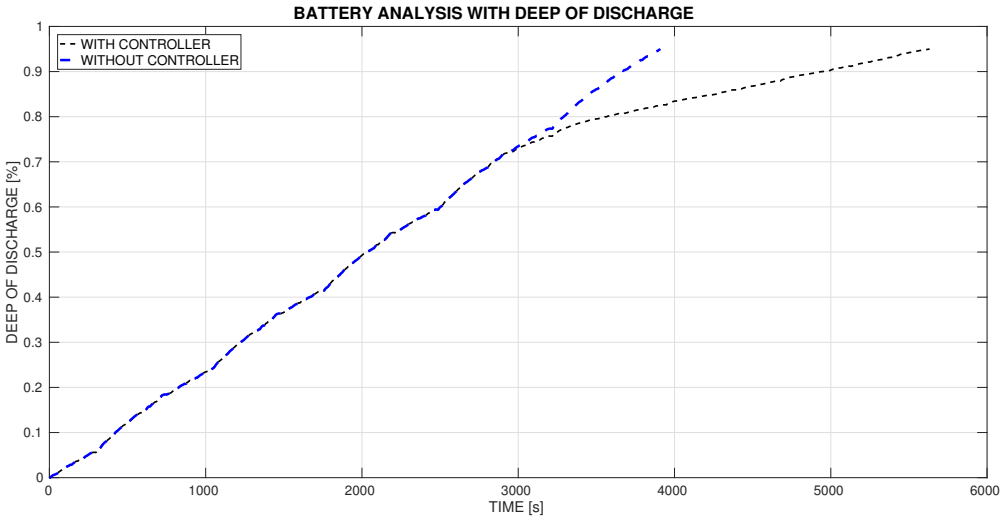

Figure 27 – The EV battery DoD in HWFET driving cycle. Source: The Author

The Figure 28, shows the relation of deep of discharge and the distance travelled by the vehicle. In the controlled cycle, thirteen extra kilometers are added to the trip. This longer

range provided by the controller is due to the speed reduction, affecting directly in the EV consumption.

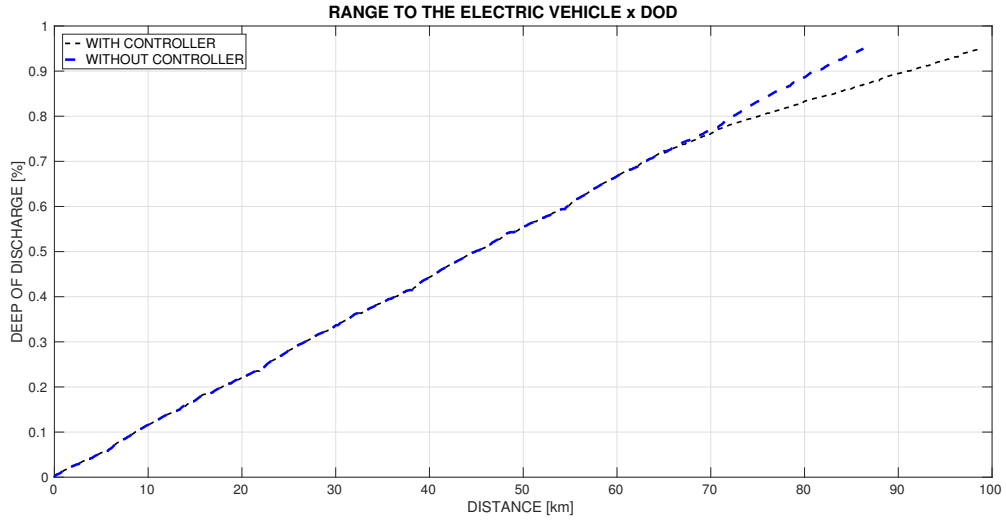

(a)

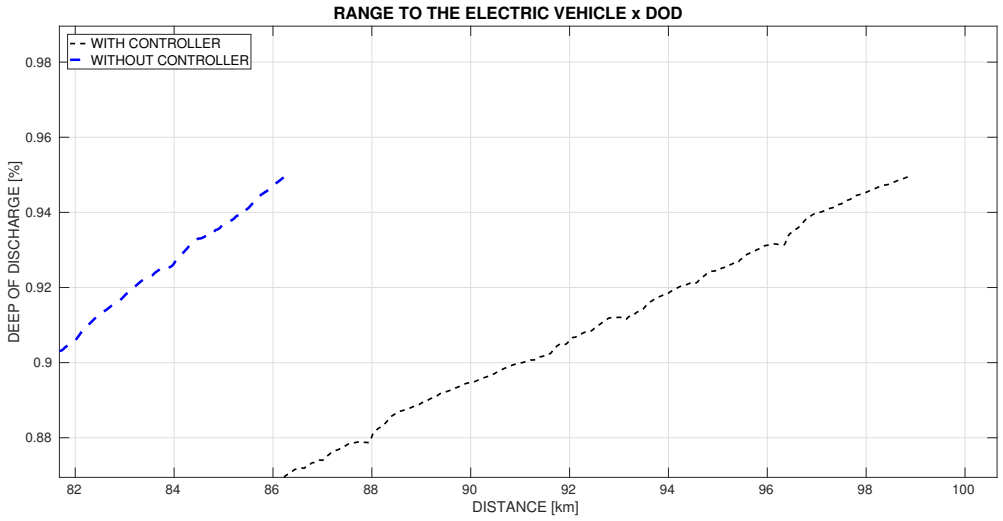

(b)

Figure 28 – The EV battery DoD x Distance travelled in HWFET driving cycle. a) Original picture of DoD x Distance travelled; b) Zoomed picture of DoD x Distance travelled. Source: The Author

4.2.2 Real driving cycle (Araranguá - Porto Alegre)

Using an Android software called *Speed Logger* obtained in the Google Play Store, a driving cycle from Araranguá (SC) and Porto Alegre (RS) was developed. It is used a free

version of the software. With the ability of the mobile phone GPS, the software gets 50 acceleration and velocity readings per second, generating a graphic representation of the driving cycle. One of the main features of this application is the possibility to export the data to a spreadsheet *.csv* format. This action turns easier data exchanging between devices. The Figure 29 shows the application interface and its features.

Figure 29 – The application Speed Logger interface. Source: The Author

This scenario aims to emulate a real trip between these two cities, using the data recorded as input for the simulation used. Firstly, the EV velocity obtained from the app and the velocity from the FLC are shown in Figure 30, whereas the controller acting in the EV performance is visible with the black line and yellow one for the mean value. This driving cycle was produced respecting the speed limits imposed for the federal highway. Represents a non stop trip between this two cities.

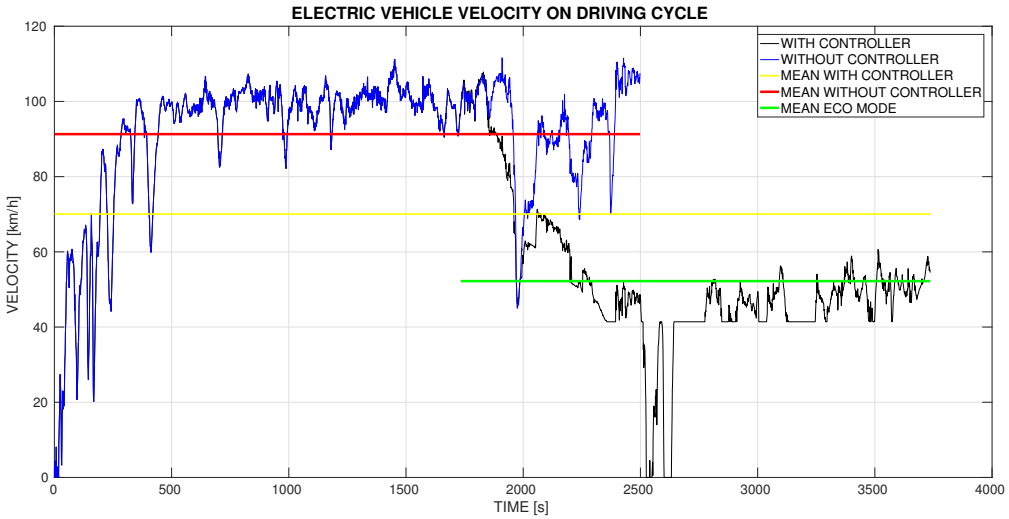

Figure 30 – The EV velocity in Araranguá/Porto Alegre driving cycle. Source: The Author

In Figure 31, the EV energy consumption in the driving cycle with and without controller are illustrated. A longer driving range with the controller is evident in the graphic. In Table 15 are shown the mean EV energy consumption values during this cycle.

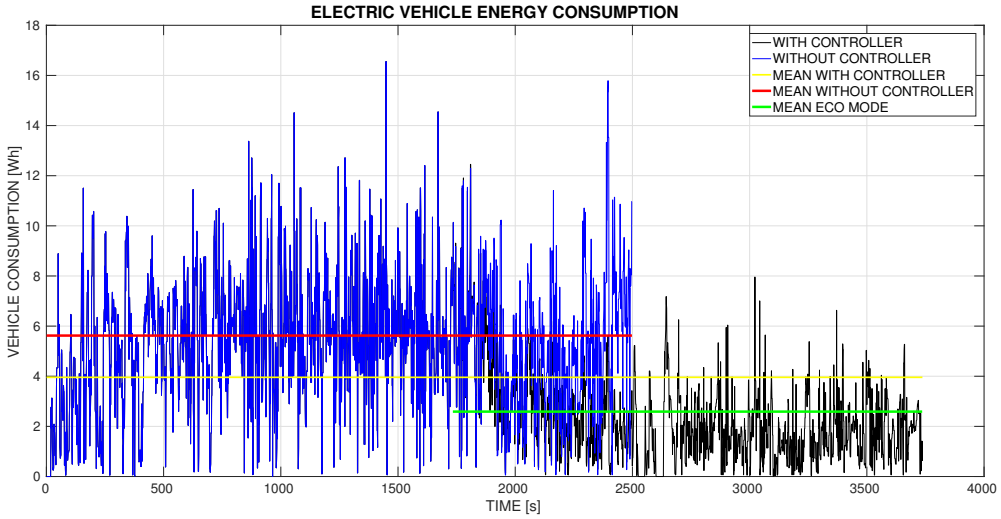

(a)

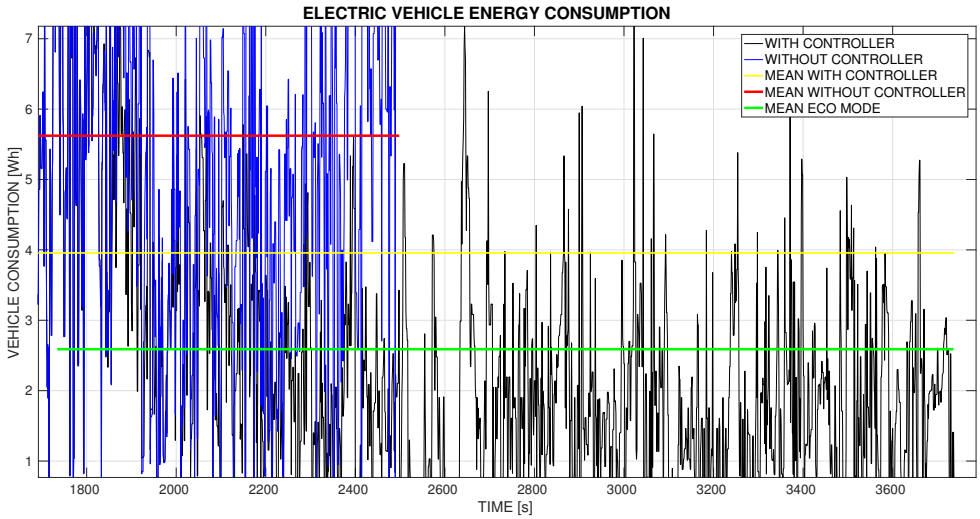

(b)

Figure 31 – The EV consumption in Araranguá/Porto Alegre driving cycle. a) Original picture of the energy consumption; b) Zoomed picture of the energy consumption. Source: The Author

Table 15 – Mean values of EV energy consumption in Araranguá/Porto Alegre driving cycle

Parameter	**Results for the electric vehicle GM EV1**	**Improvements (%)**
Energy consumption without controller	5.6224 Wh	—
Energy consumption with controller	3.9567 Wh	29.62
Energy consumption in Safe power mode	2.5892 Wh	53.94

Source: The Author

The power losses are presented in the Figure 32. In all graphics of this driving cycle, lower values are occurred on account of the SPMS. In the Table 16, the mean values of the EV powertrain losses are presented. There are higher results compared with HWFET case, due to higher velocities shown in Figure 30. A overall improvement of 35.87 % occurred with SPMS application.

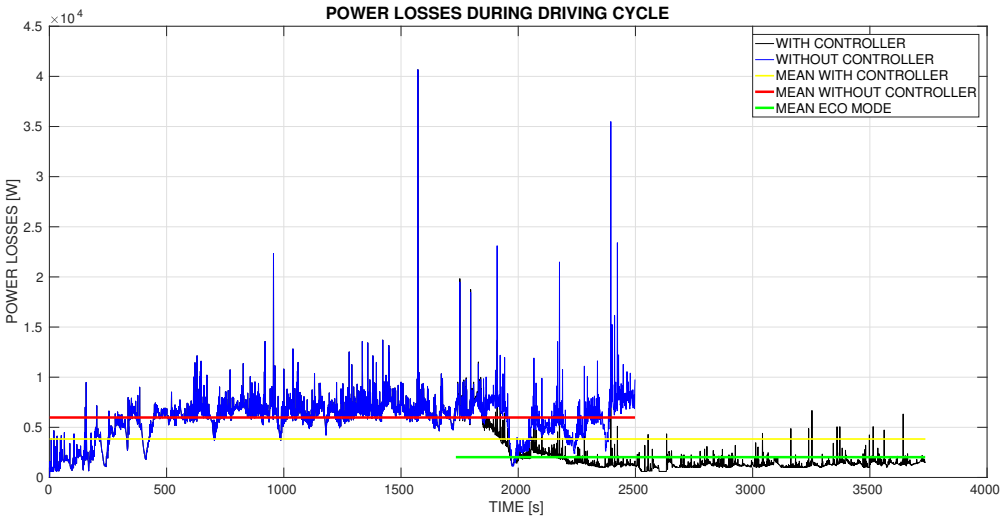

(a)

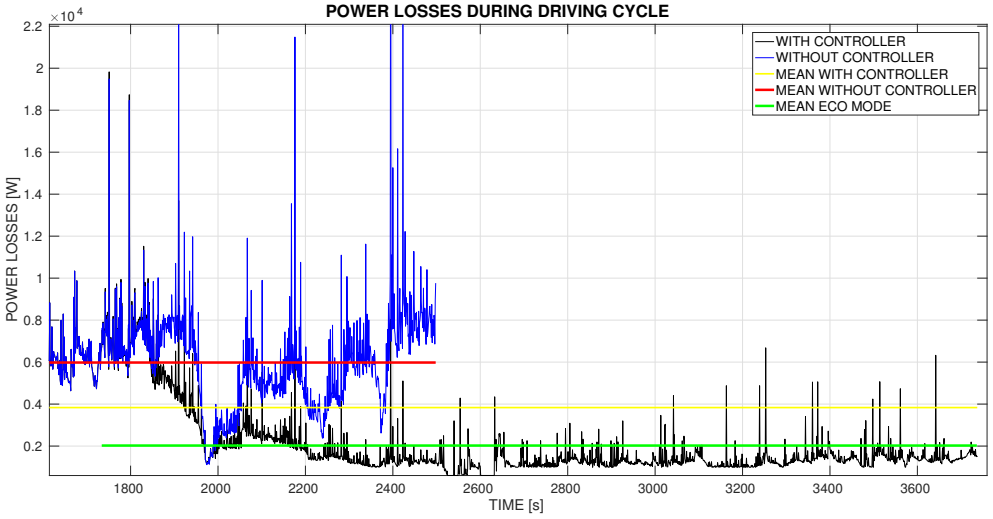

(b)

Figure 32 – The EV power losses in (Araranguá - Porto Alegre) driving cycle. a) Original picture of the power losses; b) Zoomed picture of the power losses. Source: The Author

Table 16 – Mean values of EV powertrain power losses during the Araranguá/driving cycle

Parameter	**Results for the electric vehicle GM EV1**	**Improvements (%)**
Power losses without controller	5979 W	—
Power losses with controller	3834 W	35.87
Power losses in Safe power mode	2024 W	66.14

Source: The Author

The next graphic, Figure 33, the battery electric current is illustrated with its results for each case proposed. The Table 17 presents the mean values. A overall improvement of 30 % occurred with the SPMS application.

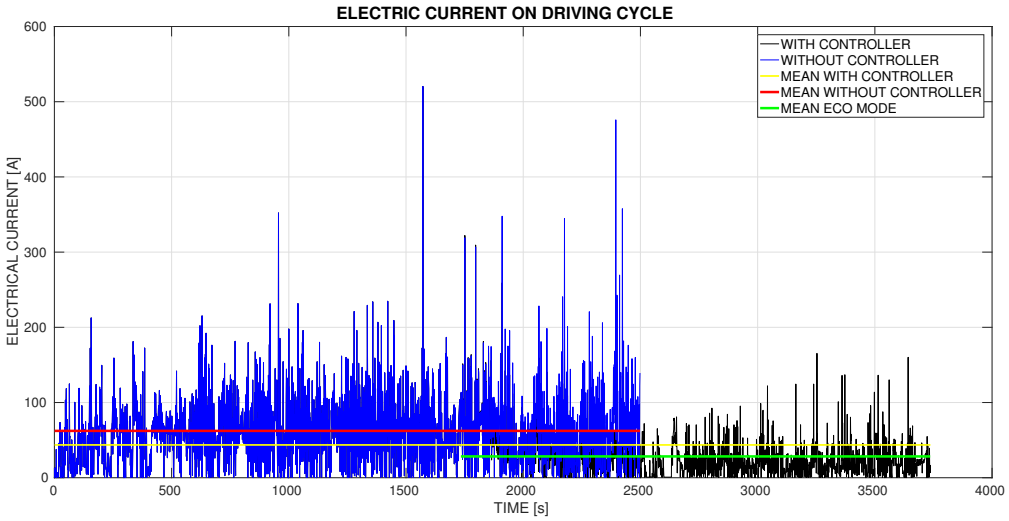

(a)

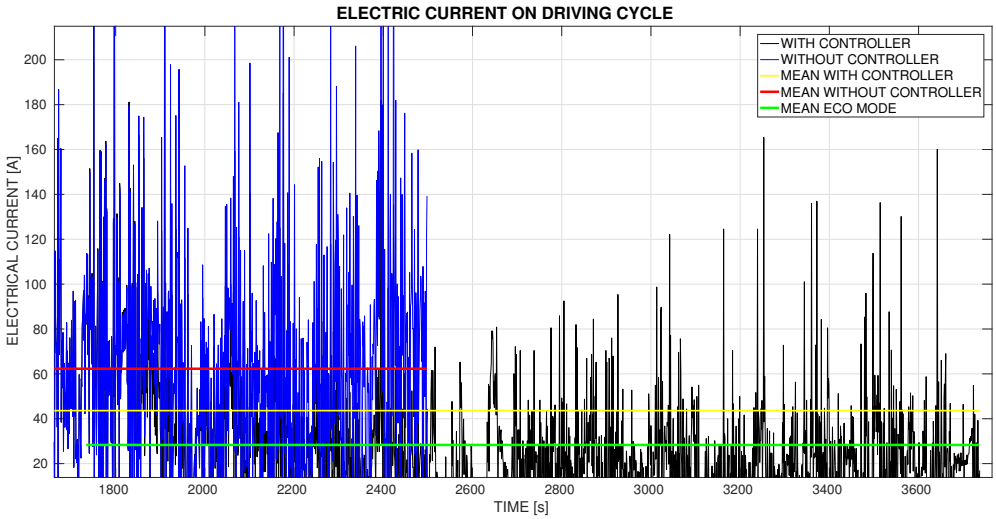

(b)

Figure 33 – The EV battery current in Araranguá/Porto Alegre driving cycle. a) Original picture of the battery electric current; b) Zoomed picture of the battery electric current. Source: The Author

Table 17 – Mean values of EV battery electric current during the Araranguá/Porto Alegre driving cycle

Parameter	**Results for the electric vehicle GM EV1**	**Improvements (%)**
Battery electric current without controller	62.28 A	—
Battery electric current with controller	43.60 A	30
Battery electric current in Safe power mode	28.33 A	54.51

Source: The Author

The Figure 34, illustrates the deep of discharge behaviour during the cycle. As this trip occurs in a highway with rarely braking periods, the regenerative breaking is few activated. A longer driving range is seen in the graphic representation.

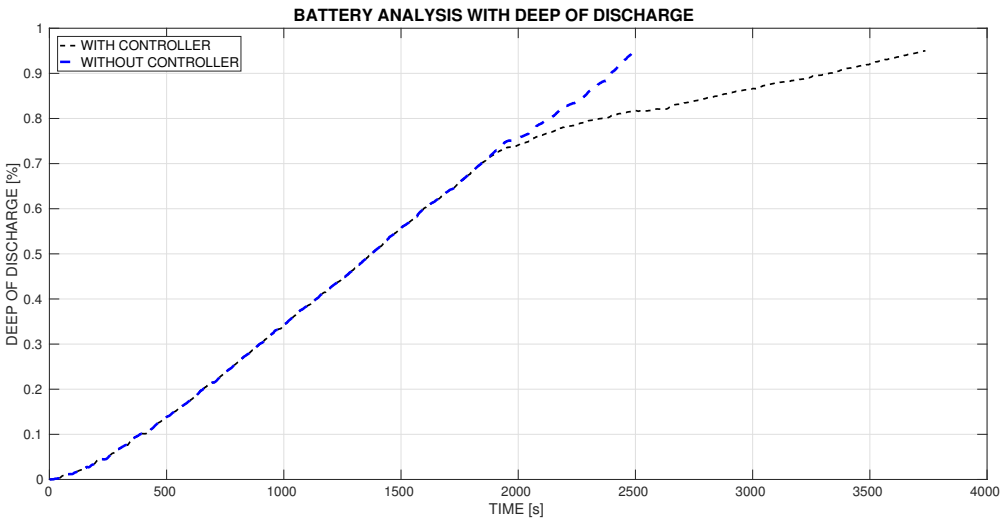

Figure 34 – The EV battery DoD in Araranguá/Porto Alegre driving cycle. Source: The Author

With the representation of the DoD versus distance travelled by the vehicle, in the Figure 35, the relationship between these two parameters could be analyzed. The main result, obtained from the graph, is the longer distance travelled by the vehicle. An extra ten kilometers are added to the trip caused by the utilization of the SPMS.

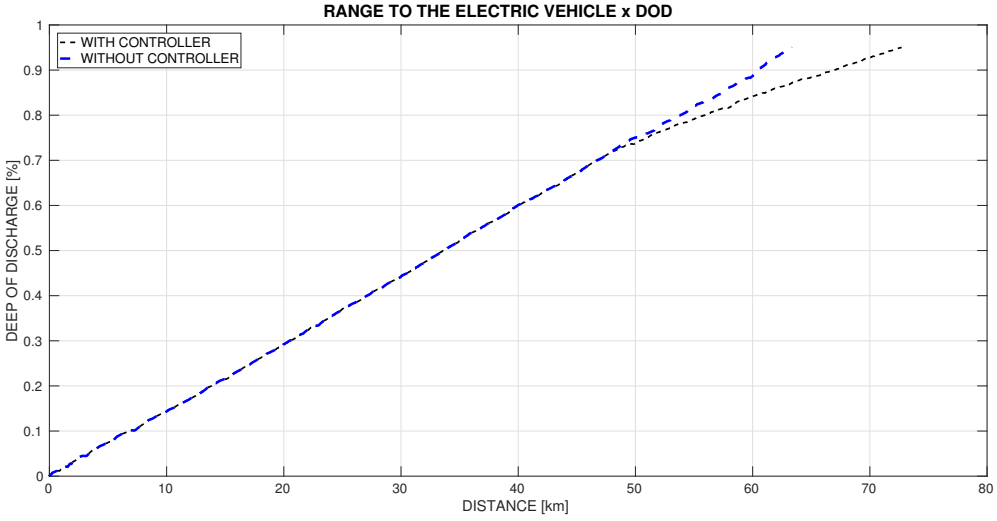

(a)

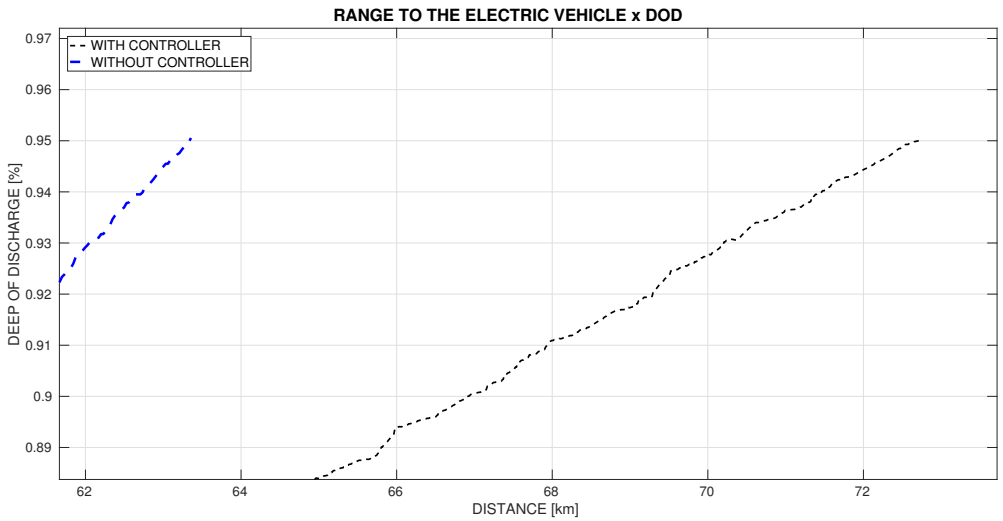

(b)

Figure 35 – The EV battery Dod x Distance travelled in Araranguá/Porto Alegre driving cycle. a) Original picture of DoD x Distance travelled; b) Zoomed picture of DoD x Distance travelled. Source: The Author

4.3 Uphill driving scenario

To test the SPMS in a road with gradient, a uphill driving cycle was created. Following what Yang et al. (2014) cited in the article, which argued how to develop this kind of conditions. A feasible option is the modal driving cycle cited before in the text. Setting a constant velocity and a constant slope for testing. According to this study, a hypothetical situation was developed to the SPMS test. Imagining a vehicle with a constant urban speed V = 60 km/h, where the car slows down to V = 40 km/h for the uphill driving and keep the same velocity for the whole test. Consequently no modifications in the slope has done, performing a steady state condition until the EV battery gets flat. So the slope vary from $0 - 12°$ in the driving cycle.

However, the downhill scenario was not studied and projected for testing, due to the negative tractive force generated by it. That situation means , if Fte is negative the tractive force will not be applied from the electric motor to the wheels, but from the wheels to the motor; and the current will flow into the battery, charging it (MAIA et al., 2011). The forces that could get negative is the hill climbing force in downhill and the acceleration force in braking cases. As the vehicle do not use power to drive and brakes constantly for safety, the battery is recharged. Those situations are both considered as regenerative braking scenarios (CHUANWEI et al., 2004; FERREIRA et al., 2008). The Figure 36 illustrates the velocity in the cycle. The behaviour mentioned to the velocity, is shown in this figure. The mean EV velocities reached in the cycle are

illustrated also in the same figure. Nonetheless, in the Figure 37 the EV consumption during the driving cycle is demonstrated. Lower energy consumption values for the controlling type are presented. Overall the improvements with the controller was 39.35 %.

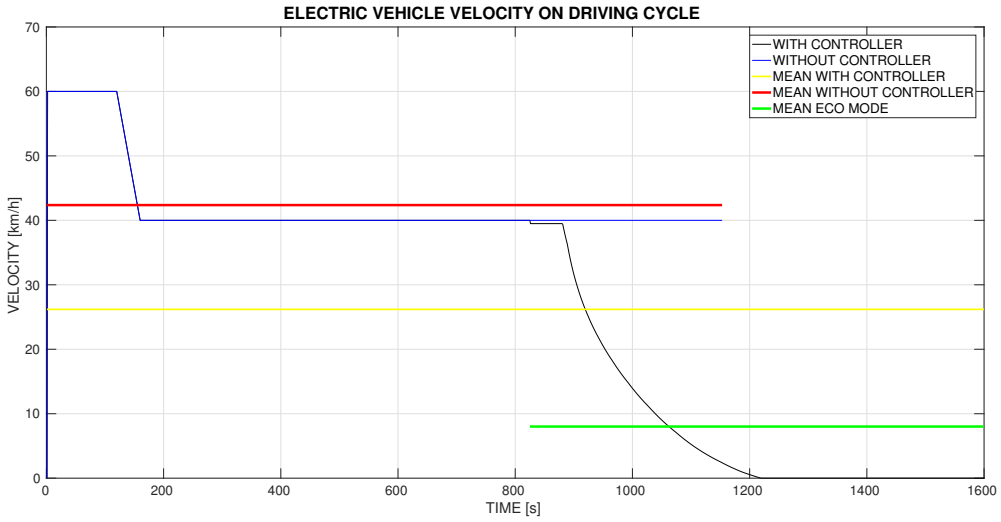

Figure 36 – The EV velocity in the Uphill driving cycle. Source: The Author

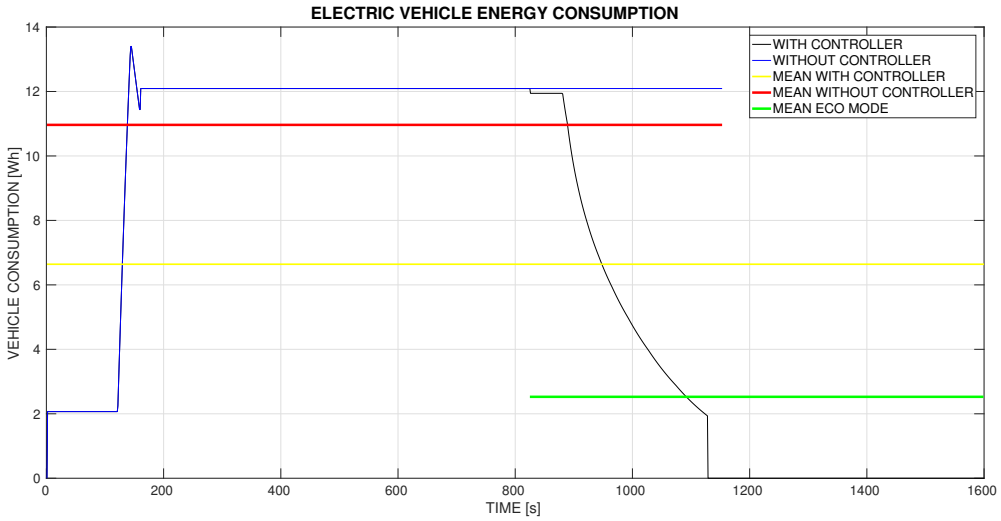

Figure 37 – The EV energy consumption Wh in Uphill driving cycle. Source: The Author

Table 18 – Mean values of EV energy consumption in Uphill driving cycle

Parameter	**Results for the electric vehicle GM EV1**	**Improvements (%)**
Energy consumption without controller	10.9510 Wh	—
Energy consumption with controller	6.6409 Wh	39.35
Energy consumption in Safe power mode	2.5313 Wh	76.88

Source: The Author

The power losses are presented in the Figure 38. It is visible, as in all the graphics of this driving cycle, that lower values are occurred on account of the SPMS. In the Table 19 the mean values of the powertrain losses are presented. Higher values compared with the other cycles are generated, due to the effort of the vehicle to overcome the road gradient. A overall improvement of 29.03 % occurred with SPMS application.

Figure 38 – The EV power losses in Uphill driving cycle. Source: The Author

Table 19 – Mean values of EV powertrain power losses during the driving cycle (W)

Parameter	**Results for the electric vehicle GM EV1**	**Improvements (%)**
Power losses without controller	5239 W	—
Power losses with controller	3718 W	29.03
Power losses in Safe power mode	2291 W	56.27

Source: The Author

The next graphic, Figure 39, the battery electric current is illustrated with its mean values for each case proposed. In the Table 17, these mean values are shown. As mentioned before, in the model developed in Rajamani (2011), these electric currents were too high in the simulations. This parameter implies deeply for the vehicle consumption. In Yang et al. (2014) is mentioned, that some electric vehicles are restricted to run on high road slopes due to a fast battery discharging. For that situation, this longitudinal vehicle dynamics model was not adopted. Therefore, in the Table 20 the mean values generated from the uphill driving cycle are demonstrated. A overall improvement of 38.68 % occurred with the SPMS application.

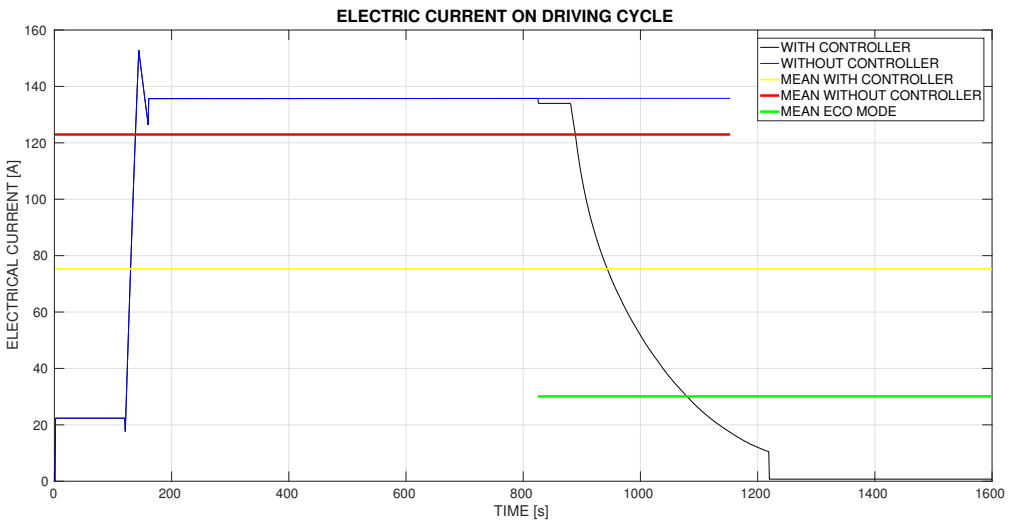

Figure 39 – The EV battery electric current in Uphill driving cycle. Source: The Author

Table 20 – Mean values of EV battery electric current during the Uphill driving cycle

Parameter	**Results for the electric vehicle GM EV1**	**Improvements (%)**
Battery electric current without controller	122.80 A	—
Battery electric current with controller	75.30 A	38.68
Battery electric current in Safe power mode	30.16 A	75.43

Source: The Author

The Figure 40, presents the deep of discharge behaviour during the cycle. A interesting point observed in this graph, is how the EV behaves in low DoD. It appears to turn constant during the period, having a reduced consumption due to the low EV speeds. To clarify that, the cycle with controller has a run-time of 1600 s and without controller 1153 s. It is a difference of 447 seconds (0.1242 hours). That means, without SPMS the battery gets flat and with the SPMS the battery still in low state of charge. To explain the situation occurred, some mathematical manipulations are done. Using the velocity uphill of 40 km/h, a simple calculation with the formula $V = \frac{ds}{dt}$ demonstrate that extra five kilometers are added to the trip.

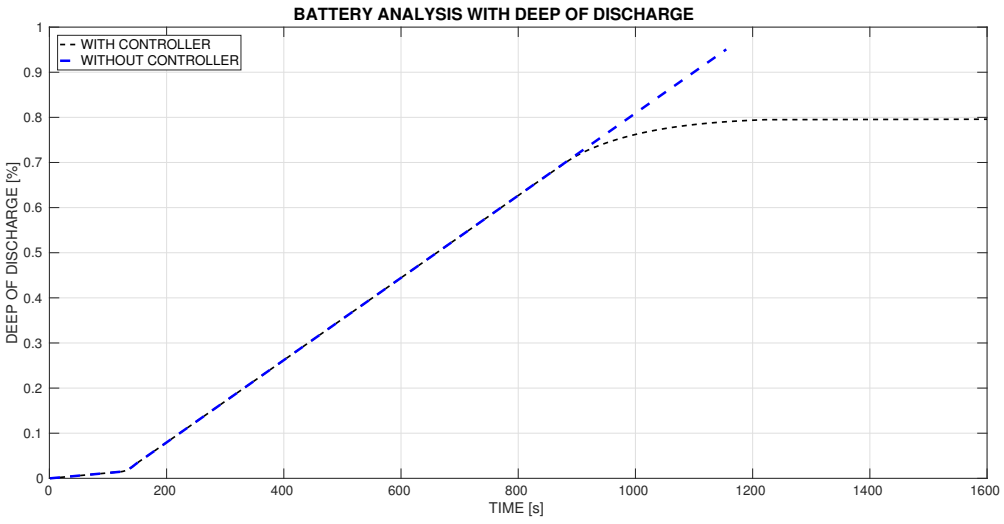

Figure 40 – The EV battery DoD in Uphill driving cycle. Source: The Author

5 FINAL CONCLUSIONS

In this section the final conclusions of this study would be elucidated to understand the results from the simulated scenarios. Those, with the controller embedded in the vehicle, returned desired results. In all of them, lower values for all the parameters analyzed were generated, demonstrating the effectiveness of the Safe Power Management System implementation. The electric energy consumption had reduction in all tests, giving integrity and safety to the FLC proposed. The longer range achieved by the FLC, is a necessary result to real driving application, avoiding empty battery and giving opportunity to the driver find a next recharge station.

Firstly, analyzing the urban scenario, all the parameters studied, had lower numbers with the SPMS implemented. In the FTP-75 driving cycle, lower velocities compared to Arroio do Silva-Araranguá driving cycle were occurred. For that reason, reduced values in the EV consumption appeared in all data compiled. That behaviour was found also, in all the parameters due to the lower velocity. A small gain in extra trip distance was given by the SPMS.

For the highway scenario the same situation appeared in the simulation. A lower velocity for the HWFET occurred, creating reduced values for all the studied parameters. However, a longer extra distance offered by the SPMS were generated. This situation offered by the controlling system in the highway, compared to the urban scenario, is an important point to be analyzed.

Therefore, that situation occurs due to the lower energy consumed in the city, generating a longer cycle. When the controller is activated, the new velocity has a short difference than original one, giving a few kilometers to the vehicle. Nonetheless, in the highway environment the Safe Power Mode has a bigger impact in the velocity. That point appeared due to a higher velocity gradient of the original velocity by the controlled one. However, the highway EV behaviour leads to a shorter time durance trip and a bigger impact in the energy consumption, giving more distance to be travelled with the EV.

In the uphill scenario lower consumption with SPMS was occurred. A stabilization in a low state of charge during the trip was performed. That behaviour demonstrates the efficiency of the FLC in the system for that environment. The rules for the Mamdani FIS type are respected. If very low SoC's in an uphill environment to be proceed as the vehicle system conditions, consequently turns the velocity in a very low state, offering the lowest energy consumption scenario.

Considering the modelling blocks, all the them had desirable performance into the sys-

tem analysis. To prove that, some calculations using the FTP-75 scenario could be done. The parameters for that procedure are: mean Battery Power without controller = 5.3051 kW; mean velocity without controller = 34.12 km/h. With a empirical equation $E = P_{bat}/V_{EV}$, V_{EV} being the mean EV velocity without controller, a consumption of E = 0.1555 kWh/km is found, very similar to the pure electric vehicle Nissan Leaf, E = 0.143 kWh/km obtained in urban conditions. That is a 8.7413$\%$ higher than real conditions. For that reason GM EV1 vehicular dynamics, DC power losses model and the chemical battery internal resistance model, were a good choice to describe the EV powertrain.

Table 21 illustrates the improvements with the SPMS system, using the mean values collected from the simulation. A overall improvement of 22.47 % in the EV energy consumption confirm, the better performance with the FLC system. In Table 22 also a decrease of 23.38 % in power losses and 22.37 % in electric current, shown on Table 23, demonstrating the improvements to the system with the SPMS action.

Table 21 – The SPMS improvements on EV energy consumption

Scenario	**Energy consumption improvements (%)**
FTP-75	6.67
Arroio do Silva / Araranguá	8.48
HWFET	28.25
Araranguá / Porto Alegre	29.62
Uphill	39.35

Source: The Author

Table 22 – The SPMS improvements on EV power losses

Scenario	**Power losses improvements (%)**
FTP-75	8.11
Arroio do Silva / Araranguá	12.24
HWFET	31.67
Araranguá / Porto Alegre	35.87
Uphill	29.03

Source: The Author

Table 23 – The SPMS improvements on EV electric current

Scenario	**Electric current improvements (%)**
FTP-75	6.18
Arroio do Silva / Araranguá	8.58
HWFET	28.42
Araranguá / Porto Alegre	30
Uphill	38.68

Source: The Author

The SPMS action produces similar values for each type of scenario used. As a occurrence of higher velocity gradients in the highway, a bigger improvement is done by the controller. That explanation could relate to the uphill environment as well. Therefore, to improve the system analysis and perform different researches about the topics adopted in the project, suggestions to future studies are done below:

- Improvement of the EV powertrain model, as using a AC motor model, Li-Ion battery model,a more accurate regenerative braking model, power electronic models; seeking a description in a time domain modelling;
- Applying new types of controllers, even the modern types as neural networks, or the classics as PID for comparison;
- Perform tests to find a better choice of MF in the FLC development;
- Optimization of the FLC, with machine learning techniques;
- Optimization of the whole system, as mentioned in Larminie and Lowry (2004) being a option to EMS construction, using running restrictions as energy consumption, for example.

SISTEMA DE GERENCIAMENTO DO MODO ECONOMIA DE ENERGIA EM VEÍCULOS ELÉTRICOS UTILIZANDO CONTROLADOR FUZZY

RESUMO

A tecnologia veicular está passando por um novo paradigma. Novas diretrizes devem ser determinadas, para o controle veicular de emissão de poluntes e o uso inteligente das fontes não-renováveis. Os carros elétricos são uma opção hoje em dia para mitigar estes problemas. Visto como um dispositivo eletrônico, a energia consumida deve ser gerenciada efetivamente devido a baixa autonomia e o custo elevado das baterias químicas. É desenvolvido neste trabalho de conclusão de curso, um sistema de gerenciamento para o modo economia de energia em veículos elétricos , sendo este um bloco do sistema veicular de gerenciamento de energia. Um gerenciador de energia é um distribuidor de potência dentro do veículo elétrico, buscando a integridade do sistema e a redução no consumo de energia. O sistema utiliza um controlador fuzzy como estratégia de controle da energia consumida pelo veículo.

Palavras-chave: Veículo elétrico, Sistema de Gerenciamento de Energia, Sistema de Gerenciamento Modo Economia, Consumo de energia, Controlador Fuzzy

REFERENCES

ARAÚJO, B. J. d. O. *Desenvolvimento de um modelo de caracterização energética de ciclos de condução*. Dissertação (Doutorado), 2015.

ARMENTA, J. et al. An advanced energy management system for controlling the ultracapacitor discharge and improving the electric vehicle range. *Journal of Power Sources*, Elsevier, v. 284, p. 452–458, 2015.

ARUN, N. et al. Development of driving cycles for passenger cars and motorcycles in chennai, india. *Sustainable Cities and Society*, Elsevier, v. 32, p. 508–512, 2017.

BAI, Y.; WANG, D. Fundamentals of fuzzy logic control—fuzzy sets, fuzzy rules and defuzzifications. In: *Advanced Fuzzy Logic Technologies in Industrial Applications*. [S.l.]: Springer, 2006. p. 17–36.

BAŠIĆ, M.; VUKADINOVIĆ, D.; POLIĆ, M. Fuzzy logic vs. classical pi voltage controller for a self-excited induction generator. In: *4th European Conference for the Applied Mathematics and Informatics (AMATHI'13)*. [S.l.: s.n.], 2013.

BEAUDIN, M.; ZAREIPOUR, H. Home energy management systems: A review of modelling and complexity. *Renewable and Sustainable Energy Reviews*, Elsevier, v. 45, p. 318–335, 2015.

BECKER, J.; SCHAEPER, C.; SAUER, D. Energy management system for a multi-source storage system electric vehicle. In: IEEE. *Vehicle Power and Propulsion Conference (VPPC), 2012 IEEE*. [S.l.], 2012. p. 407–412.

BENTO, J. P. M. *Análise da viabilidade de adaptação de motores elétricos nos cubos de rodas traseiros de veículos de passeio*. Dissertação (Bachelor Thesis) — Engenharia Automotiva - Universidade de Brasília, November 2015.

CAPO, P. Ícaro M. *Modelagem matemática e simulação de um veículo elétrico movido a células de combustível*. Dissertação (Bachelor Thesis) — Engenharia de Energia - Universidade Federal de Santa Catarina, December 2016.

CARBONI, A.; RAGAINI, E.; FERRERO, A. A fuzzy inference system for power systems. In: IEEE. *Research and Technologies for Society and Industry (RTSI), 2017 IEEE 3rd International Forum on*. [S.l.], 2017. p. 1–5.

CHAN, C. C. The state of the art of electric, hybrid, and fuel cell vehicles. *Proceedings of the IEEE*, IEEE, v. 95, n. 4, p. 704–718, 2007.

CHAPMAN, S. *Electric machinery fundamentals*. [S.l.]: McGraw-Hill Education, 2013.

CHAPMAN, S. J. *Essentials of MATLAB programming*. [S.l.]: Cengage Learning, 2016.

CHEN, C. et al. On-road emission characteristics of heavy-duty diesel vehicles in shanghai. *Atmospheric Environment*, Elsevier, v. 41, n. 26, p. 5334–5344, 2007.

CHENG, K. W. E. et al. Battery-management system (bms) and soc development for electrical vehicles. *IEEE Transactions on Vehicular Technology*, IEEE, v. 60, n. 1, p. 76–88, 2011.

CHUANWEI, Z. et al. Study on regenerative braking of electric vehicle. In: IEEE. *Power Electronics and Motion Control Conference, 2004. IPEMC 2004. The 4th International*. [S.l.], 2004. v. 2, p. 836–839.

DIB, W. et al. Optimal energy management for an electric vehicle in eco-driving applications. *Control Engineering Practice*, Elsevier, v. 29, p. 299–307, 2014.

EMADI, A. *Advanced electric drive vehicles*. [S.l.]: CRC Press, 2014.

FARIAS, L. da R. *Aplicação de lógica fuzzy no controle do consumo de energia em veículos elétricos*. Dissertação (Bachelor Thesis) — Tecnologias da Informação e Comunicação - Universidade Federal de Santa Catarina, December 2014.

FERREIRA, A. A. et al. Energy management fuzzy logic supervisory for electric vehicle power supplies system. *IEEE Transactions on Power Electronics*, IEEE, v. 23, n. 1, p. 107–115, 2008.

FOTOUHI, A. et al. A review on electric vehicle battery modelling: From lithium-ion toward lithium–sulphur. *Renewable and Sustainable Energy Reviews*, Elsevier, v. 56, p. 1008–1021, 2016.

GALDI, V.; PICCOLO, A.; SIANO, P. A fuzzy based safe power management algorithm for energy storage systems in electric vehicles. In: IEEE. *Vehicle Power and Propulsion Conference, 2006. VPPC'06. IEEE*. [S.l.], 2006. p. 1–6.

HAIZHOU, Z. Modeling of lithium-ion battery for charging/discharging characteristics based on circuit model. *International Journal of Online Engineering (iJOE)*, v. 13, n. 06, p. 86–95, 2017.

HEMI, H.; GHOUILI, J.; CHERITI, A. A real time fuzzy logic power management strategy for a fuel cell vehicle. *Energy conversion and Management*, Elsevier, v. 80, p. 63–70, 2014.

HIBBELER, R. *Engineering Mechanics Dynamics. 2016*. [S.l.]: Upper Saddle River, NJ: Pearson Prentice Hall, 2016.

HOWEY, D. A. et al. Comparative measurements of the energy consumption of 51 electric, hybrid and internal combustion engine vehicles. *Transportation Research Part D: Transport and Environment*, Elsevier, v. 16, n. 6, p. 459–464, 2011.

JANG, J.-S. Anfis: adaptive-network-based fuzzy inference system. *IEEE transactions on systems, man, and cybernetics*, IEEE, v. 23, n. 3, p. 665–685, 1993.

JI, S. et al. Electric vehicles in china: emissions and health impacts. *Environmental science & technology*, ACS Publications, v. 46, n. 4, p. 2018–2024, 2012.

JOSSEN, A. Fundamentals of battery dynamics. *Journal of Power Sources*, Elsevier, v. 154, n. 2, p. 530–538, 2006.

KALAVATHI, M. S.; REDDY, C. S. R. Performance evaluation of classical and fuzzy logic control techniques for brushless dc motor drive. In: IEEE. *Power Modulator and High Voltage Conference (IPMHVC), 2012 IEEE International*. [S.l.], 2012. p. 488–491.

KAUR, A.; KAUR, A. Comparison of fuzzy logic and neuro-fuzzy algorithms for air conditioning system. *International journal of soft computing and engineering*, v. 2, n. 1, p. 417–20, 2012.

KLEY, F.; LERCH, C.; DALLINGER, D. New business models for electric cars—a holistic approach. *Energy Policy*, Elsevier, v. 39, n. 6, p. 3392–3403, 2011.

KLOMP, M. *Longitudinal force distribution and road vehicle handling*. [S.l.]: Chalmers University of Technology, 2010.

LARMINIE, J.; LOWRY, J. *Electric vehicle technology explained*. [S.l.]: John Wiley & Sons, 2004.

LI, C. et al. Fuel economy optimization of hybrid electric vehicles. In: IEEE. *Control and Decision Conference (CCDC), 2015 27th Chinese*. [S.l.], 2015. p. 810–815.

LOVATT, H.; RAMSDEN, V.; MECROW, B. Design of an in-wheel motor for a solar-powered electric vehicle. *IEE Proceedings-Electric Power Applications*, IET, v. 145, n. 5, p. 402–408, 1998.

MAIA, R. et al. Electric vehicle simulator for energy consumption studies in electric mobility systems. In: IEEE. *Integrated and Sustainable Transportation System (FISTS), 2011 IEEE Forum on*. [S.l.], 2011. p. 227–232.

MAMDANI, E. H. Application of fuzzy logic to approximate reasoning using linguistic synthesis. In: IEEE COMPUTER SOCIETY PRESS. *Proceedings of the sixth international symposium on Multiple-valued logic*. [S.l.], 1976. p. 196–202.

MELO, P.; ARAUJO, R. E.; CASTRO, R. de. Overview on energy management strategies for electric vehicles-modelling, trends and research perspectives. In: IEEE. *Energetics (IYCE), Proceedings of the 2011 3rd International Youth Conference on*. [S.l.], 2011. p. 1–8.

MIERS, S. A. et al. *Drive cycle analysis of butanol/diesel blends in a light-duty vehicle*. [S.l.], 2008.

MORENO, J.; ORTÚZAR, M. E.; DIXON, J. W. Energy-management system for a hybrid electric vehicle, using ultracapacitors and neural networks. *IEEE transactions on Industrial Electronics*, IEEE, v. 53, n. 2, p. 614–623, 2006.

MUNEER, T.; KOLHE, M.; DOYLE, A. *Electric Vehicles: Prospects and Challenges*. [S.l.]: Elsevier, 2017.

MUNSON, B. R.; YOUNG, D. F.; OKIISHI, T. H. *Fundamentals of fluid mechanics*. [S.l.: s.n.], 2004.

MURPHEY, Y. L. et al. Intelligent hybrid vehicle power control—part i: Machine learning of optimal vehicle power. *IEEE Transactions on Vehicular Technology*, IEEE, v. 61, n. 8, p. 3519–3530, 2012.

NISE, N. S. *Engenharia de sistemas de controle*. [S.l.]: LTC, 2012.

PISTOIA, G. *Electric and hybrid vehicles: Power sources, models, sustainability, infrastructure and the market*. [S.l.]: Elsevier, 2010.

RAJAMANI, R. *Vehicle dynamics and control*. [S.l.]: Springer Science & Business Media, 2011.

RAJHI, A. A. et al. *Economic Development in Saudi Arabia*. [S.l.]: Routledge, 2012.

RIADI, R. et al. Decentralized temperature fuzzy logic control of a passive air conditioning unit. In: IEEE. *Control & Automation, 2007. MED'07. Mediterranean Conference on*. [S.l.], 2007. p. 1–6.

SAKHDARI, B.; AZAD, N. An optimal energy management system for battery electric vehicles. *IFAC-PapersOnLine*, Elsevier, v. 48, n. 15, p. 86–92, 2015.

SERRAO, L. et al. Optimal energy management of hybrid electric vehicles including battery aging. In: IEEE. *American Control Conference (ACC), 2011*. [S.l.], 2011. p. 2125–2130.

SHAKOURI, P. et al. Longitudinal vehicle dynamics using simulink/matlab. IET, 2010.

SZCZEPANIAK, P. S.; LISBOA, P. J. *Fuzzy systems in medicine*. [S.l.]: Physica, 2012.

TANG, K. L.; MULHOLLAND, R. J. Comparing fuzzy logic with classical controller designs. *IEEE Transactions on Systems, Man, and Cybernetics*, IEEE, v. 17, n. 6, p. 1085–1087, 1987.

WANG, J. et al. Investigation of speciated voc in gasoline vehicular exhaust under ece and eudc test cycles. *Science of the Total Environment*, Elsevier, v. 445, p. 110–116, 2013.

WANG, N.; PAN, H.; ZHENG, W. Assessment of the incentives on electric vehicle promotion in china. *Transportation Research Part A: Policy and Practice*, Elsevier, v. 101, p. 177–189, 2017.

WANG, T. et al. Application of energy management strategy based on state machine in fuel cell hybrid power system. In: IEEE. *Transportation Electrification Asia-Pacific (ITEC Asia-Pacific), 2017 IEEE Conference and Exp*. [S.l.], 2017. p. 1–5.

WENG, C.; SUN, J.; PENG, H. A unified open-circuit-voltage model of lithium-ion batteries for state-of-charge estimation and state-of-health monitoring. *Journal of power Sources*, Elsevier, v. 258, p. 228–237, 2014.

WU, D. Twelve considerations in choosing between gaussian and trapezoidal membership functions in interval type-2 fuzzy logic controllers. In: IEEE. *Fuzzy Systems (FUZZ-IEEE), 2012 IEEE International Conference on*. [S.l.], 2012. p. 1–8.

YANG, S. et al. Electric vehicle's electricity consumption on a road with different slope. *Physica A: Statistical Mechanics and its Applications*, Elsevier, v. 402, p. 41–48, 2014.

YOUNG, K. et al. Electric vehicle battery technologies. In: *Electric Vehicle Integration into Modern Power Networks*. [S.l.]: Springer, 2013. p. 15–56.

ZADEH, L. A. Fuzzy sets. *Information and control*, Elsevier, v. 8, n. 3, p. 338–353, 1965.

ZHANG, F.; GUO, F.; HUANG, H. A study of driving cycle for electric special-purpose vehicle in beijing. *Energy Procedia*, Elsevier, v. 105, p. 4884–4889, 2017.

ACKNOWLEDGMENTS

Esta parte gostaria de realizá-la em português para meus amigos e familiares que não compreendem muito bem a língua inglesa. Primeiramente gostaria de agradeçer aos meus pais, mentores, progenitores e amigos. Meu pai e mestre Sérgio Lucchesi e minha mãe amada Marli Schmidt. Sem a sua ajuda psicológica até a financeira, nada teria acontecido. Os amo eternamente por serem meus pais e tenho um imenso orgulho de carregar seus sobrenomes. Aos meus grandes irmãos de vida Thiago Cardias e Marcelo Cavalcante, aqueles que me apoiaram em todas as situações, sendo elas de glória e derrota desejo os meus calorosos agradecimentos. A minha amiga Regina que foi minha mentora psicológica guiando me para fora das turbulências. Aos meus professores e amigos Anderson Perez, César Scharlau e Leonardo Bremermann que me apoiaram em todo o período do desenvolvimento deste projeto.

Gostaria de agradecer ao professor Anderson pela amizade, apoio como co-orientador e detentor da idéia em criar o recheio da casca do sorvete, analogia feita pelo complemento deste trabalho ao projeto desenvolvido pelo colega Luiz Farias. Ao professor César, por nossa história acadêmica feita de projetos e boas conversas sobre o nosso Tricolor. Ao professor Leonardo por ter me apoiado como orientador na relização do projeto de TCC e por sua amizade e solicitude às perguntas feitas informalmente e formalmente para o desenvolvimento deste projeto. Ao professor que extrapolou os meus limites cognitivos durante a matéria de Estática e Dinâmica à qual nunca esquecerei, deixo meu agradecimento ao amigo e surfista Éverton Fabian.

Sou muito agradecido por todos os momentos ocorridos neste período em Araranguá e a todos os professores que me ajudaram durante esta árdua caminhada. Gostaria de agradecer aos meus amigos do laboratório LARM, onde desenvolvi o projeto aqui descrito. Fizeram deste um local familiar e ótimo para produtividade em minhas pesquisas. Esse período de graduação foi uma escola da vida, onde inúmeros momentos difíceis ocorreram, entretanto com uma frase mencionada pelo personagem Rocky Balboa, a qual assessorou minha vida durante as tempestades neste vasto oceano. Salientada principalmente pelo mestre que me guiou igual à um treinador neste periodo, a mesma é descrita com os próximos versos:

O mundo não é um mar de rosas; é um lugar sujo, um lugar cruel, que não quer saber o quanto você é durão. Vai botar você de joelhos e você vai ficar de joelhos para sempre se você deixar. Você, eu, ninguém vai bater tão forte como a vida, mas não se trata de bater forte. Se trata de quanto você aguenta apanhar e seguir em frente, o quanto você é capaz de aguentar e continuar tentando. É assim que se consegue vencer. Agora se você sabe do o seu valor, então vá atrás do que você merece, mas tem que estar preparado para apanhar. E nada de apontar dedos, dizer que você não consegue por causa dele ou dela, ou de quem quer que seja. Só covardes fazem isso e você não é covarde, você é melhor que isso. (Rocky Balboa)

Deixo aqui uma frase desenvolvida por minha autoria que descreveu muito bem o meu período durante à graduação em Engenharia de Energia:

Inversamente proporcional ao meu desejo de evoluir, é minha ansiedade de querer produzir. (Rodrigo Schmidt Lucchesi)

ATTACHMENT A – Fuzzy rules used to develop the Mamdani Fuzzy Logic Control

1. If (slope is poucoAclive) and (DoD is ultraHighBattery) and (velocity is ultraLow) then (newVelocity is ultraLow)
2. If (slope is poucoAclive) and (DoD is ultraHighBattery) and (velocity is low) then (newVelocity is low)
3. If (slope is poucoAclive) and (DoD is ultraHighBattery) and (velocity is lowNormal) then (newVelocity is lowNormal)
4. If (slope is poucoAclive) and (DoD is ultraHighBattery) and (velocity is high) then (newVelocity is high)
5. If (slope is poucoAclive) and (DoD is ultraHighBattery) and (velocity is normal) then (newVelocity is normal)
6. If (slope is poucoAclive) and (DoD is ultraHighBattery) and (velocity is highNormal) then (newVelocity is highNormal)
7. If (slope is poucoAclive) and (DoD is ultraHighBattery) and (velocity is ultraHigh) then (newVelocity is ultraHigh)
8. If (slope is poucoAclive) and (DoD is ultraHighBattery) and (velocity is highLimit) then (newVelocity is highLimit)
9. If (slope is declive) and (DoD is ultraHighBattery) and (velocity is ultraLow) then (newVelocity is ultraLow)
10. If (slope is declive) and (DoD is ultraHighBattery) and (velocity is low) then (newVelocity is low)
11. If (slope is declive) and (DoD is ultraHighBattery) and (velocity is lowNormal) then (newVelocity is lowNormal)
12. If (slope is declive) and (DoD is ultraHighBattery) and (velocity is high) then (newVelocity is high)
13. If (slope is declive) and (DoD is ultraHighBattery) and (velocity is normal) then (newVelocity is normal)
14. If (slope is declive) and (DoD is ultraHighBattery) and (velocity is highNormal) then (newVelocity is highNormal)
15. If (slope is declive) and (DoD is ultraHighBattery) and (velocity is ultraHigh) then (newVelocity is ultraHigh)
16. If (slope is declive) and (DoD is ultraHighBattery) and (velocity is highLimit) then (newVelocity is highLimit)
17. If (slope is plano) and (DoD is ultraHighBattery) and (velocity is ultraLow) then (newVelocity is ultraLow)
18. If (slope is plano) and (DoD is ultraHighBattery) and (velocity is low) then (newVelocity is low)
19. If (slope is plano) and (DoD is ultraHighBattery) and (velocity is lowNormal) then (newVelocity is lowNormal)
20. If (slope is plano) and (DoD is ultraHighBattery) and (velocity is high) then (newVelocity is high)
21. If (slope is plano) and (DoD is ultraHighBattery) and (velocity is normal) then (newVelocity is normal)
22. If (slope is plano) and (DoD is ultraHighBattery) and (velocity is highNormal) then (newVelocity is highNormal)
23. If (slope is plano) and (DoD is ultraHighBattery) and (velocity is ultraHigh) then (newVelocity is ultraHigh)
24. If (slope is plano) and (DoD is ultraHighBattery) and (velocity is highLimit) then (newVelocity is highLimit)
25. If (slope is poucoDeclive) and (DoD is ultraHighBattery) and (velocity is ultraLow) then (newVelocity is ultraLow)
26. If (slope is poucoDeclive) and (DoD is ultraHighBattery) and (velocity is low) then (newVelocity is low)
27. If (slope is poucoDeclive) and (DoD is ultraHighBattery) and (velocity is lowNormal) then (newVelocity is lowNormal)
28. If (slope is poucoDeclive) and (DoD is ultraHighBattery) and (velocity is high) then (newVelocity is high)
29. If (slope is poucoDeclive) and (DoD is ultraHighBattery) and (velocity is normal) then (newVelocity is normal)
30. If (slope is poucoDeclive) and (DoD is ultraHighBattery) and (velocity is highNormal) then (newVelocity is highNormal)
31. If (slope is poucoDeclive) and (DoD is ultraHighBattery) and (velocity is ultraHigh) then (newVelocity is ultraHigh)
32. If (slope is poucoDeclive) and (DoD is ultraHighBattery) and (velocity is highLimit) then (newVelocity is highLimit)
33. If (slope is declivePlano) and (DoD is ultraHighBattery) and (velocity is ultraLow) then (newVelocity is ultraLow)
34. If (slope is declivePlano) and (DoD is ultraHighBattery) and (velocity is low) then (newVelocity is low)
35. If (slope is declivePlano) and (DoD is ultraHighBattery) and (velocity is lowNormal) then (newVelocity is lowNormal)
36. If (slope is declivePlano) and (DoD is ultraHighBattery) and (velocity is high) then (newVelocity is high)
37. If (slope is declivePlano) and (DoD is ultraHighBattery) and (velocity is normal) then (newVelocity is normal)
38. If (slope is declivePlano) and (DoD is ultraHighBattery) and (velocity is highNormal) then (newVelocity is highNormal)
39. If (slope is declivePlano) and (DoD is ultraHighBattery) and (velocity is ultraHigh) then (newVelocity is ultraHigh)
40. If (slope is declivePlano) and (DoD is ultraHighBattery) and (velocity is highLimit) then (newVelocity is highLimit)
41. If (slope is aclivePlano) and (DoD is ultraHighBattery) and (velocity is ultraLow) then (newVelocity is ultraLow)
42. If (slope is aclivePlano) and (DoD is ultraHighBattery) and (velocity is low) then (newVelocity is low)
43. If (slope is aclivePlano) and (DoD is ultraHighBattery) and (velocity is lowNormal) then (newVelocity is lowNormal)
44. If (slope is aclivePlano) and (DoD is ultraHighBattery) and (velocity is high) then (newVelocity is high)
45. If (slope is aclivePlano) and (DoD is ultraHighBattery) and (velocity is normal) then (newVelocity is normal)
46. If (slope is aclivePlano) and (DoD is ultraHighBattery) and (velocity is highNormal) then (newVelocity is highNormal)
47. If (slope is aclivePlano) and (DoD is ultraHighBattery) and (velocity is ultraHigh) then (newVelocity is ultraHigh)
48. If (slope is aclivePlano) and (DoD is ultraHighBattery) and (velocity is highLimit) then (newVelocity is highLimit)
49. If (slope is aclive) and (DoD is ultraHighBattery) and (velocity is ultraLow) then (newVelocity is ultraLow)
50. If (slope is aclive) and (DoD is ultraHighBattery) and (velocity is low) then (newVelocity is low)
51. If (slope is aclive) and (DoD is ultraHighBattery) and (velocity is lowNormal) then (newVelocity is lowNormal)
52. If (slope is aclive) and (DoD is ultraHighBattery) and (velocity is normal) then (newVelocity is normal)
53. If (slope is aclive) and (DoD is ultraHighBattery) and (velocity is high) then (newVelocity is normal)
54. If (slope is aclive) and (DoD is ultraHighBattery) and (velocity is highNormal) then (newVelocity is normal)
55. If (slope is aclive) and (DoD is ultraHighBattery) and (velocity is ultraHigh) then (newVelocity is normal)
56. If (slope is aclive) and (DoD is ultraHighBattery) and (velocity is highLimit) then (newVelocity is normal)
57. If (slope is poucoAclive) and (DoD is HighBattery) and (velocity is ultraLow) then (newVelocity is ultraLow)
58. If (slope is poucoAclive) and (DoD is HighBattery) and (velocity is low) then (newVelocity is low)
59. If (slope is poucoAclive) and (DoD is HighBattery) and (velocity is lowNormal) then (newVelocity is lowNormal)
60. If (slope is poucoAclive) and (DoD is HighBattery) and (velocity is high) then (newVelocity is high)
61. If (slope is poucoAclive) and (DoD is HighBattery) and (velocity is normal) then (newVelocity is normal)
62. If (slope is poucoAclive) and (DoD is HighBattery) and (velocity is highNormal) then (newVelocity is highNormal)
63. If (slope is poucoAclive) and (DoD is HighBattery) and (velocity is ultraHigh) then (newVelocity is ultraHigh)
64. If (slope is poucoAclive) and (DoD is HighBattery) and (velocity is highLimit) then (newVelocity is highLimit)
65. If (slope is declive) and (DoD is HighBattery) and (velocity is ultraLow) then (newVelocity is ultraLow)
66. If (slope is declive) and (DoD is HighBattery) and (velocity is low) then (newVelocity is low)
67. If (slope is declive) and (DoD is HighBattery) and (velocity is lowNormal) then (newVelocity is lowNormal)
68. If (slope is declive) and (DoD is HighBattery) and (velocity is high) then (newVelocity is high)
69. If (slope is declive) and (DoD is HighBattery) and (velocity is normal) then (newVelocity is normal)
70. If (slope is declive) and (DoD is HighBattery) and (velocity is highNormal) then (newVelocity is highNormal)
71. If (slope is declive) and (DoD is HighBattery) and (velocity is ultraHigh) then (newVelocity is ultraHigh)
72. If (slope is declive) and (DoD is HighBattery) and (velocity is highLimit) then (newVelocity is highLimit)
73. If (slope is plano) and (DoD is HighBattery) and (velocity is ultraLow) then (newVelocity is ultraLow)
74. If (slope is plano) and (DoD is HighBattery) and (velocity is low) then (newVelocity is low)
75. If (slope is plano) and (DoD is HighBattery) and (velocity is lowNormal) then (newVelocity is lowNormal)
76. If (slope is plano) and (DoD is HighBattery) and (velocity is high) then (newVelocity is high)
77. If (slope is plano) and (DoD is HighBattery) and (velocity is normal) then (newVelocity is normal)
78. If (slope is plano) and (DoD is HighBattery) and (velocity is highNormal) then (newVelocity is highNormal)

79. If (slope is plano) and (DoD is HighBattery) and (velocity is ultraHigh) then (newVelocity is ultraHigh)
80. If (slope is plano) and (DoD is HighBattery) and (velocity is highLimit) then (newVelocity is highLimit)
81. If (slope is poucoDeclive) and (DoD is HighBattery) and (velocity is ultraLow) then (newVelocity is ultraLow)
82. If (slope is poucoDeclive) and (DoD is HighBattery) and (velocity is low) then (newVelocity is low)
83. If (slope is poucoDeclive) and (DoD is HighBattery) and (velocity is lowNormal) then (newVelocity is lowNormal)
84. If (slope is poucoDeclive) and (DoD is HighBattery) and (velocity is high) then (newVelocity is high)
85. If (slope is poucoDeclive) and (DoD is HighBattery) and (velocity is normal) then (newVelocity is normal)
86. If (slope is poucoDeclive) and (DoD is HighBattery) and (velocity is highNormal) then (newVelocity is highNormal)
87. If (slope is poucoDeclive) and (DoD is HighBattery) and (velocity is ultraHigh) then (newVelocity is ultraHigh)
88. If (slope is poucoDeclive) and (DoD is HighBattery) and (velocity is highLimit) then (newVelocity is highLimit)
89. If (slope is declivePlano) and (DoD is HighBattery) and (velocity is ultraLow) then (newVelocity is ultraLow)
90. If (slope is declivePlano) and (DoD is HighBattery) and (velocity is low) then (newVelocity is low)
91. If (slope is declivePlano) and (DoD is HighBattery) and (velocity is lowNormal) then (newVelocity is lowNormal)
92. If (slope is declivePlano) and (DoD is HighBattery) and (velocity is high) then (newVelocity is high)
93. If (slope is declivePlano) and (DoD is HighBattery) and (velocity is normal) then (newVelocity is normal)
94. If (slope is declivePlano) and (DoD is HighBattery) and (velocity is highNormal) then (newVelocity is highNormal)
95. If (slope is declivePlano) and (DoD is HighBattery) and (velocity is ultraHigh) then (newVelocity is ultraHigh)
96. If (slope is declivePlano) and (DoD is HighBattery) and (velocity is highLimit) then (newVelocity is highLimit)
97. If (slope is aclivePlano) and (DoD is HighBattery) and (velocity is ultraLow) then (newVelocity is ultraLow)
98. If (slope is aclivePlano) and (DoD is HighBattery) and (velocity is low) then (newVelocity is low)
99. If (slope is aclivePlano) and (DoD is HighBattery) and (velocity is lowNormal) then (newVelocity is lowNormal)
100. If (slope is aclivePlano) and (DoD is HighBattery) and (velocity is high) then (newVelocity is high)
101. If (slope is aclivePlano) and (DoD is HighBattery) and (velocity is normal) then (newVelocity is normal)
102. If (slope is aclivePlano) and (DoD is HighBattery) and (velocity is highNormal) then (newVelocity is highNormal)
103. If (slope is aclivePlano) and (DoD is HighBattery) and (velocity is ultraHigh) then (newVelocity is ultraHigh)
104. If (slope is aclivePlano) and (DoD is HighBattery) and (velocity is highLimit) then (newVelocity is highLimit)
105. If (slope is aclive) and (DoD is HighBattery) and (velocity is ultraLow) then (newVelocity is ultraLow)
106. If (slope is aclive) and (DoD is HighBattery) and (velocity is low) then (newVelocity is low)
107. If (slope is aclive) and (DoD is HighBattery) and (velocity is lowNormal) then (newVelocity is lowNormal)
108. If (slope is aclive) and (DoD is HighBattery) and (velocity is normal) then (newVelocity is normal)
109. If (slope is aclive) and (DoD is HighBattery) and (velocity is highNormal) then (newVelocity is normal)
110. If (slope is aclive) and (DoD is HighBattery) and (velocity is ultraHigh) then (newVelocity is normal)
111. If (slope is aclive) and (DoD is HighBattery) and (velocity is highLimit) then (newVelocity is normal)
112. If (slope is poucoAclive) and (DoD is normalBattery) and (velocity is ultraLow) then (newVelocity is ultraLow)
113. If (slope is poucoAclive) and (DoD is normalBattery) and (velocity is low) then (newVelocity is low)
114. If (slope is poucoAclive) and (DoD is normalBattery) and (velocity is lowNormal) then (newVelocity is lowNormal)
115. If (slope is poucoAclive) and (DoD is normalBattery) and (velocity is high) then (newVelocity is high)
116. If (slope is poucoAclive) and (DoD is normalBattery) and (velocity is normal) then (newVelocity is normal)
117. If (slope is poucoAclive) and (DoD is normalBattery) and (velocity is highNormal) then (newVelocity is highNormal)
118. If (slope is poucoAclive) and (DoD is normalBattery) and (velocity is ultraHigh) then (newVelocity is ultraHigh)
119. If (slope is poucoAclive) and (DoD is normalBattery) and (velocity is highLimit) then (newVelocity is highLimit)
120. If (slope is declive) and (DoD is normalBattery) and (velocity is ultraLow) then (newVelocity is ultraLow)
121. If (slope is declive) and (DoD is normalBattery) and (velocity is low) then (newVelocity is low)
122. If (slope is declive) and (DoD is normalBattery) and (velocity is lowNormal) then (newVelocity is lowNormal)
123. If (slope is declive) and (DoD is normalBattery) and (velocity is high) then (newVelocity is high)
124. If (slope is declive) and (DoD is normalBattery) and (velocity is normal) then (newVelocity is normal)
125. If (slope is declive) and (DoD is normalBattery) and (velocity is highNormal) then (newVelocity is highNormal)
126. If (slope is declive) and (DoD is normalBattery) and (velocity is ultraHigh) then (newVelocity is ultraHigh)
127. If (slope is declive) and (DoD is normalBattery) and (velocity is highLimit) then (newVelocity is highLimit)
128. If (slope is plano) and (DoD is normalBattery) and (velocity is ultraLow) then (newVelocity is ultraLow)
129. If (slope is plano) and (DoD is normalBattery) and (velocity is low) then (newVelocity is low)
130. If (slope is plano) and (DoD is normalBattery) and (velocity is lowNormal) then (newVelocity is lowNormal)
131. If (slope is plano) and (DoD is normalBattery) and (velocity is high) then (newVelocity is high)
132. If (slope is plano) and (DoD is normalBattery) and (velocity is normal) then (newVelocity is normal)
133. If (slope is plano) and (DoD is normalBattery) and (velocity is highNormal) then (newVelocity is highNormal)
134. If (slope is plano) and (DoD is normalBattery) and (velocity is ultraHigh) then (newVelocity is ultraHigh)
135. If (slope is plano) and (DoD is normalBattery) and (velocity is highLimit) then (newVelocity is highLimit)
136. If (slope is poucoDeclive) and (DoD is normalBattery) and (velocity is ultraLow) then (newVelocity is ultraLow)
137. If (slope is poucoDeclive) and (DoD is normalBattery) and (velocity is low) then (newVelocity is low)
138. If (slope is poucoDeclive) and (DoD is normalBattery) and (velocity is lowNormal) then (newVelocity is lowNormal)
139. If (slope is poucoDeclive) and (DoD is normalBattery) and (velocity is high) then (newVelocity is high)
140. If (slope is poucoDeclive) and (DoD is normalBattery) and (velocity is normal) then (newVelocity is normal)
141. If (slope is poucoDeclive) and (DoD is normalBattery) and (velocity is highNormal) then (newVelocity is highNormal)
142. If (slope is poucoDeclive) and (DoD is normalBattery) and (velocity is ultraHigh) then (newVelocity is ultraHigh)
143. If (slope is poucoDeclive) and (DoD is normalBattery) and (velocity is highLimit) then (newVelocity is highLimit)
144. If (slope is declivePlano) and (DoD is normalBattery) and (velocity is ultraLow) then (newVelocity is ultraLow)
145. If (slope is declivePlano) and (DoD is normalBattery) and (velocity is low) then (newVelocity is low)
146. If (slope is declivePlano) and (DoD is normalBattery) and (velocity is lowNormal) then (newVelocity is lowNormal)
147. If (slope is declivePlano) and (DoD is normalBattery) and (velocity is high) then (newVelocity is high)
148. If (slope is declivePlano) and (DoD is normalBattery) and (velocity is normal) then (newVelocity is normal)
149. If (slope is declivePlano) and (DoD is normalBattery) and (velocity is highNormal) then (newVelocity is highNormal)
150. If (slope is declivePlano) and (DoD is normalBattery) and (velocity is ultraHigh) then (newVelocity is ultraHigh)
151. If (slope is declivePlano) and (DoD is normalBattery) and (velocity is highLimit) then (newVelocity is highLimit)
152. If (slope is aclivePlano) and (DoD is normalBattery) and (velocity is ultraLow) then (newVelocity is ultraLow)
153. If (slope is aclivePlano) and (DoD is normalBattery) and (velocity is low) then (newVelocity is low)
154. If (slope is aclivePlano) and (DoD is normalBattery) and (velocity is lowNormal) then (newVelocity is lowNormal)
155. If (slope is aclivePlano) and (DoD is normalBattery) and (velocity is high) then (newVelocity is high)
156. If (slope is aclivePlano) and (DoD is normalBattery) and (velocity is normal) then (newVelocity is normal)
157. If (slope is aclivePlano) and (DoD is normalBattery) and (velocity is highNormal) then (newVelocity is highNormal)

158. If (slope is aclivePlano) and (DoD is normalBattery) and (velocity is ultraHigh) then (newVelocity is ultraHigh)
159. If (slope is aclivePlano) and (DoD is normalBattery) and (velocity is highLimit) then (newVelocity is highLimit)
160. If (slope is aclive) and (DoD is normalBattery) and (velocity is ultraLow) then (newVelocity is ultraLow)
161. If (slope is aclive) and (DoD is normalBattery) and (velocity is low) then (newVelocity is low)
162. If (slope is aclive) and (DoD is normalBattery) and (velocity is lowNormal) then (newVelocity is lowNormal)
163. If (slope is aclive) and (DoD is normalBattery) and (velocity is high) then (newVelocity is normal)
164. If (slope is aclive) and (DoD is normalBattery) and (velocity is normal) then (newVelocity is normal)
165. If (slope is aclive) and (DoD is normalBattery) and (velocity is highNormal) then (newVelocity is normal)
166. If (slope is aclive) and (DoD is normalBattery) and (velocity is ultraHigh) then (newVelocity is normal)
167. If (slope is aclive) and (DoD is normalBattery) and (velocity is highLimit) then (newVelocity is normal)
168. If (slope is aclive) and (DoD is HighBattery) and (velocity is high) then (newVelocity is normal)
169. If (slope is poucoAclive) and (DoD is EcoMode) and (velocity is ultraLow) then (newVelocity is ultraLow)
170. If (slope is poucoAclive) and (DoD is EcoMode) and (velocity is low) then (newVelocity is low)
171. If (slope is poucoAclive) and (DoD is EcoMode) and (velocity is lowNormal) then (newVelocity is lowNormal)
172. If (slope is poucoAclive) and (DoD is EcoMode) and (velocity is normal) then (newVelocity is lowNormal)
173. If (slope is poucoAclive) and (DoD is EcoMode) and (velocity is high) then (newVelocity is lowNormal)
174. If (slope is poucoAclive) and (DoD is EcoMode) and (velocity is highNormal) then (newVelocity is lowNormal)
175. If (slope is poucoAclive) and (DoD is EcoMode) and (velocity is ultraHigh) then (newVelocity is normal)
176. If (slope is poucoAclive) and (DoD is EcoMode) and (velocity is highLimit) then (newVelocity is normal)
177. If (slope is declive) and (DoD is EcoMode) and (velocity is ultraLow) then (newVelocity is ultraLow)
178. If (slope is declive) and (DoD is EcoMode) and (velocity is low) then (newVelocity is low)
179. If (slope is declive) and (DoD is EcoMode) and (velocity is lowNormal) then (newVelocity is lowNormal)
180. If (slope is declive) and (DoD is EcoMode) and (velocity is high) then (newVelocity is high)
181. If (slope is declive) and (DoD is EcoMode) and (velocity is normal) then (newVelocity is normal)
182. If (slope is declive) and (DoD is EcoMode) and (velocity is highNormal) then (newVelocity is highNormal)
183. If (slope is declive) and (DoD is EcoMode) and (velocity is ultraHigh) then (newVelocity is ultraHigh)
184. If (slope is declive) and (DoD is EcoMode) and (velocity is highLimit) then (newVelocity is highLimit)
185. If (slope is plano) and (DoD is EcoMode) and (velocity is ultraLow) then (newVelocity is ultraLow)
186. If (slope is plano) and (DoD is EcoMode) and (velocity is low) then (newVelocity is low)
187. If (slope is plano) and (DoD is EcoMode) and (velocity is lowNormal) then (newVelocity is lowNormal)
188. If (slope is plano) and (DoD is EcoMode) and (velocity is normal) then (newVelocity is lowNormal)
189. If (slope is plano) and (DoD is EcoMode) and (velocity is high) then (newVelocity is lowNormal)
190. If (slope is plano) and (DoD is EcoMode) and (velocity is highNormal) then (newVelocity is lowNormal)
191. If (slope is plano) and (DoD is EcoMode) and (velocity is ultraHigh) then (newVelocity is normal)
192. If (slope is plano) and (DoD is EcoMode) and (velocity is highLimit) then (newVelocity is normal)
193. If (slope is poucoDeclive) and (DoD is EcoMode) and (velocity is ultraLow) then (newVelocity is ultraLow)
194. If (slope is poucoDeclive) and (DoD is EcoMode) and (velocity is low) then (newVelocity is low)
195. If (slope is poucoDeclive) and (DoD is EcoMode) and (velocity is lowNormal) then (newVelocity is lowNormal)
196. If (slope is poucoDeclive) and (DoD is EcoMode) and (velocity is high) then (newVelocity is high)
197. If (slope is poucoDeclive) and (DoD is EcoMode) and (velocity is normal) then (newVelocity is normal)
198. If (slope is poucoDeclive) and (DoD is EcoMode) and (velocity is highNormal) then (newVelocity is highNormal)
199. If (slope is poucoDeclive) and (DoD is EcoMode) and (velocity is ultraHigh) then (newVelocity is ultraHigh)
200. If (slope is poucoDeclive) and (DoD is EcoMode) and (velocity is highLimit) then (newVelocity is highLimit)
201. If (slope is declivePlano) and (DoD is EcoMode) and (velocity is ultraLow) then (newVelocity is ultraLow)
202. If (slope is declivePlano) and (DoD is EcoMode) and (velocity is low) then (newVelocity is low)
203. If (slope is declivePlano) and (DoD is EcoMode) and (velocity is lowNormal) then (newVelocity is lowNormal)
204. If (slope is declivePlano) and (DoD is EcoMode) and (velocity is high) then (newVelocity is high)
205. If (slope is declivePlano) and (DoD is EcoMode) and (velocity is normal) then (newVelocity is normal)
206. If (slope is declivePlano) and (DoD is EcoMode) and (velocity is highNormal) then (newVelocity is highNormal)
207. If (slope is declivePlano) and (DoD is EcoMode) and (velocity is ultraHigh) then (newVelocity is ultraHigh)
208. If (slope is declivePlano) and (DoD is EcoMode) and (velocity is highLimit) then (newVelocity is highLimit)
209. If (slope is aclivePlano) and (DoD is EcoMode) and (velocity is ultraLow) then (newVelocity is ultraLow)
210. If (slope is aclivePlano) and (DoD is EcoMode) and (velocity is low) then (newVelocity is low)
211. If (slope is aclivePlano) and (DoD is EcoMode) and (velocity is lowNormal) then (newVelocity is lowNormal)
212. If (slope is aclivePlano) and (DoD is EcoMode) and (velocity is normal) then (newVelocity is lowNormal)
213. If (slope is aclivePlano) and (DoD is EcoMode) and (velocity is highNormal) then (newVelocity is lowNormal)
214. If (slope is aclivePlano) and (DoD is EcoMode) and (velocity is high) then (newVelocity is lowNormal)
215. If (slope is aclivePlano) and (DoD is EcoMode) and (velocity is ultraHigh) then (newVelocity is normal)
216. If (slope is aclivePlano) and (DoD is EcoMode) and (velocity is highLimit) then (newVelocity is normal)
217. If (slope is aclive) and (DoD is EcoMode) and (velocity is ultraLow) then (newVelocity is ultraLow)
218. If (slope is aclive) and (DoD is EcoMode) and (velocity is low) then (newVelocity is ultraLow)
219. If (slope is aclive) and (DoD is EcoMode) and (velocity is lowNormal) then (newVelocity is ultraLow)
220. If (slope is aclive) and (DoD is EcoMode) and (velocity is normal) then (newVelocity is low)
221. If (slope is aclive) and (DoD is EcoMode) and (velocity is highNormal) then (newVelocity is low)
222. If (slope is aclive) and (DoD is EcoMode) and (velocity is high) then (newVelocity is lowNormal)
223. If (slope is aclive) and (DoD is EcoMode) and (velocity is ultraHigh) then (newVelocity is lowNormal)
224. If (slope is aclive) and (DoD is EcoMode) and (velocity is highLimit) then (newVelocity is lowNormal)